UNIVERSITÄT BAYREUTH

BGI Bayerisches Geoinstitut

in incudibus veritas

Submicron SMS for High-Pressure Mineral Physics

Leonid Dubrovinsky

ESRF

DESY

GEFÖRDERT VOM
Bundesministerium für Bildung und Forschung

DFG Deutsche Forschungsgemeinschaft

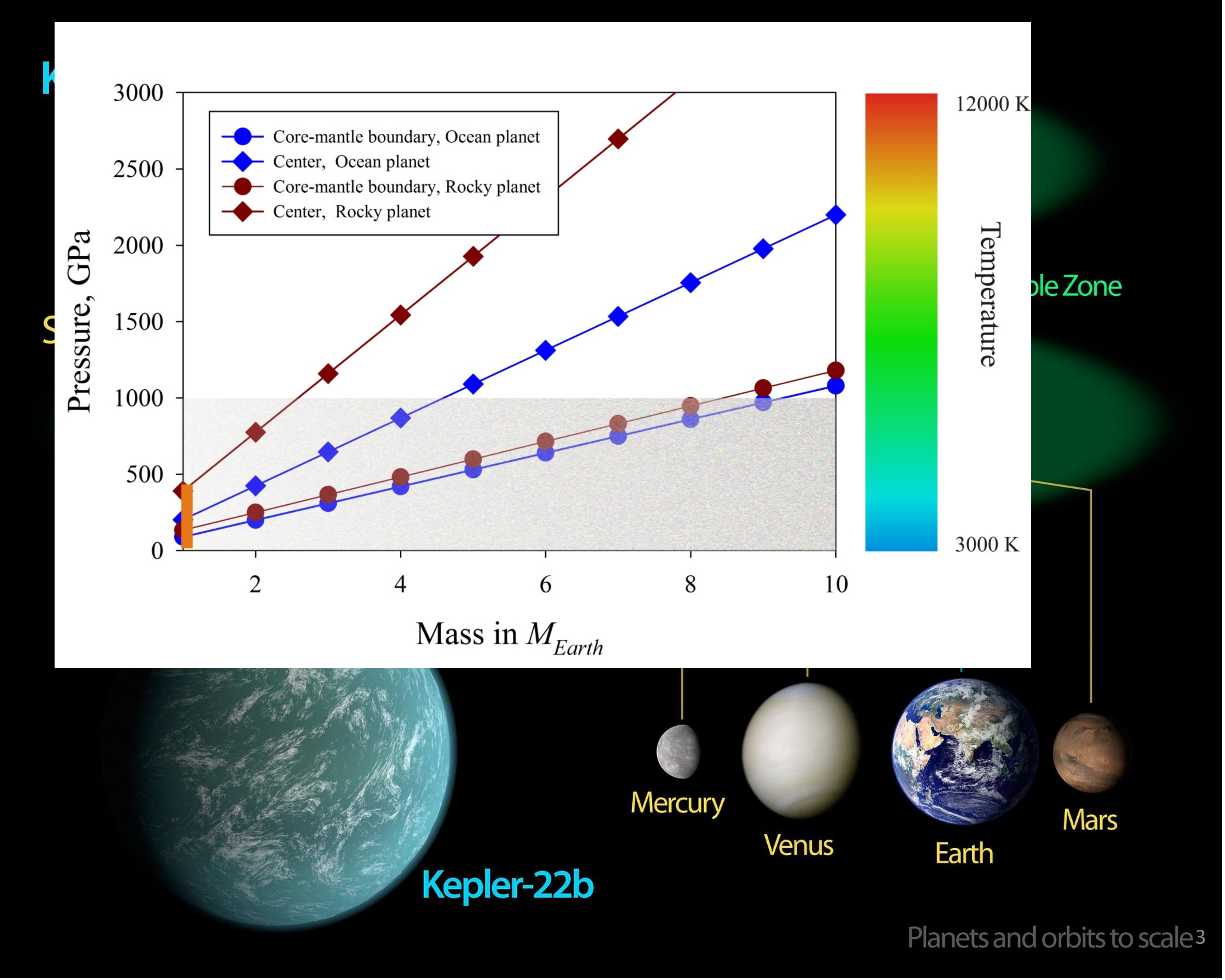

3000
2500
2000
1500
1000
500
0
Pressure, GPa
Core-mantle boundary, Ocean planet
Center, Ocean planet
Core-mantle boundary, Rocky planet
Center, Rocky planet
2
4
6
8
10
Mass in M_{Earth}
12000 K
Temperature
3000 K
ble Zone
Mercury
Venus
Earth
Mars
Kepler-22b
Planets and orbits to scale

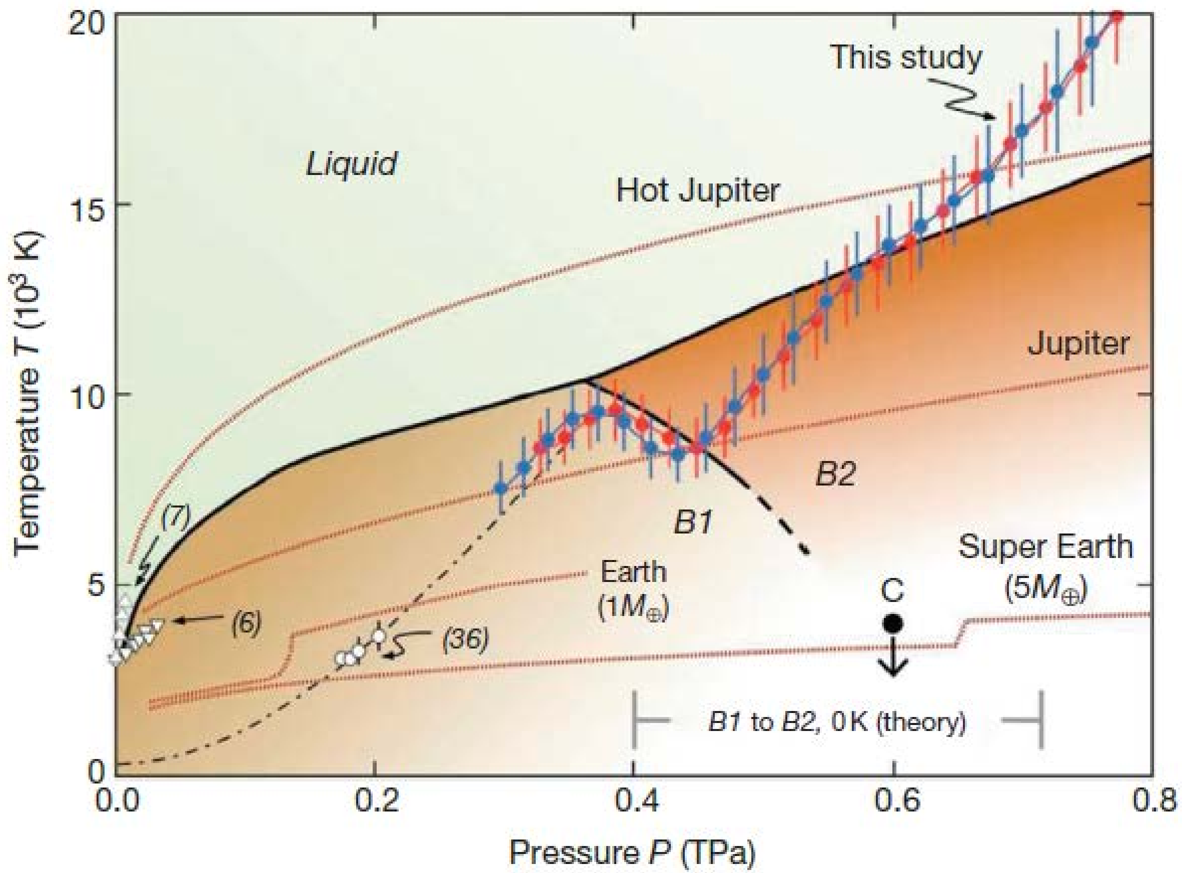

MgO is expected to be one of very important components of Super Earths

Phase diagram of MgO. Filled red and blue circles and corresponding curves are the shock pressures and temperatures from laser experiments. Brown lines show expected P–T paths for Earth, a 5 ME super-Earth, Jupiter, and a hot Jupiter. The melting curve and B1–B2 phase transition boundary are also indicated. The filled circle labeled C shows the pressure and upper bound temperature for the B1–B2 transition from ramp compression x-ray diffraction experiments (Coppari et al., 2013).

There are no static compression data on behavior of MgO above ~250 GPa

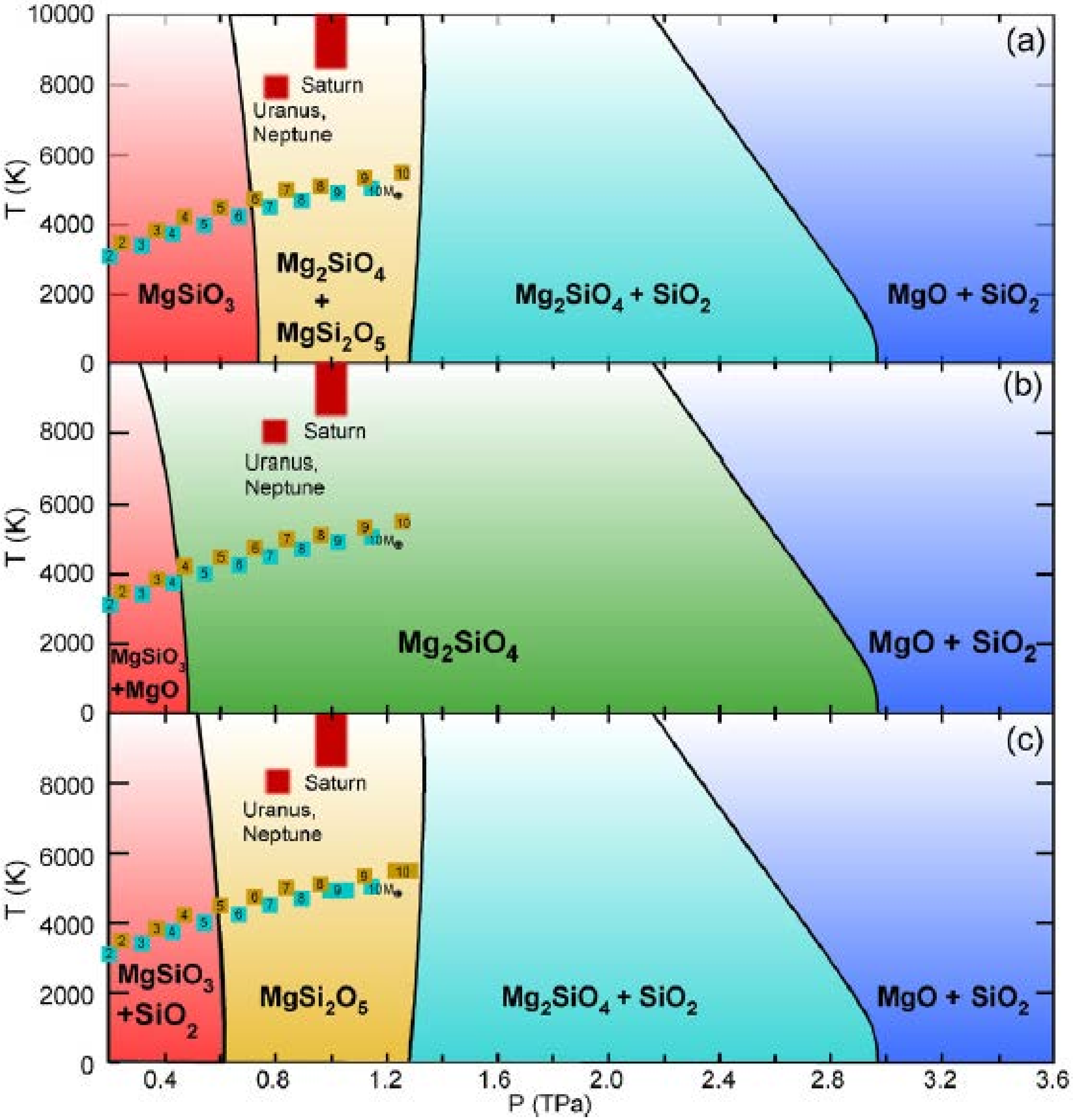

Earth and Planetary Science Letters 478 (2017) 40–45

Contents lists available at ScienceDirect

ELSEVIER

Earth and Planetary Science Letters

www.elsevier.com/locate/epsl

Phase transitions in $MgSiO_3$ post-perovskite in super-Earth mantles

Koichiro Umemoto[a,b,c,*], Renata M. Wentzcovitch[d,e,f], Shunqing Wu[c,g], Min Ji[c], Cai-Zhuang Wang[c], Kai-Ming Ho[c]

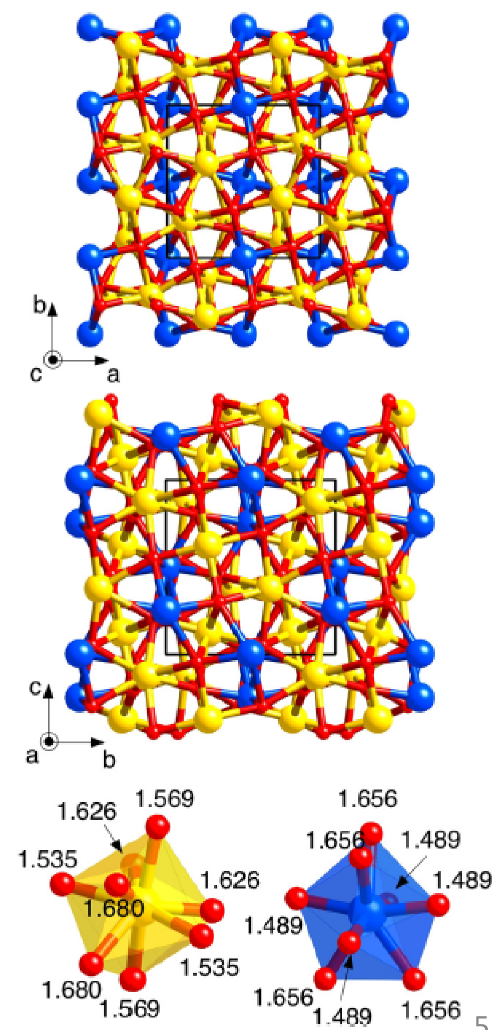

Mg_2SiO_4 above 500 GPa

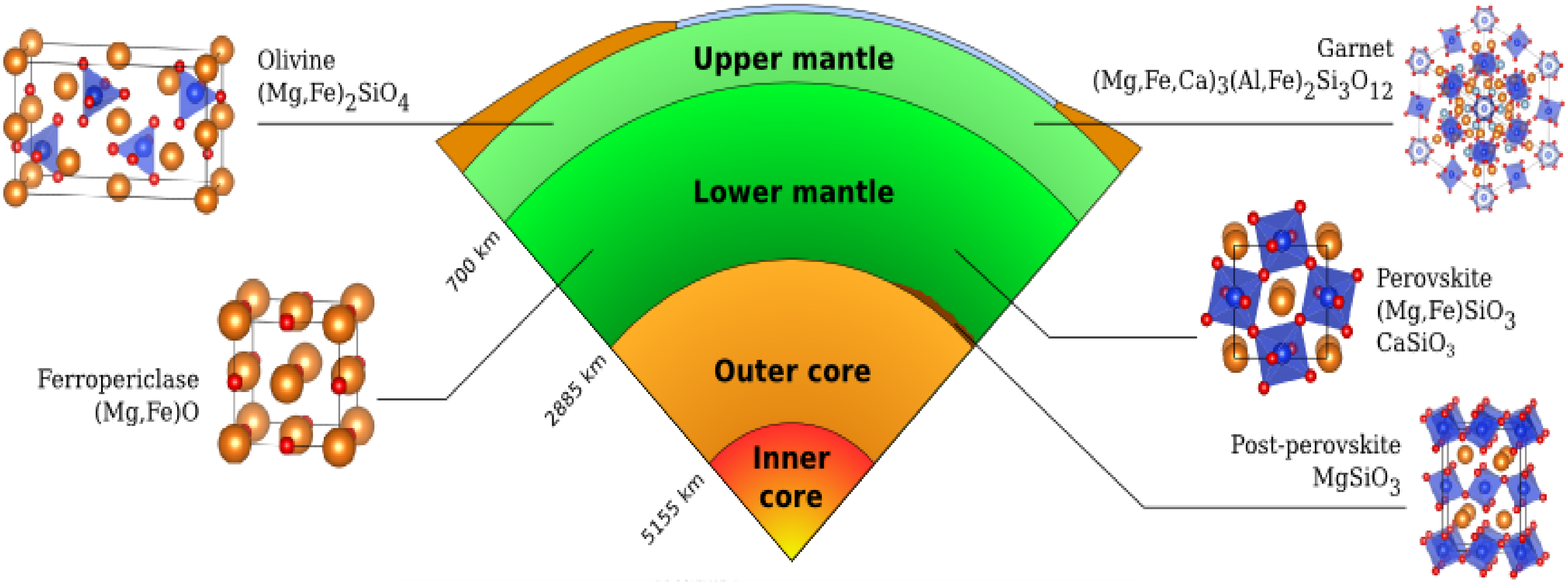

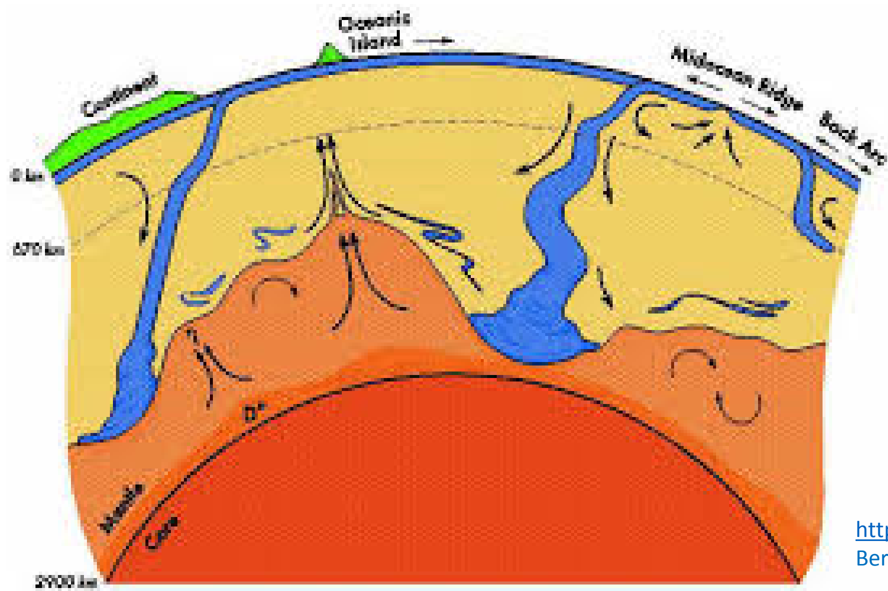

http://pierrehirel.info/

https://people.earth.yale.edu/sites/default/files/files/Bercovici/17_MantlConvection-ESEG2011-2_0.pdf

Space group *C mcm*

a=2.4626(15) Å

b=7.9970(13) Å

c=6.101(5) Å

Unique reflections: 74

Rint 1.3%

Refined parameters: 10

R1=7.2 %

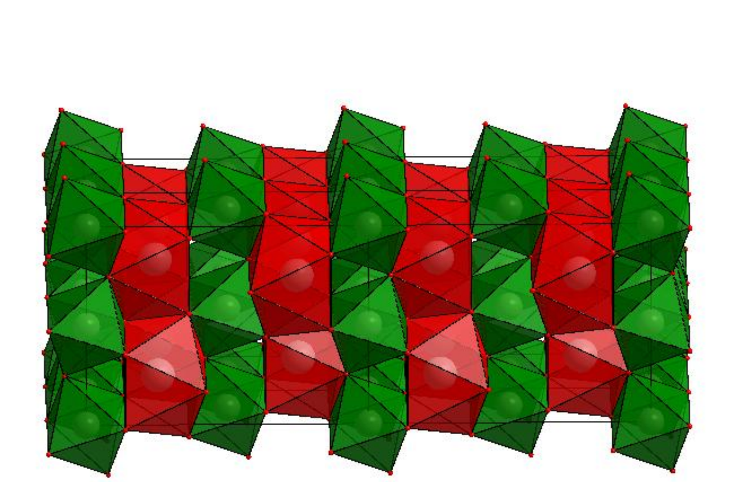

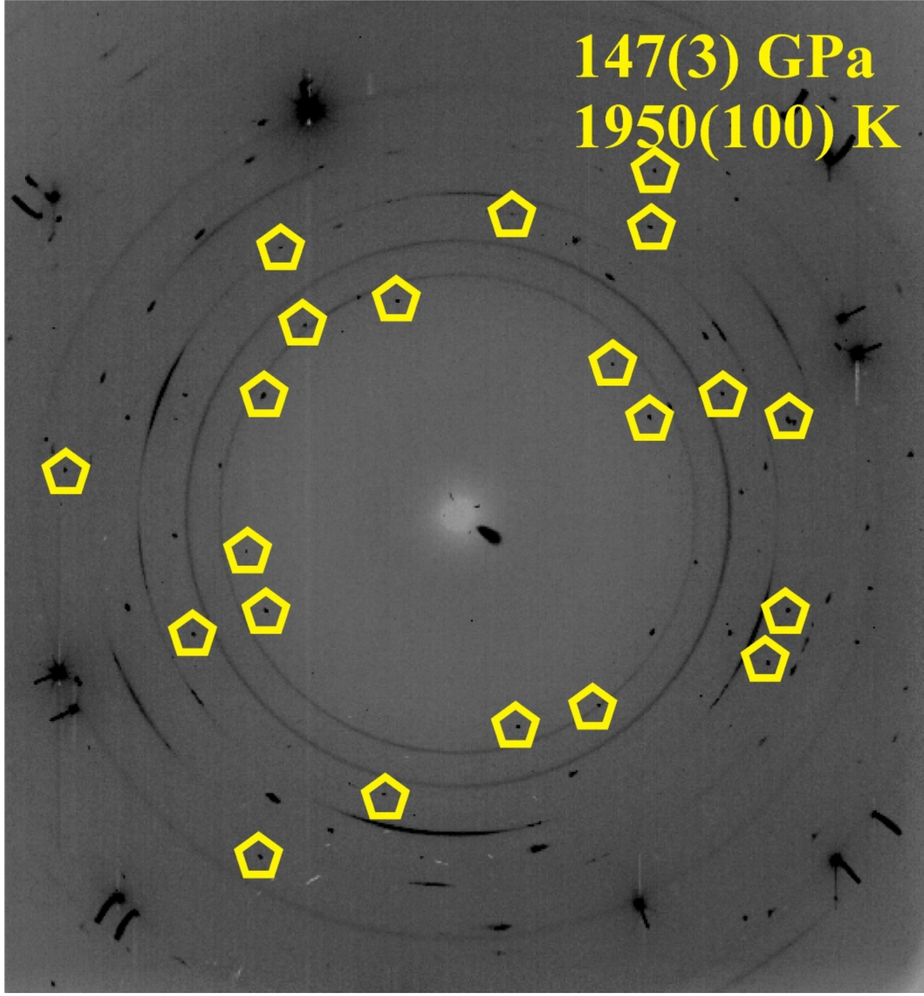

$(Mg_{0.42},Fe_{0.68})(Si_{0.57},Al_{0.37},Fe_{0.06})O_3$

$(Mg_{0.76(2)}Fe_{0.24(2)})(Si_{0.64}Al_{0.36})O_{2.98(2)}$ PPv

Koemets et al., 2019

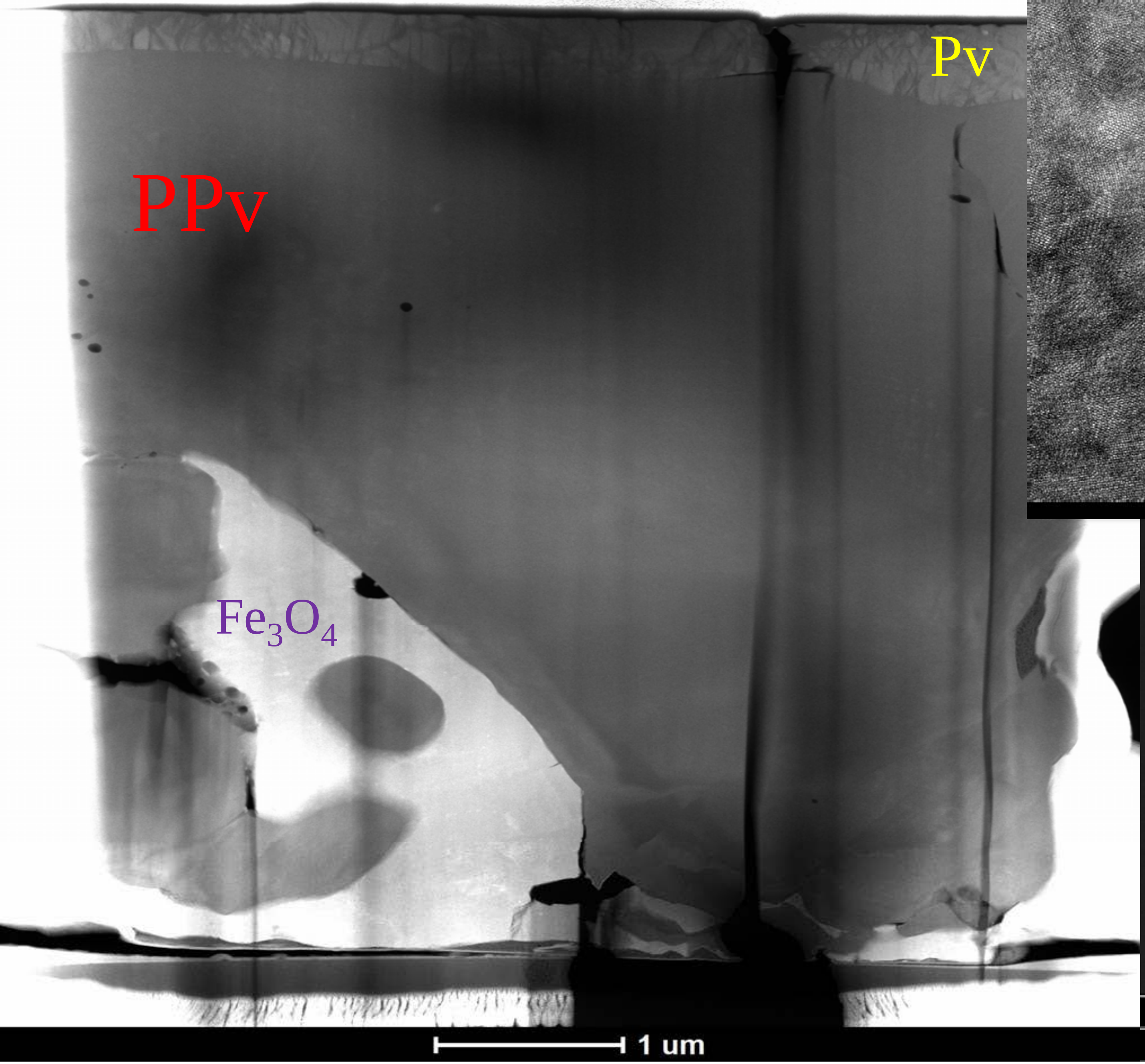

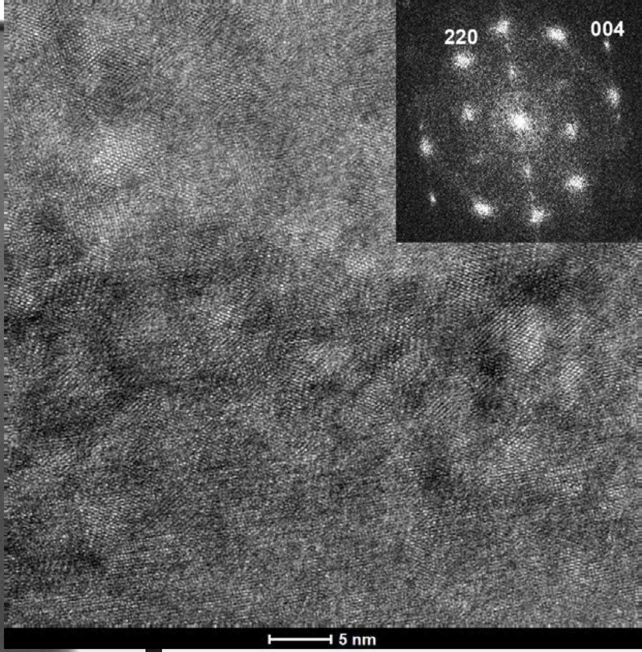

TEM/SEM

Overview HAADF-STEM image of the FIB slice

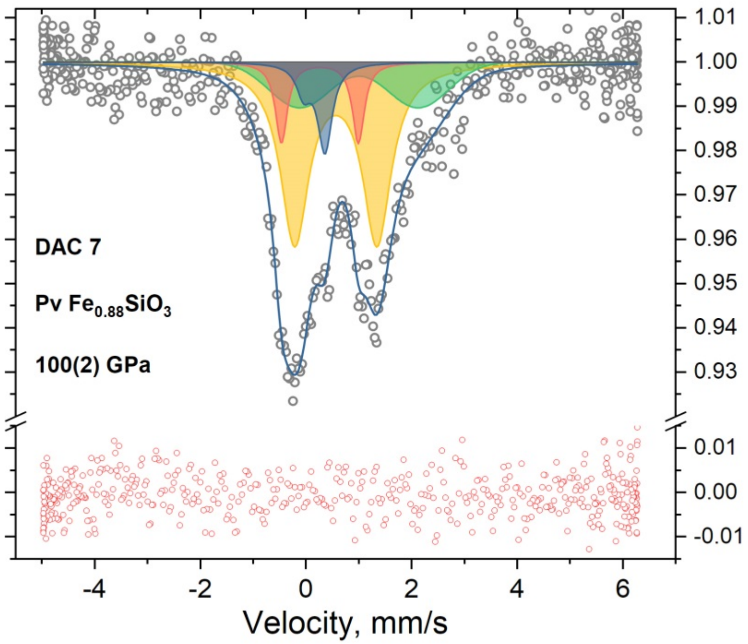

Koemets et al., 2019

High Pressure iron oxides in the presence of oxygen

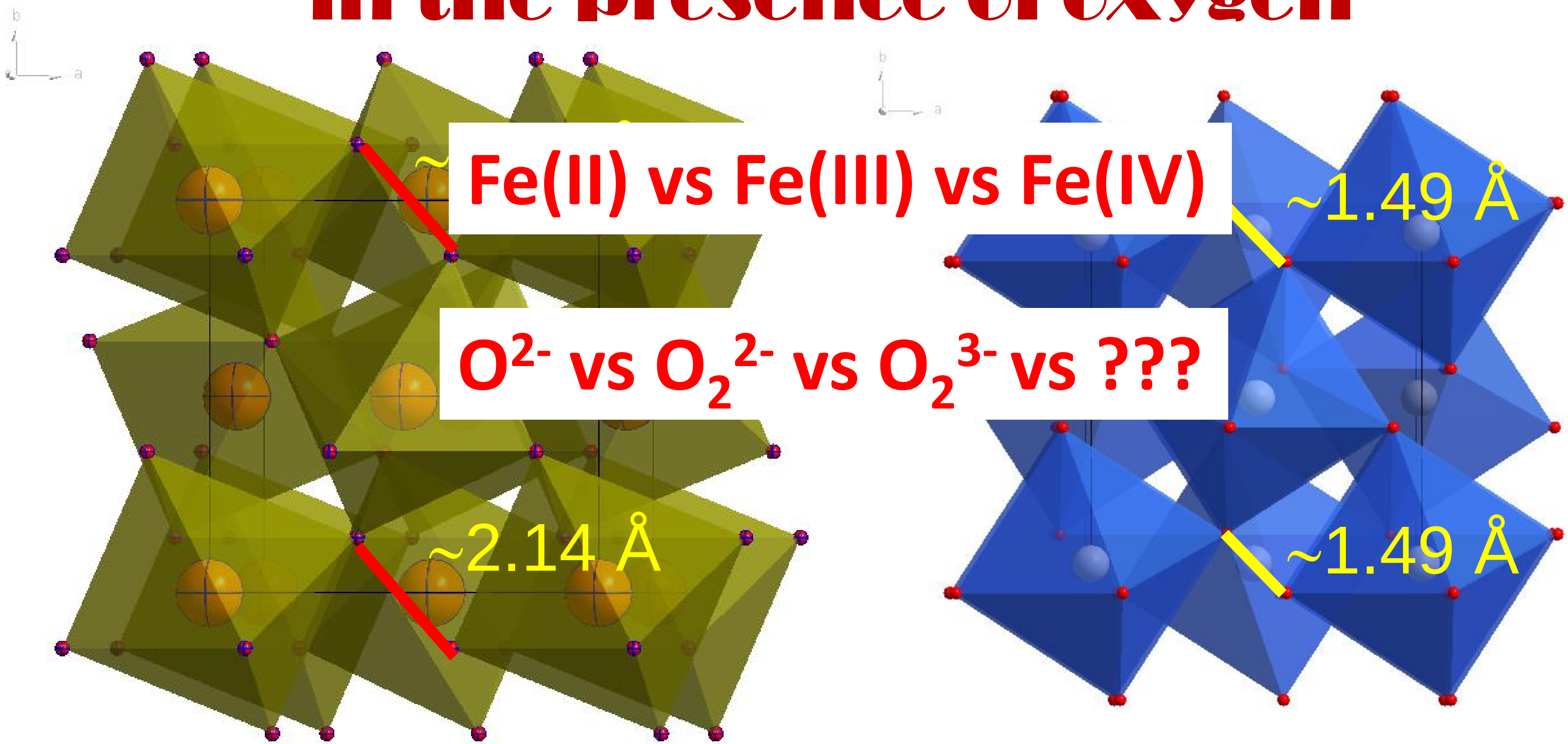

FeO_2, 68(1) GPa

HP-PdF_2-type structure

MgO_2, 0 GPa

Pyrite-type structure

O_2^{2-}

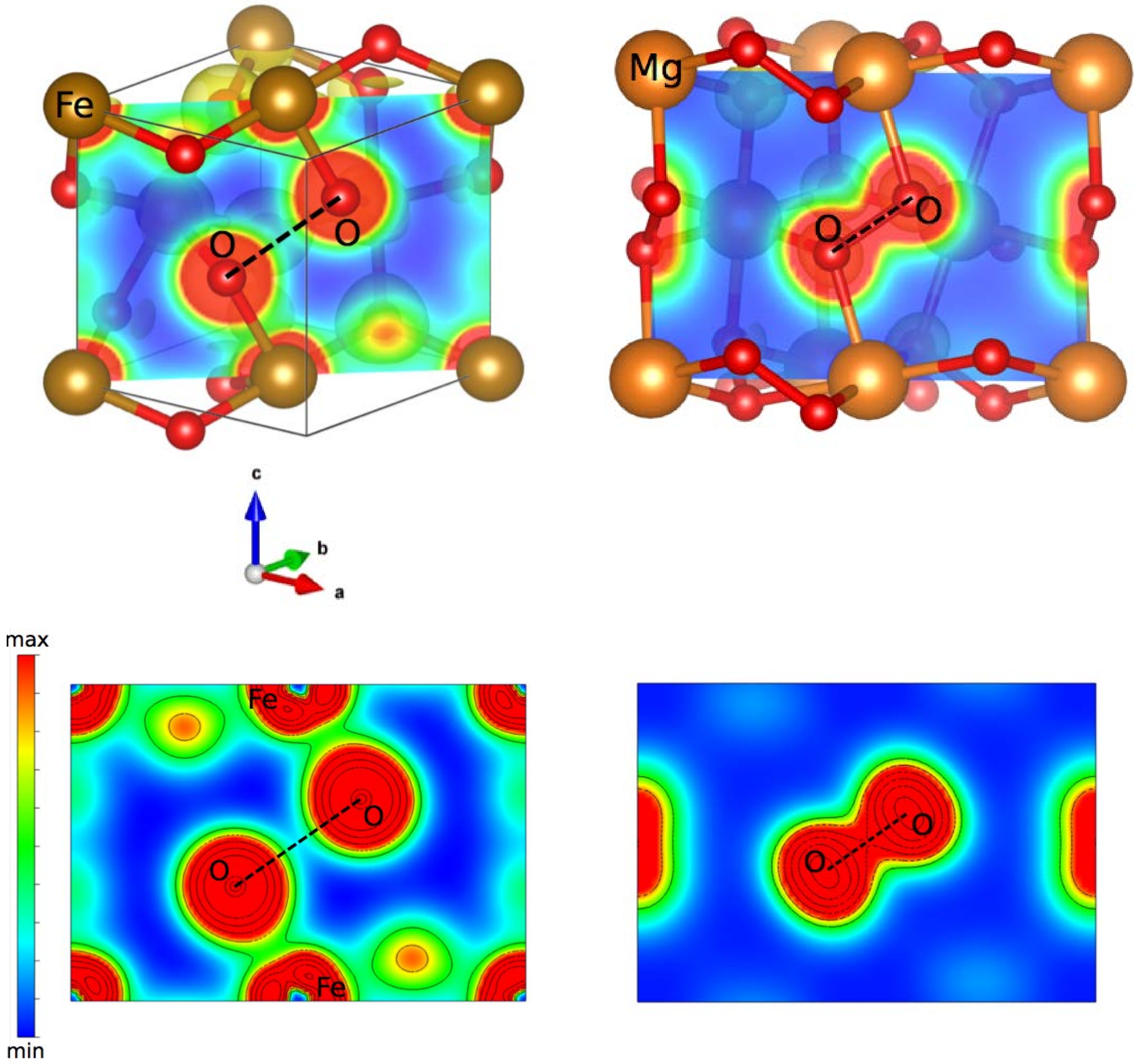

Koemets et al., 2019

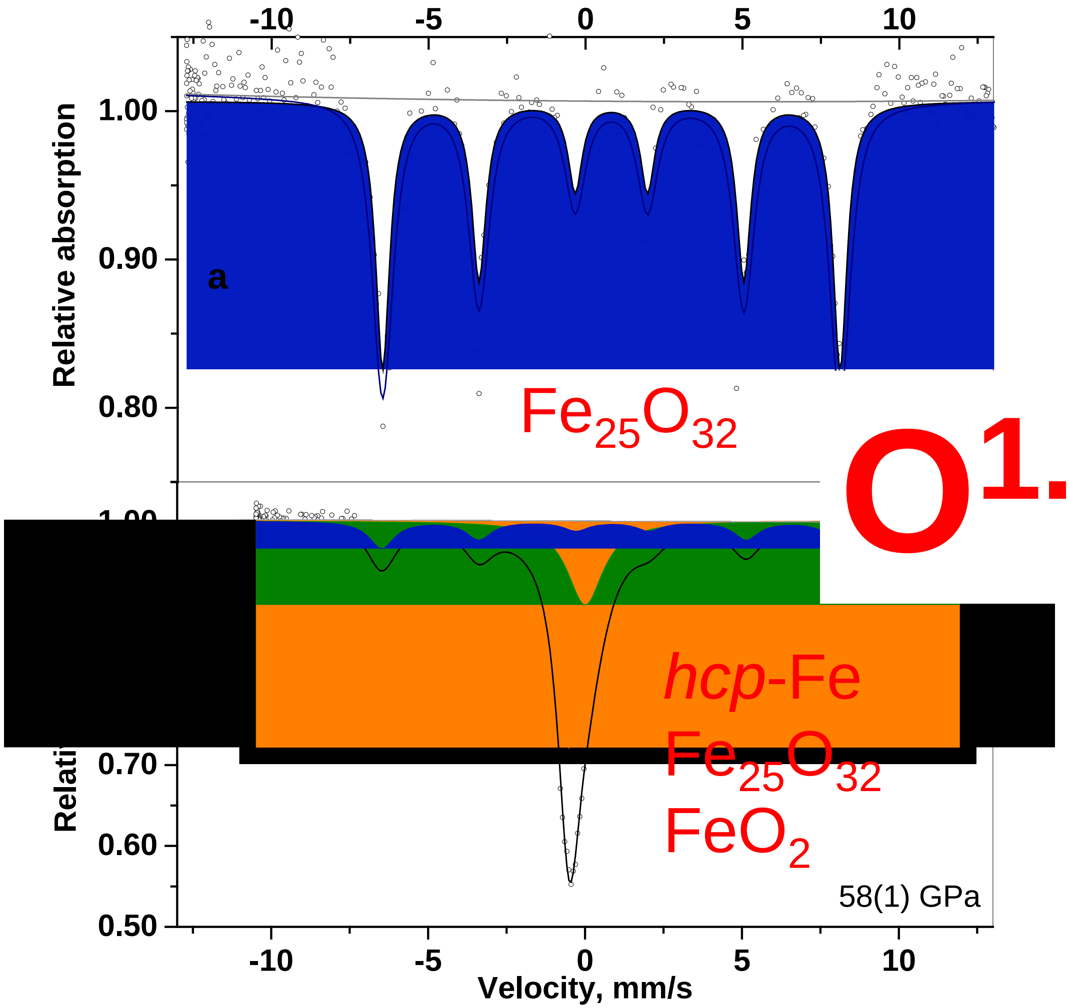

$O^{1.5-}$

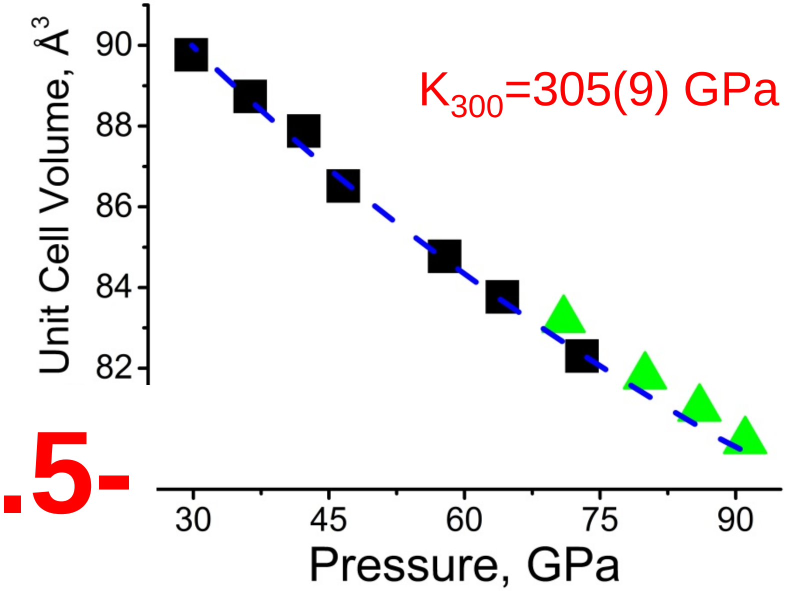

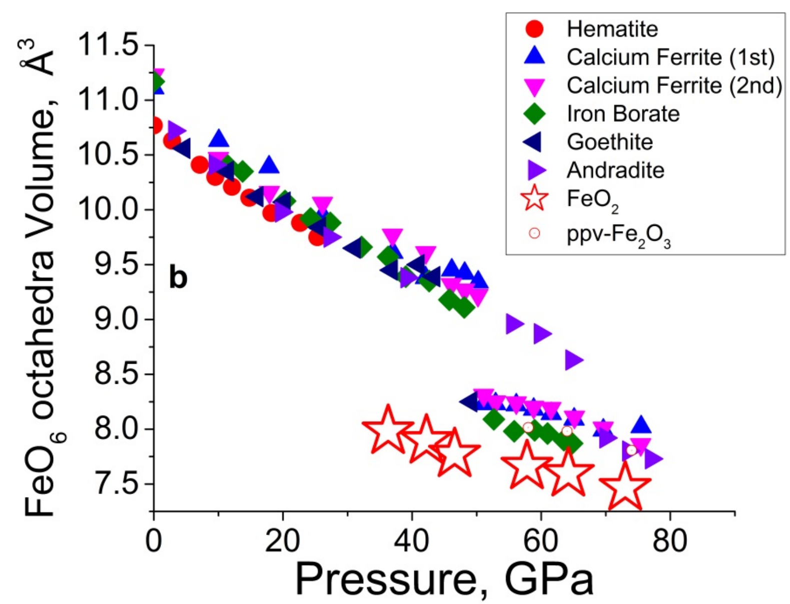

ID18, ESRF

Koemets et al., 2019

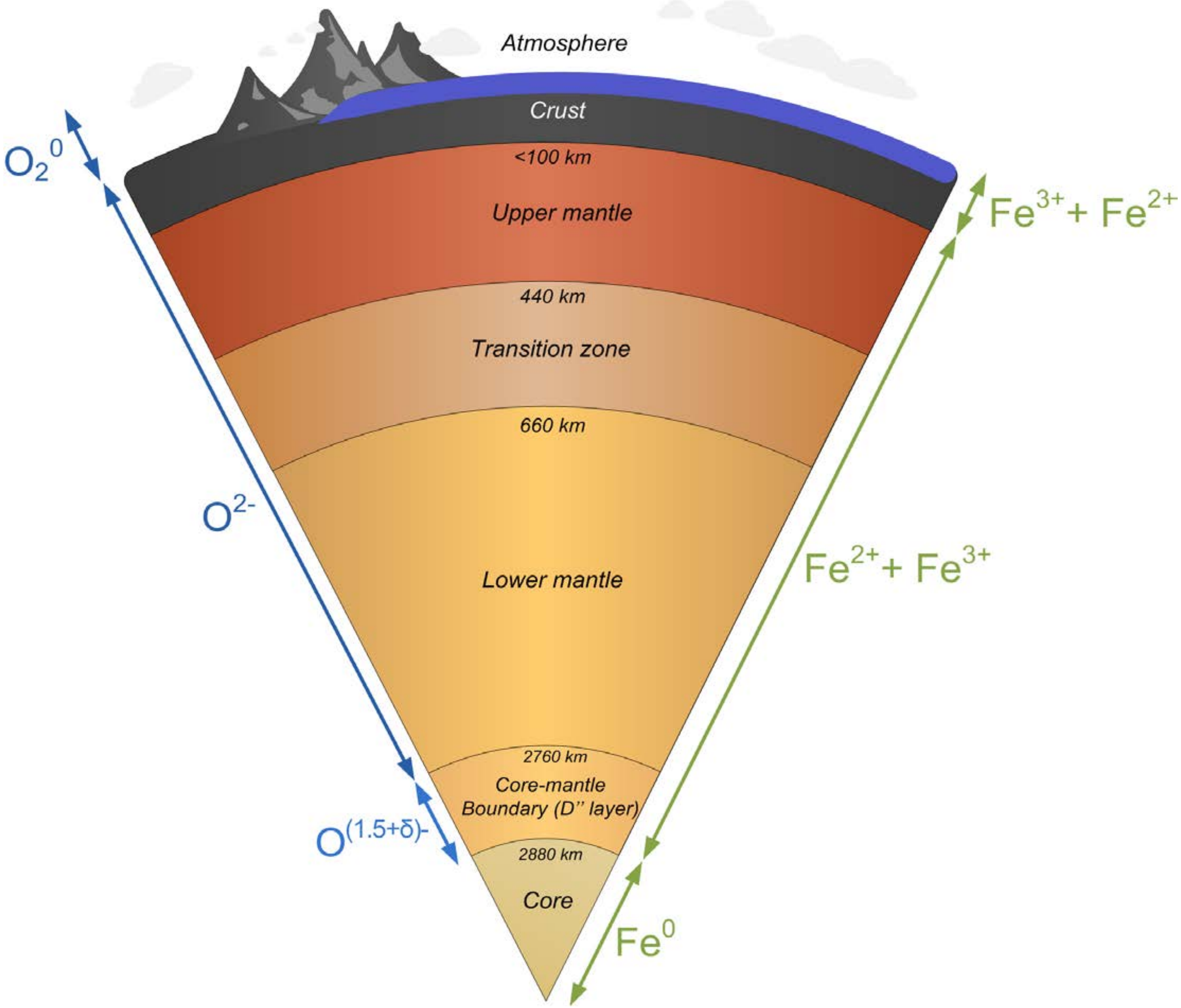

Koemets et al., 2019

Double-stage DAC (dsDAC)

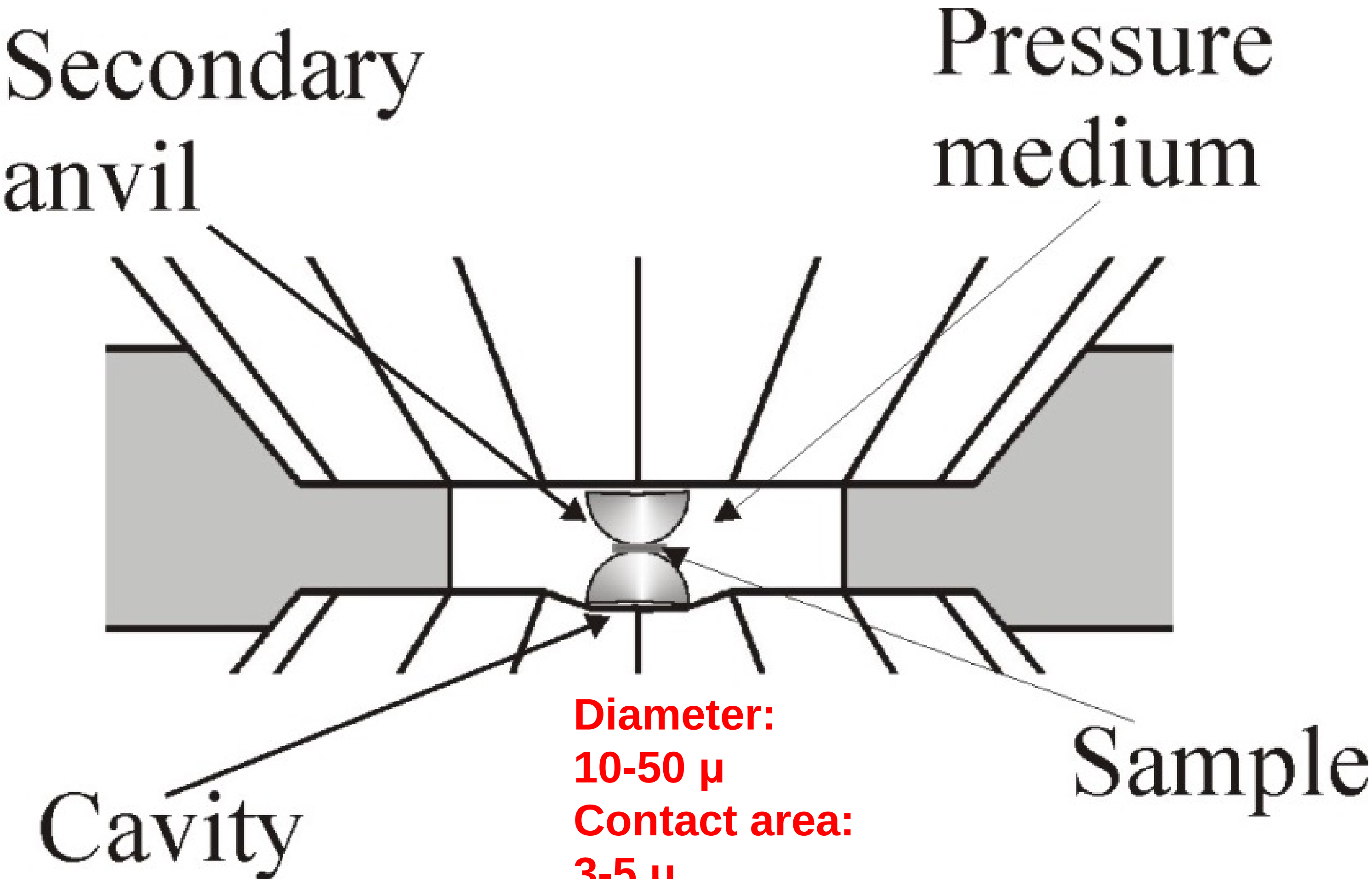

Diameter:
10-50 μ
Contact area:
3-5 μ

Dubrovinsky et al. Nature Comm. 2012

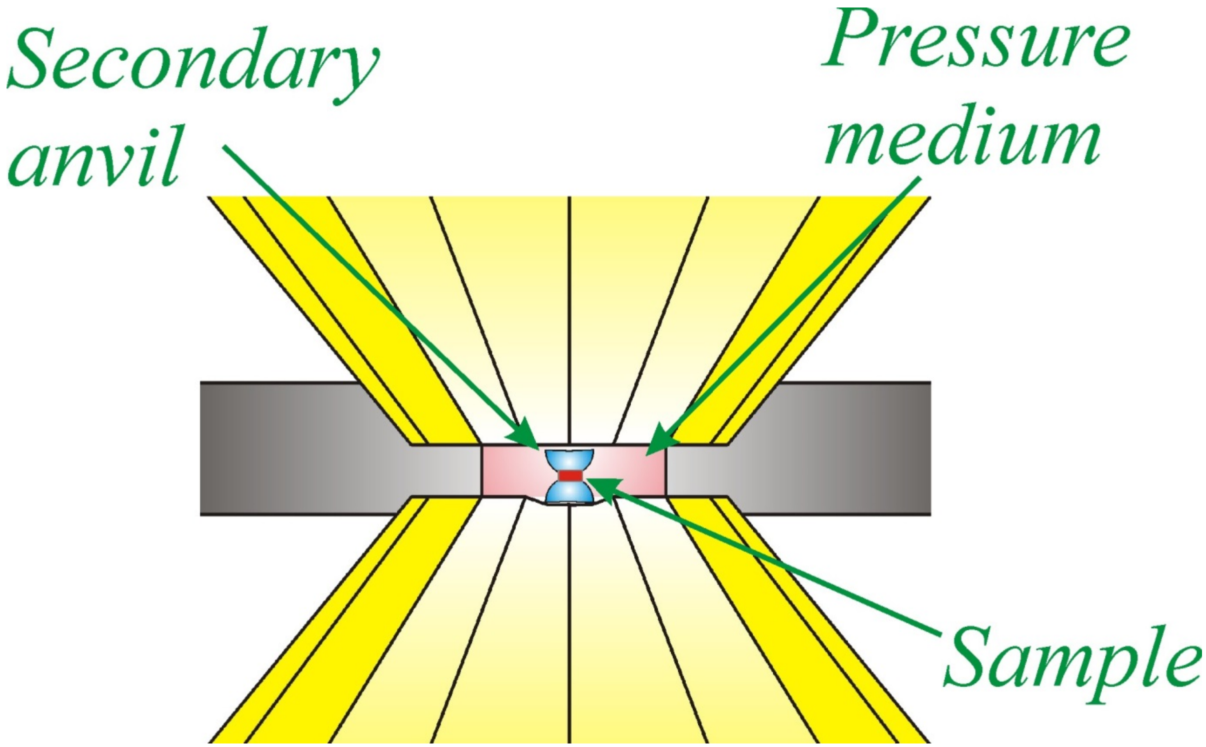

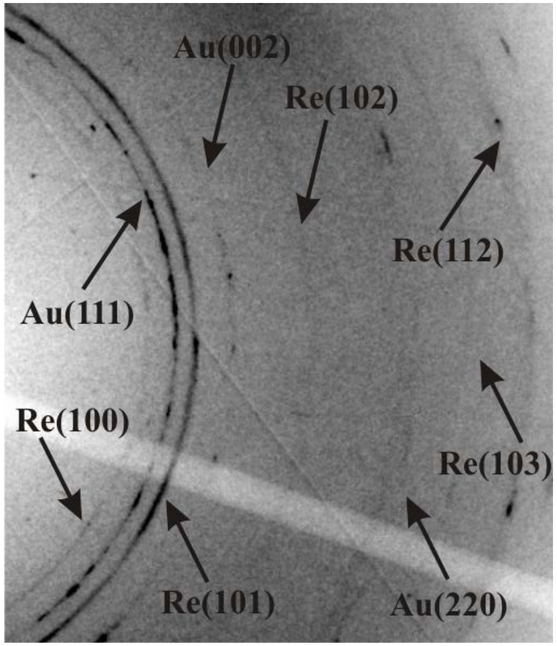

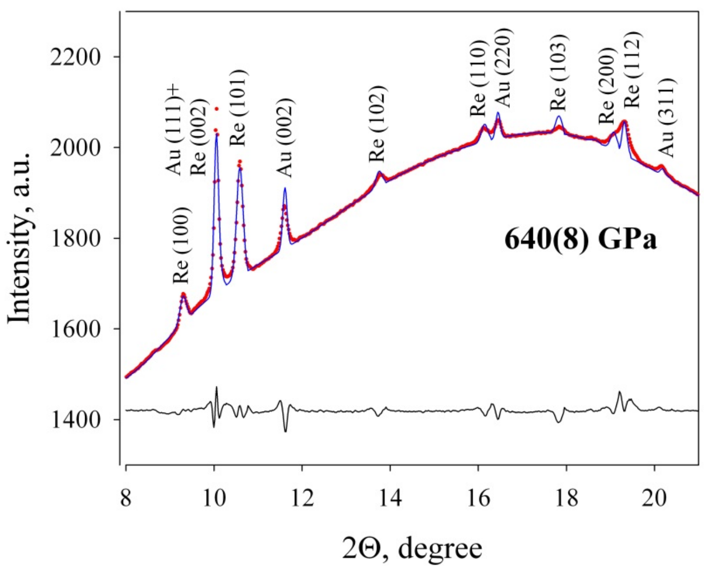

Dubrovinsky et al., Nature Commun. 2012

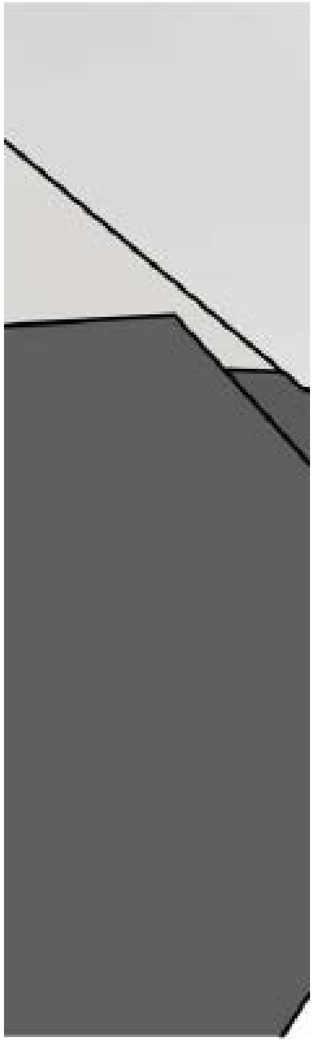

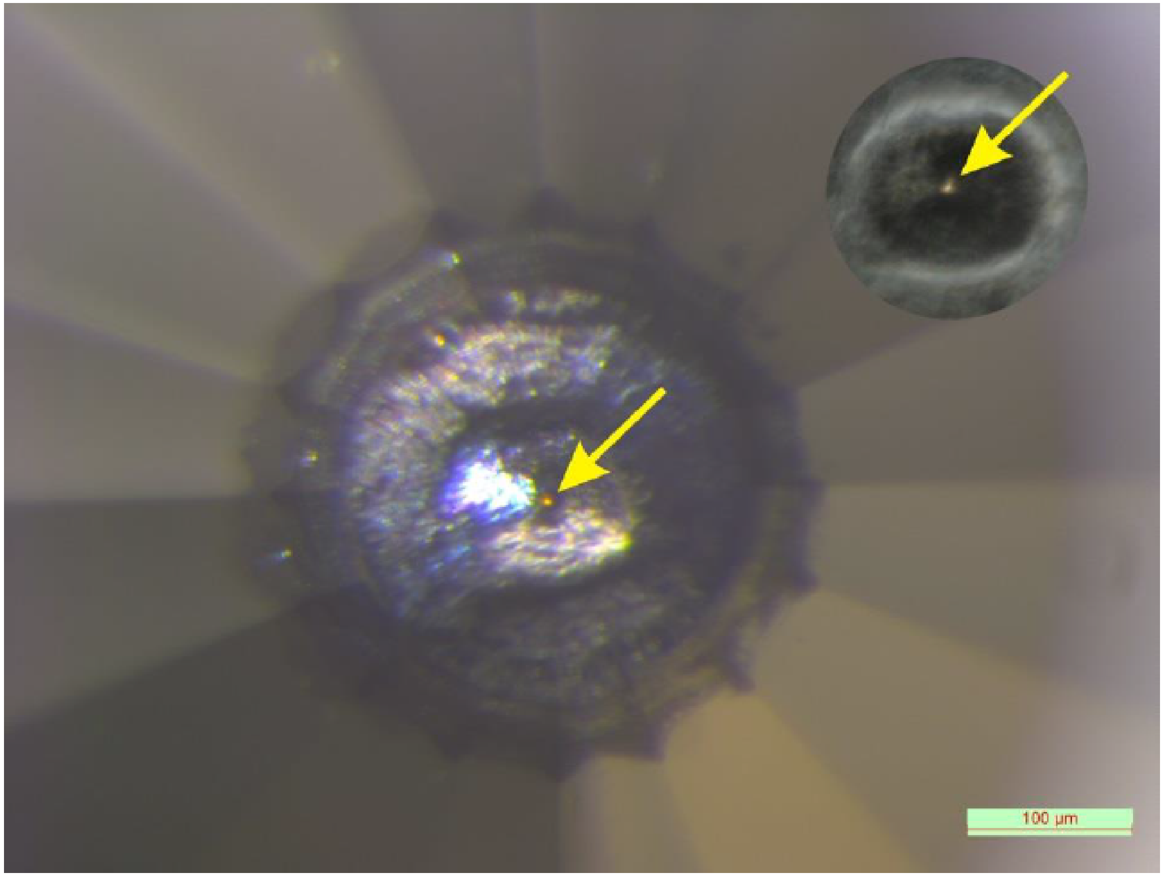

fig. S5. Optical photograph of the sample (Au and paraffin wax) compressed in a gasketed ds-DAC at 688(10) GPa, as seen through the diamonds and NCD secondary anvils. The size of the pressure chamber is of about 5 µm and gold occupies only a portion of it. As a result, one can clearly see the transmitted light (pointed out by the yellow arrow) passing through the material (paraffin wax) that confirms that NCD remains optically transparent even at such high pressures. Insert in the upper right corner shows the central part of the gasket and the pressure chamber under just slight illumination by the reflected light.

Dubrovinskaia et al., Sci Adv., 2016

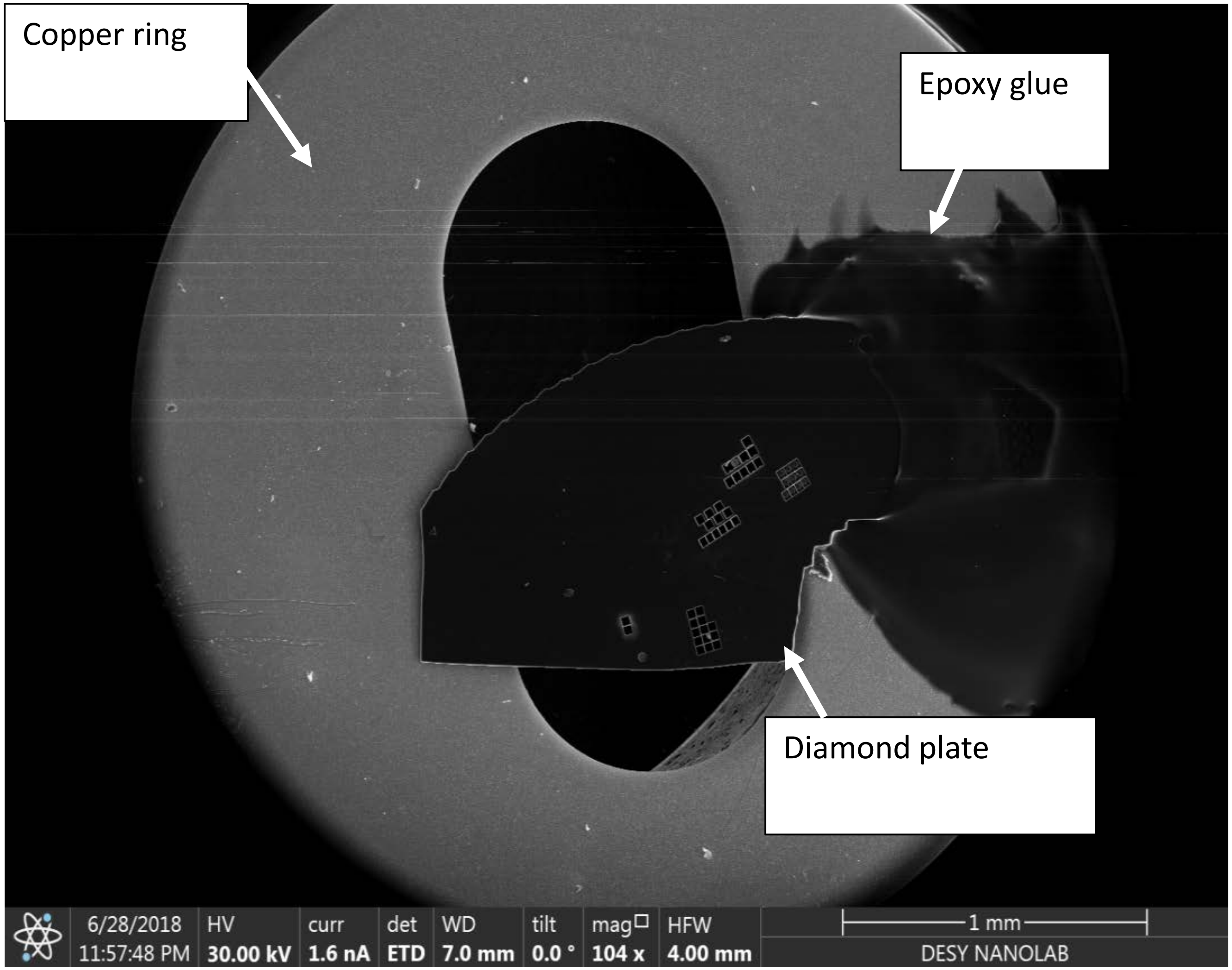

SEM-image of a single-crystal diamond plate (type Ia, diameter 3.00 mm, thickness 10 µm (100)-oriented, Almax easyLab).
The plate is glued on a copper ring (a holder for TEM-samples) with epoxy glue.

Khandarkhaeva et al., 2019

Disks or cones milling

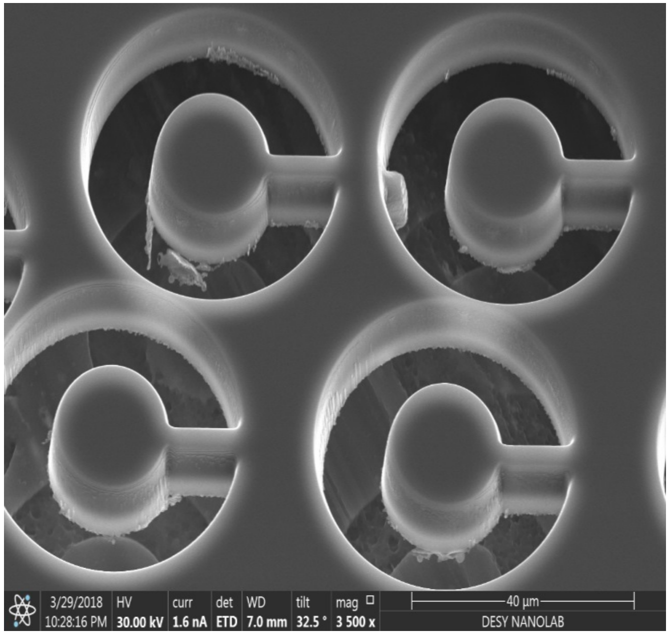

Khandarkhaeva et al., 2019

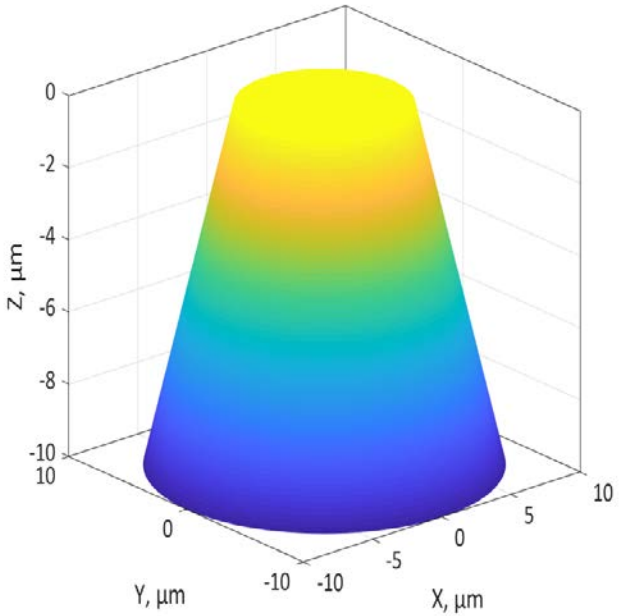

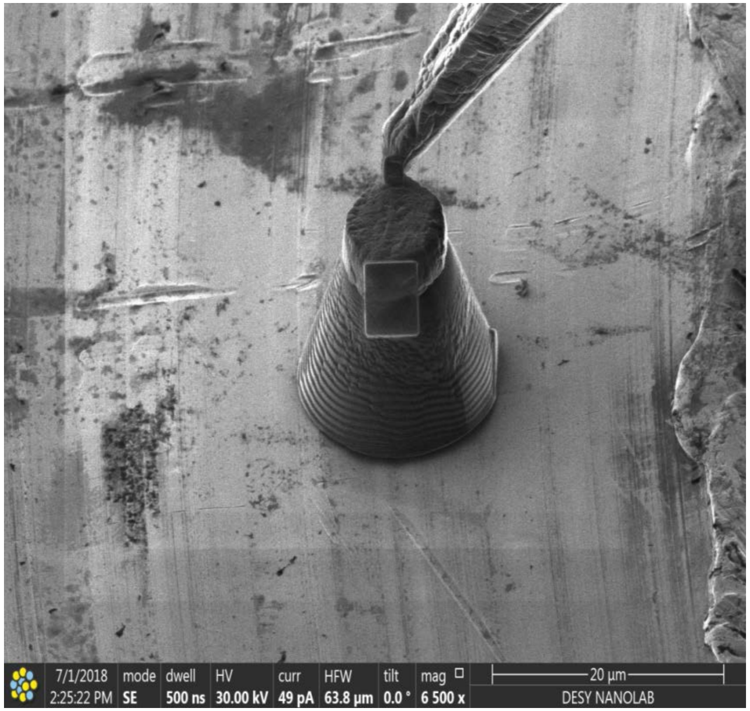

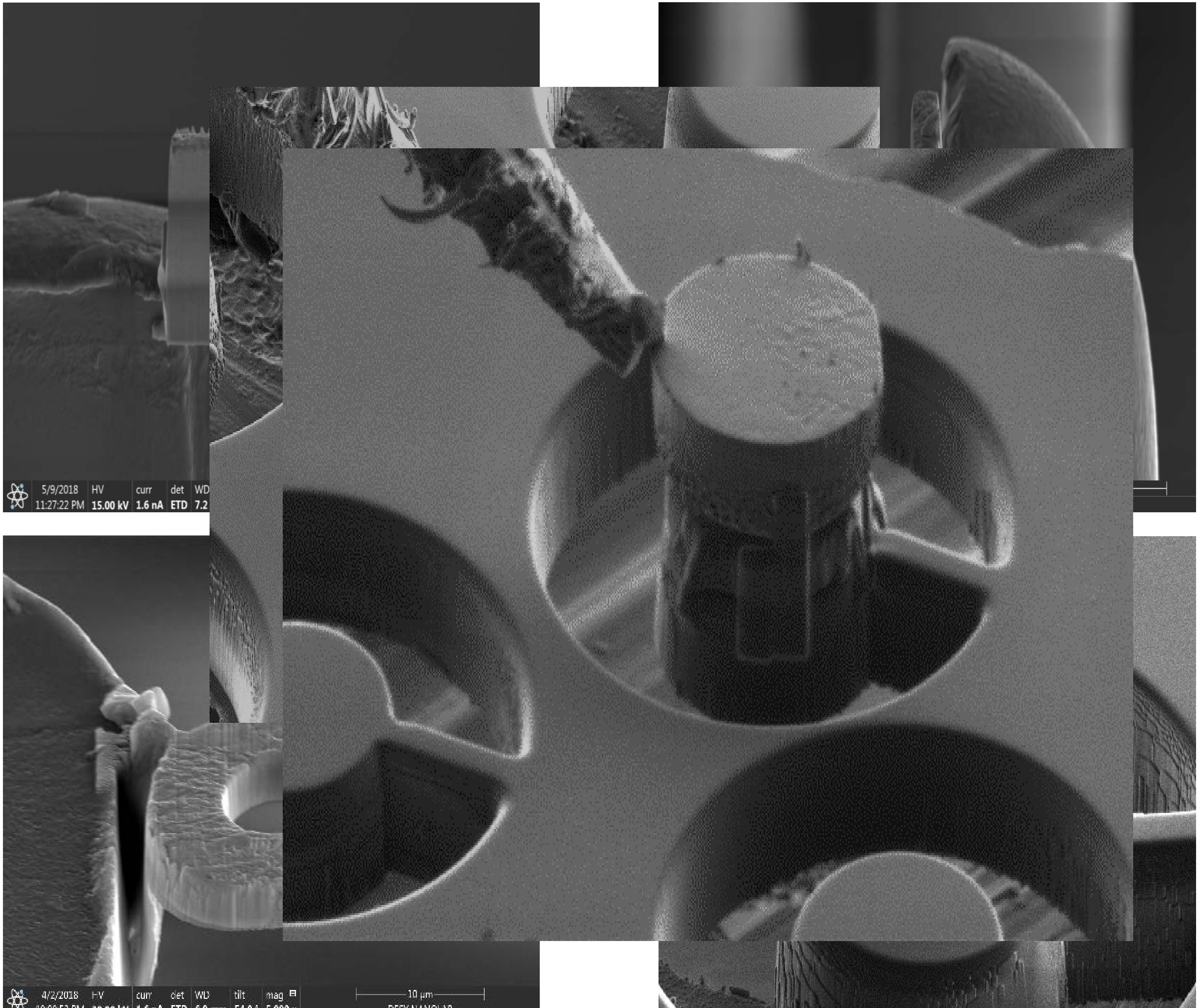
5/9/2018 HV curr det WD
11:27:22 PM 15.00 kV 1.6 nA ETD 7.2
4/2/2018 HV curr det WD tilt mag
10:00:52 PM 30.00 kV 1.6 nA ETD 6.9 mm 54.0 ° 5 000 x
10 µm
DESY NANOLAB

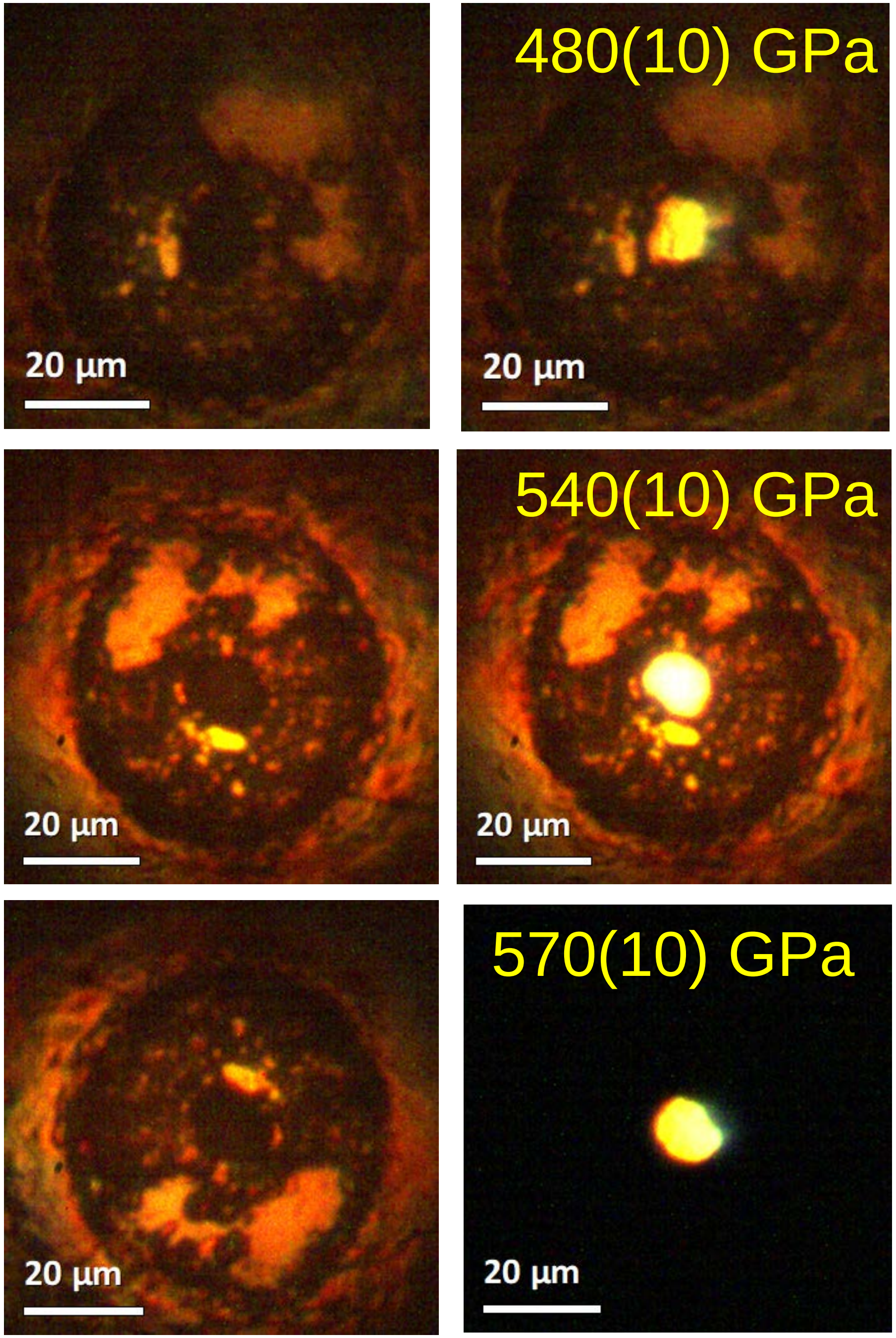

480(10) GPa
540(10) GPa
570(10) GPa
20 µm

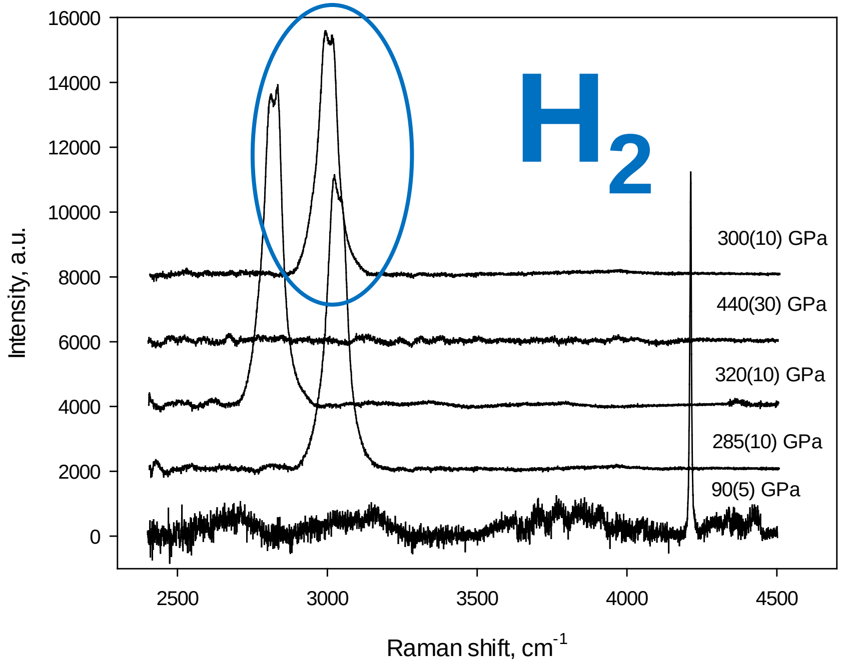

H2
Intensity, a.u.
Raman shift, cm-1
300(10) GPa
440(30) GPa
320(10) GPa
285(10) GPa
90(5) GPa

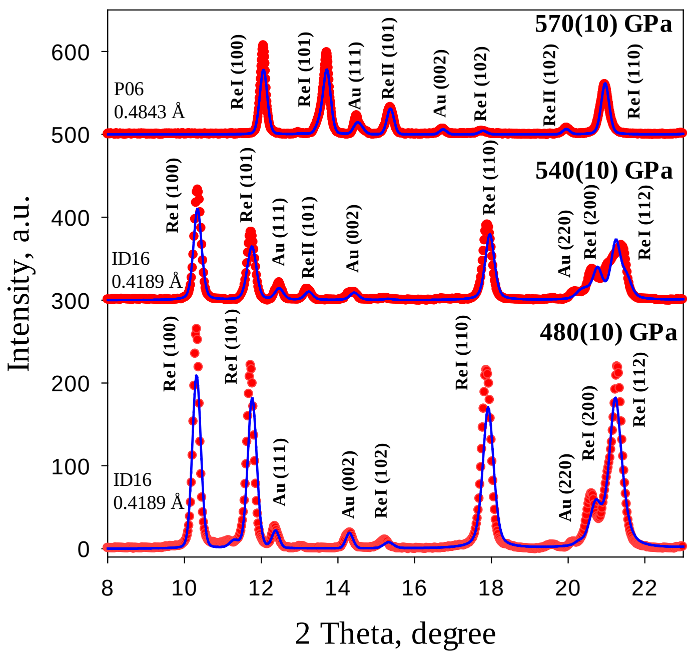

570(10) GPa
540(10) GPa
480(10) GPa
P06
0.4843 Å
ID16
0.4189 Å
ReI (100)
ReI (101)
Au (111)
ReII (101)
Au (002)
ReI (102)
ReII (102)
ReI (110)
Au (220)
ReI (200)
ReI (112)
Intensity, a.u.
2 Theta, degree

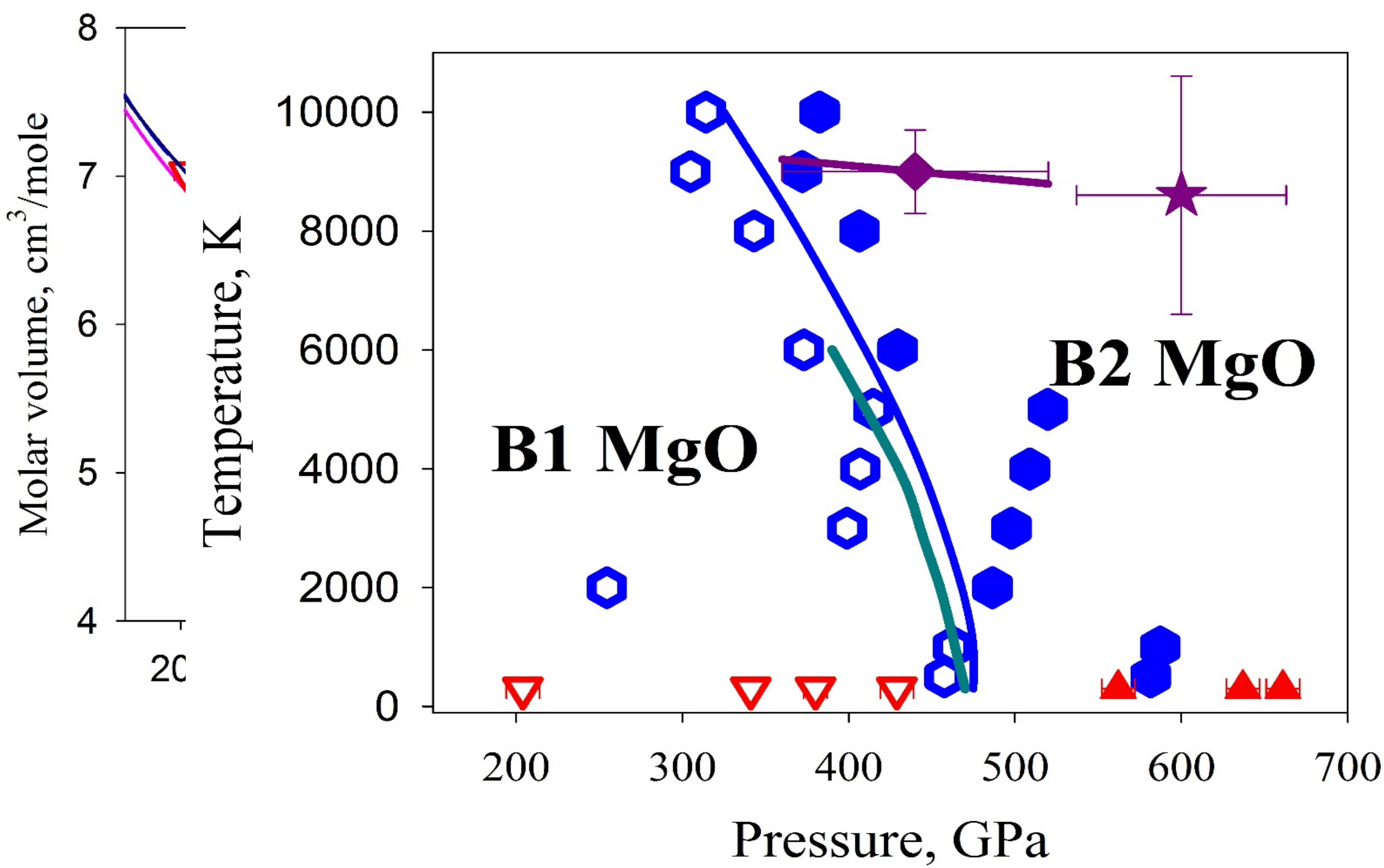

Dubrovinskaia et al., B1-B2 phase transition in MgO at ultra-high static pressure, PRX, revised

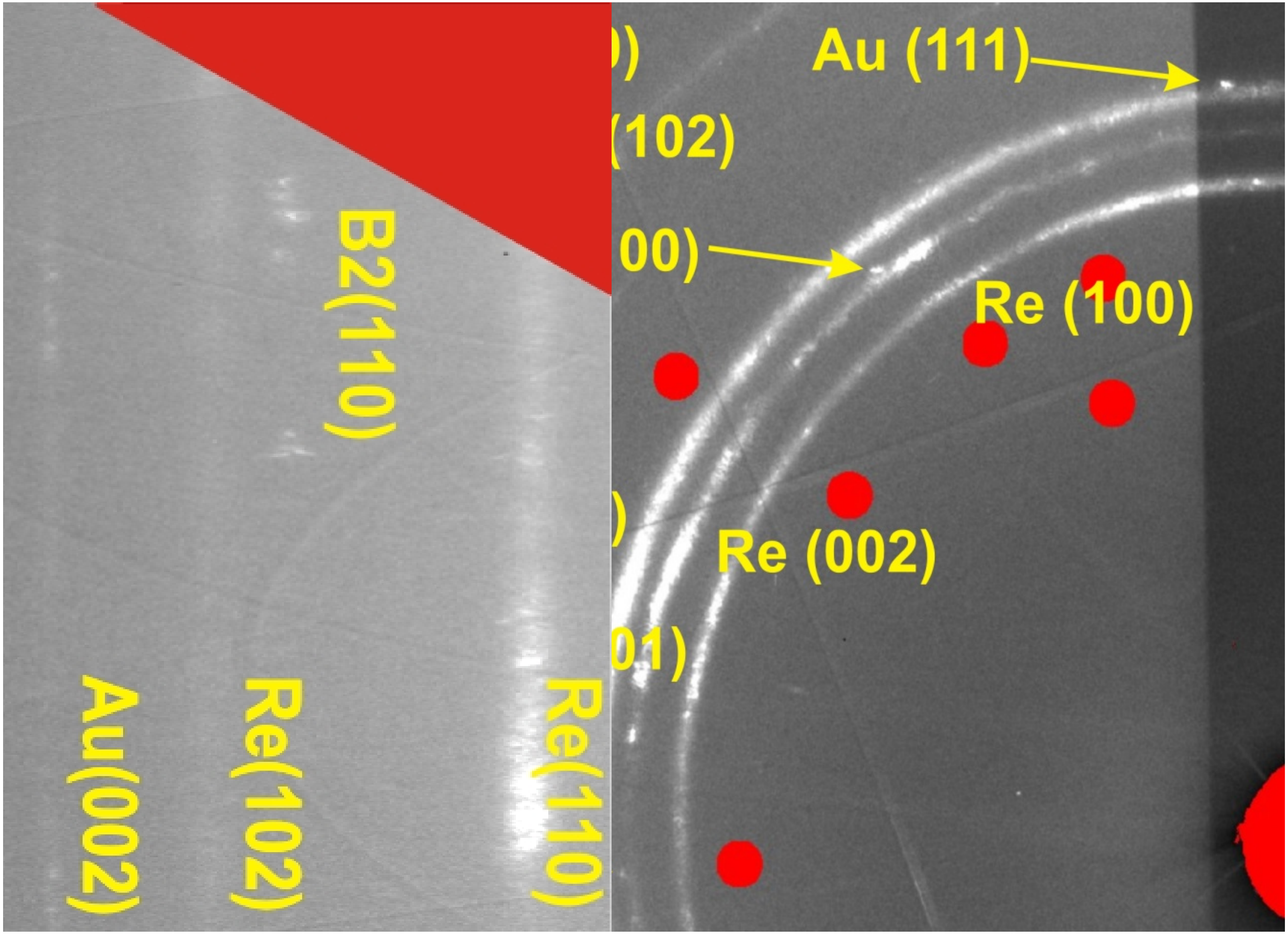

Dubrovinskaia et al., B1-B2 phase transition in MgO at ultra-high static pressure, PRX, revised

ARTICLE

DOI: 10.1038/s41467-018-05294-2

OPEN

Toroidal diamond anvil cell for detailed

ARTICLE

DOI: 10.1038/s41467-018-06071-x

OPEN

s

Single crystal toroidal diamond anvils for high pressure experiments beyond 5 megabar

Zs. Jenei[1], E.F. O'Bannon[1], S.T. Weir[1], H. Cynn[1], M.J. Lipp[1] & W.J. Evans[1]

Static compression experiments over 4 Mbar are rare, yet critical for developing accurate fundamental physics and chemistry models, relevant to a range of topics including modeling planetary interiors. Here we show that focused ion beam crafted toroidal single-crystal diamond anvils with ~9.0 μm culets are capable of producing pressures over 5 Mbar. The toroidal surface prevents gasket outflow and provides a means to stabilize the central culet. We have reached a maximum pressure of ~6.15 Mbar using Re as in situ pressure marker, a pressure regime typically accessed only by double-stage diamond anvils and dynamic compression platforms. Optimizing single-crystal diamond anvil design is key for extending the pressure range over which studies can be performed in the diamond anvil cell.

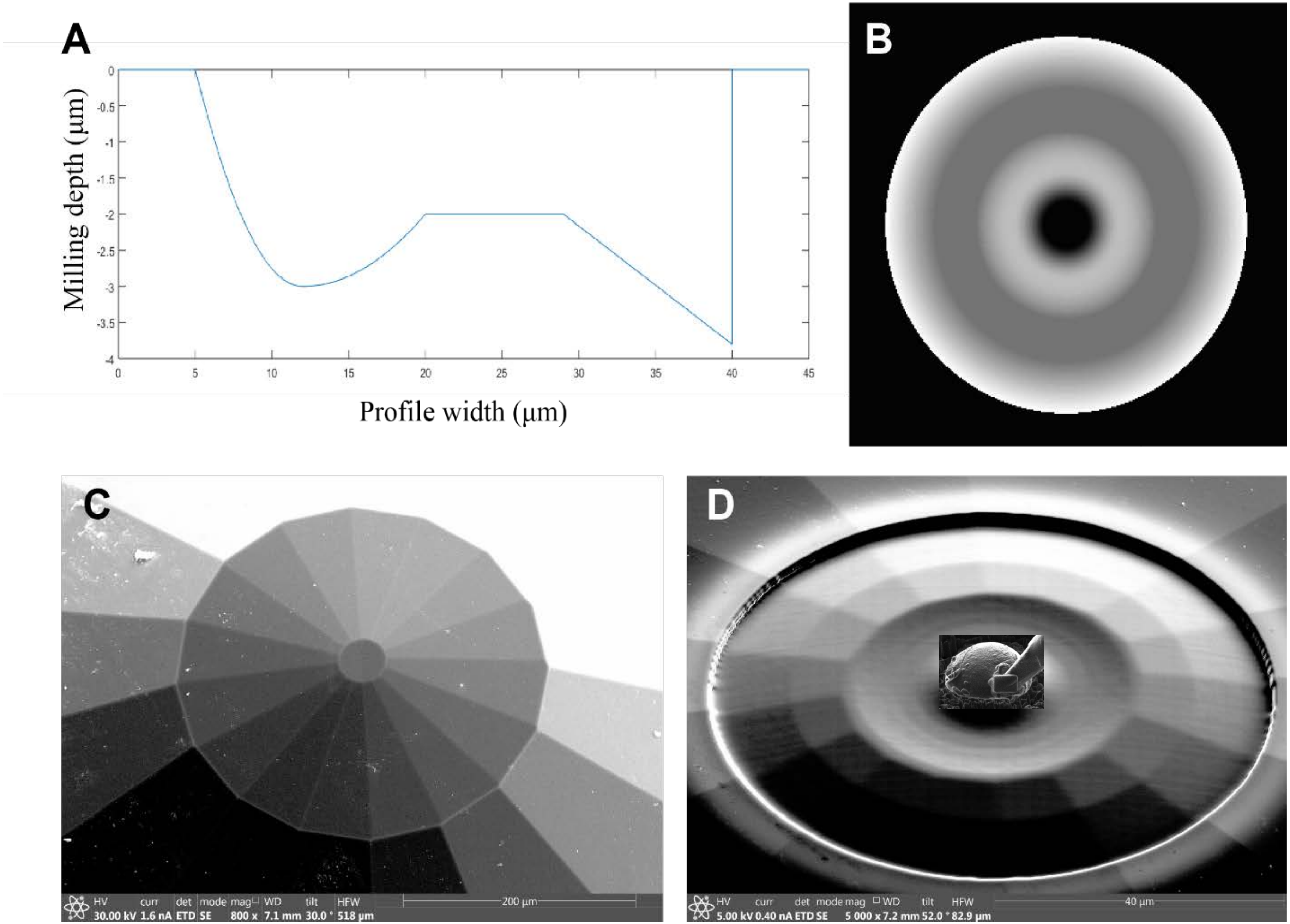

Pictures: S. Petitgirard

Pulsed laser heating in dsDAC

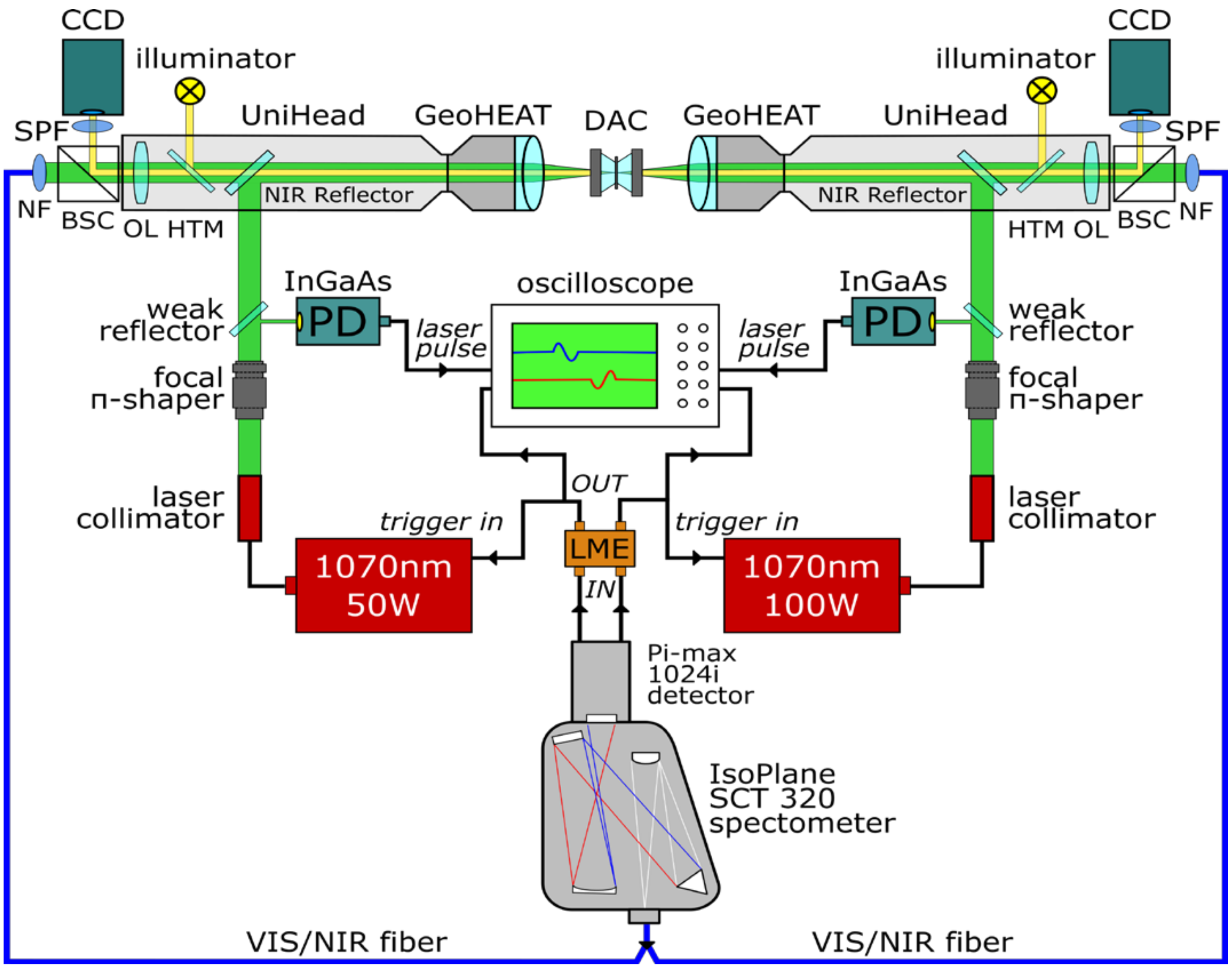

Aprilis et al., 2018

New LH setup design

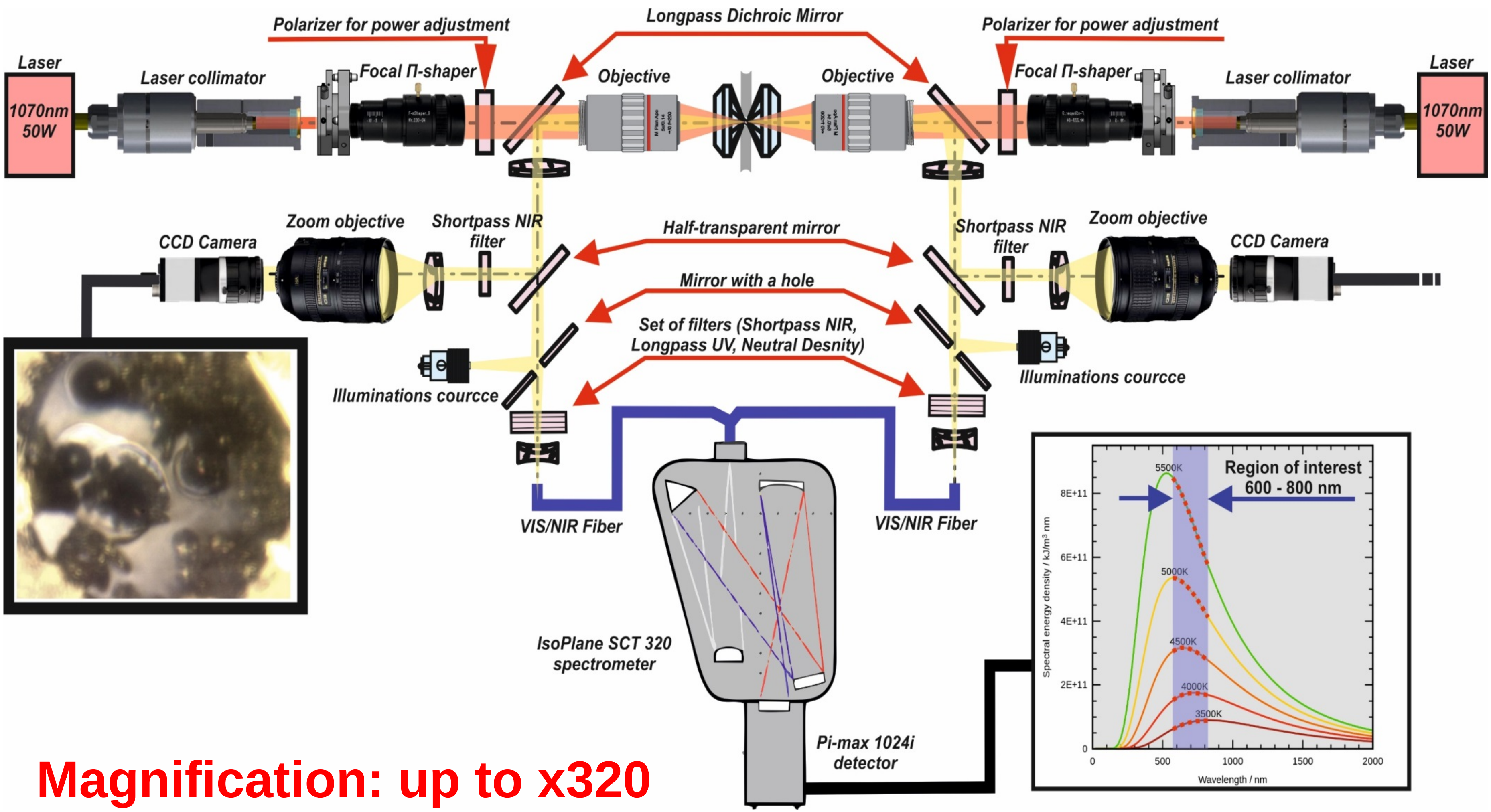

Magnification: up to x320
Beam-size: ~6 µm flat-top

Fedotenko et al., 2019; in preparation

Heating of Re-N in dsDAC

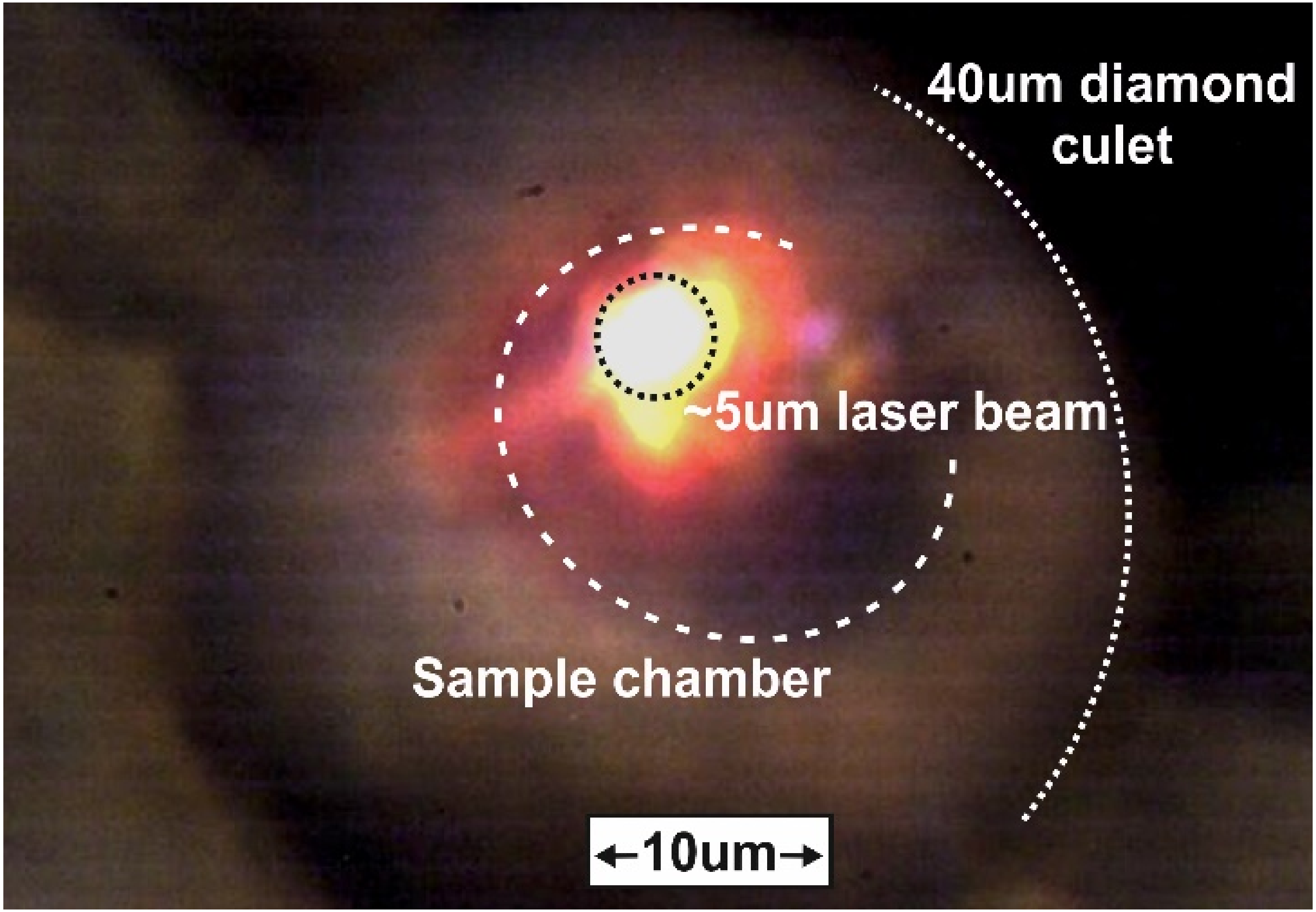

903(10) GPa (Anzellini et al., 2014)
1155(10) GPa (Dubrovinsky et al., 2012)

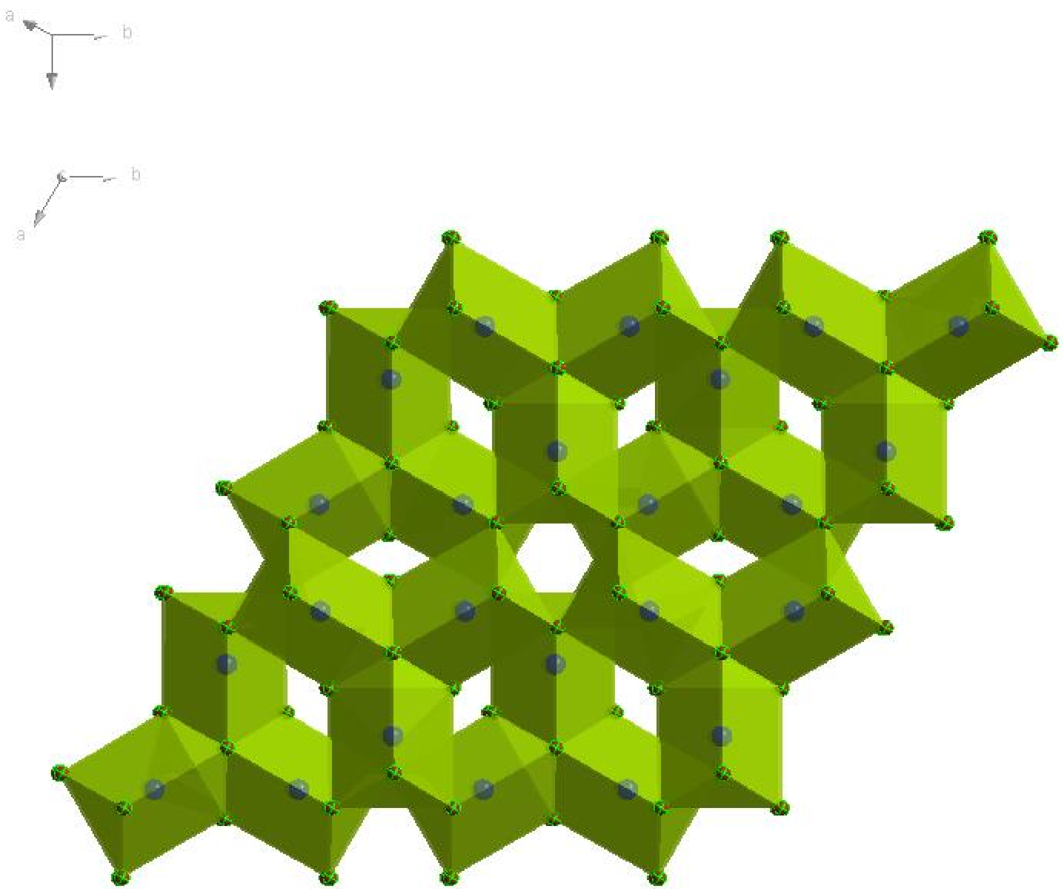

Re_7N_3

$P6_3mc$

a=6.278(2) Å

c=4.000(2) Å

V=136.57(9) Å^3

Z=2

394 reflections

Rint=2.8%

R1=7.1%

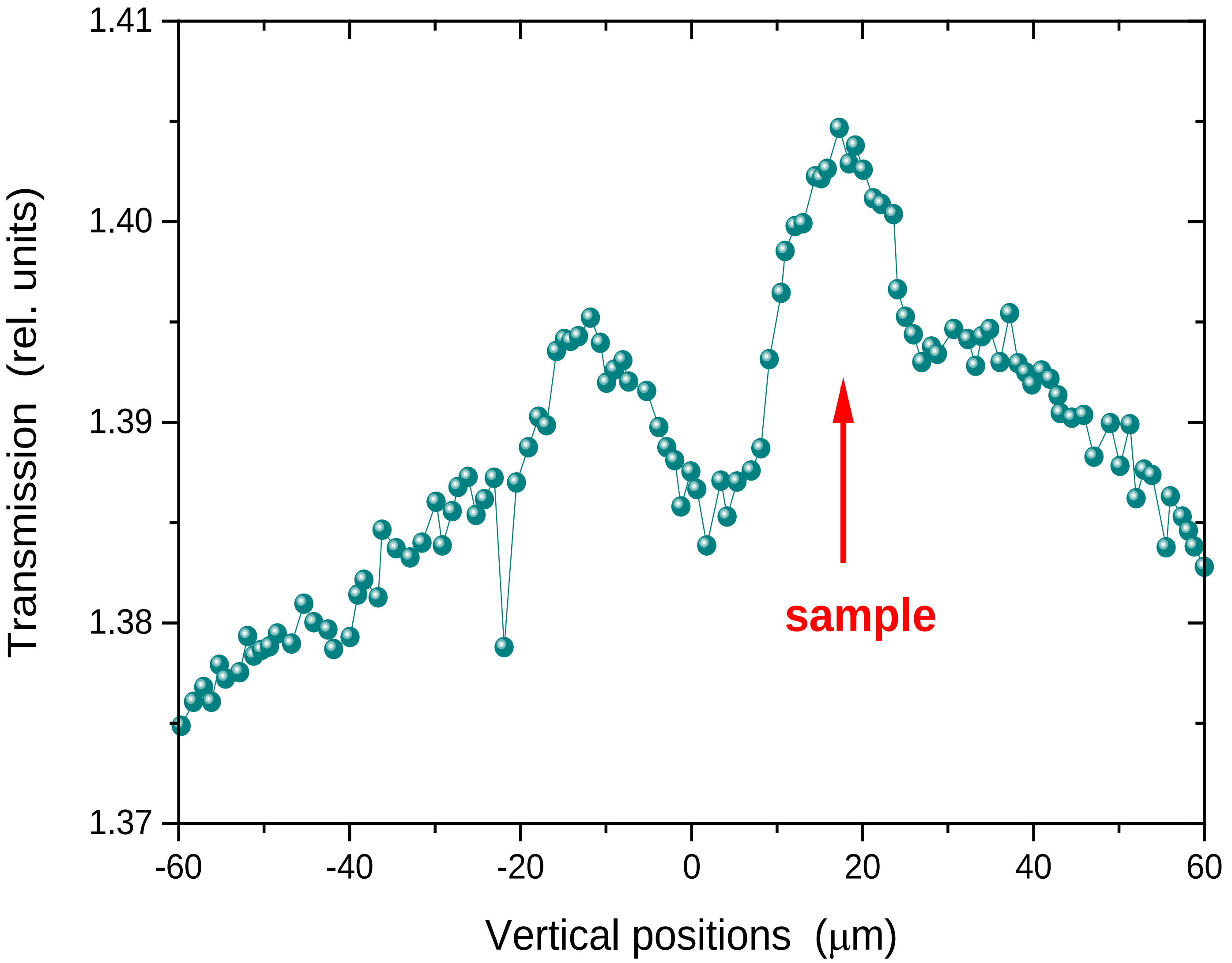

“Location of the ~2 μm sample inside the dsDAC chamber is possible. However, ~99% of radiation does not pass through the sample, precluding spectroscopy measurements.”

A. Chumakov, 2019

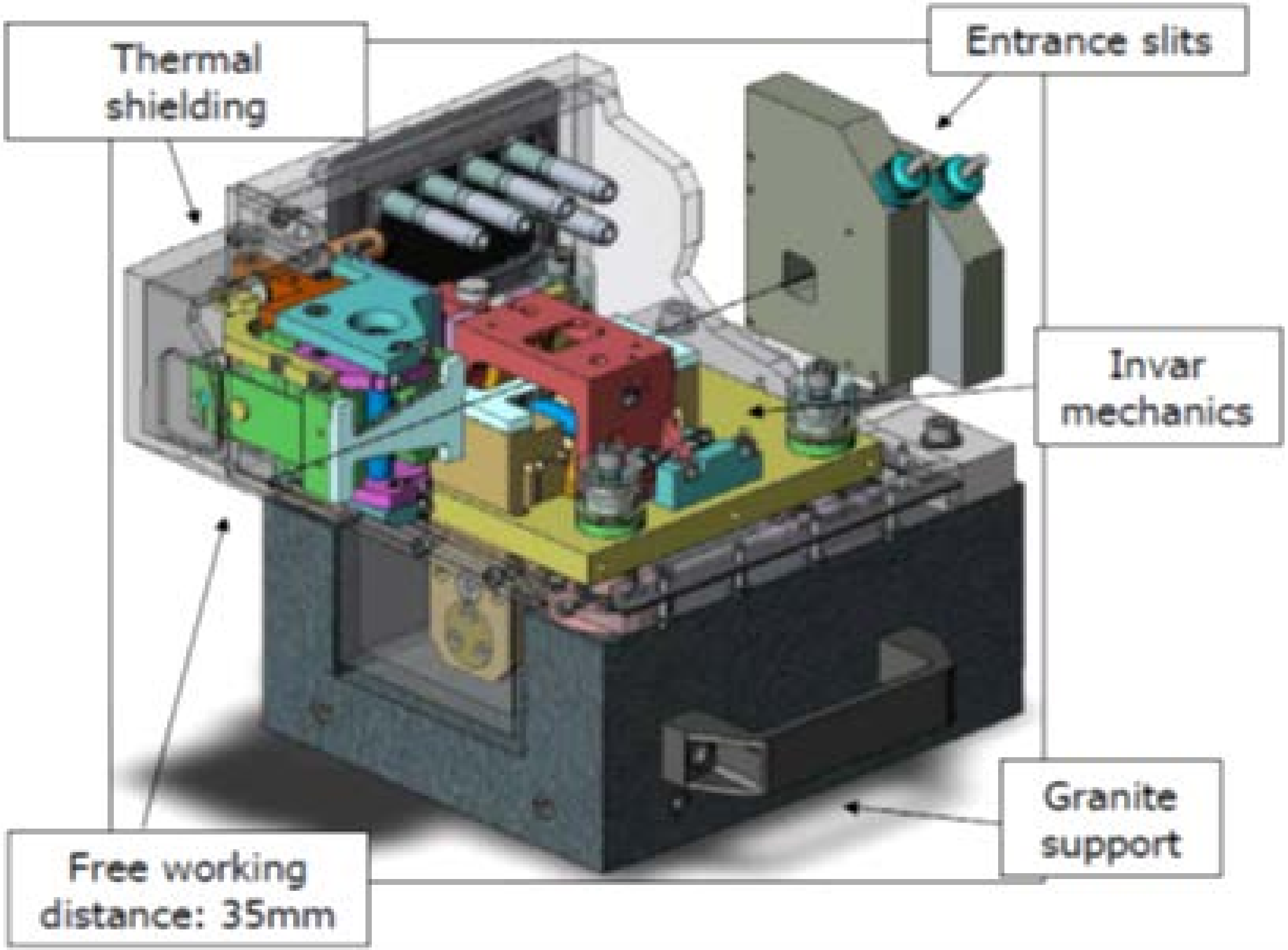

The typical setup of a short-focal-length KBM system

A. Chumakov, 2019

Acknowledgements

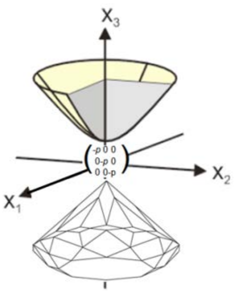

in incudibus veritas

G. Aprilis
E. Bykova
M. Bykov
S. Chariton
T. Fedotenko
S. Khandarkhaeva
E. Koemets
C. McCammon
S. Petitgirard

ID18, ID11, ID15, ID27, ID16, at ESRF
P02, P06 at PETRA III
IDD-13 at APS

UNIVERSITÄT BAYREUTH

BGI Bayerisches Geoinstitut

CarboPaT FOR2125

DESY

ARGONNE NATIONAL LABORATORY

GEFÖRDERT VOM Bundesministerium für Bildung und Forschung

DFG Deutsche Forschungsgemeinschaft

ESRF

Heisenberg-Programm Deutsche Forschungsgemeinschaft

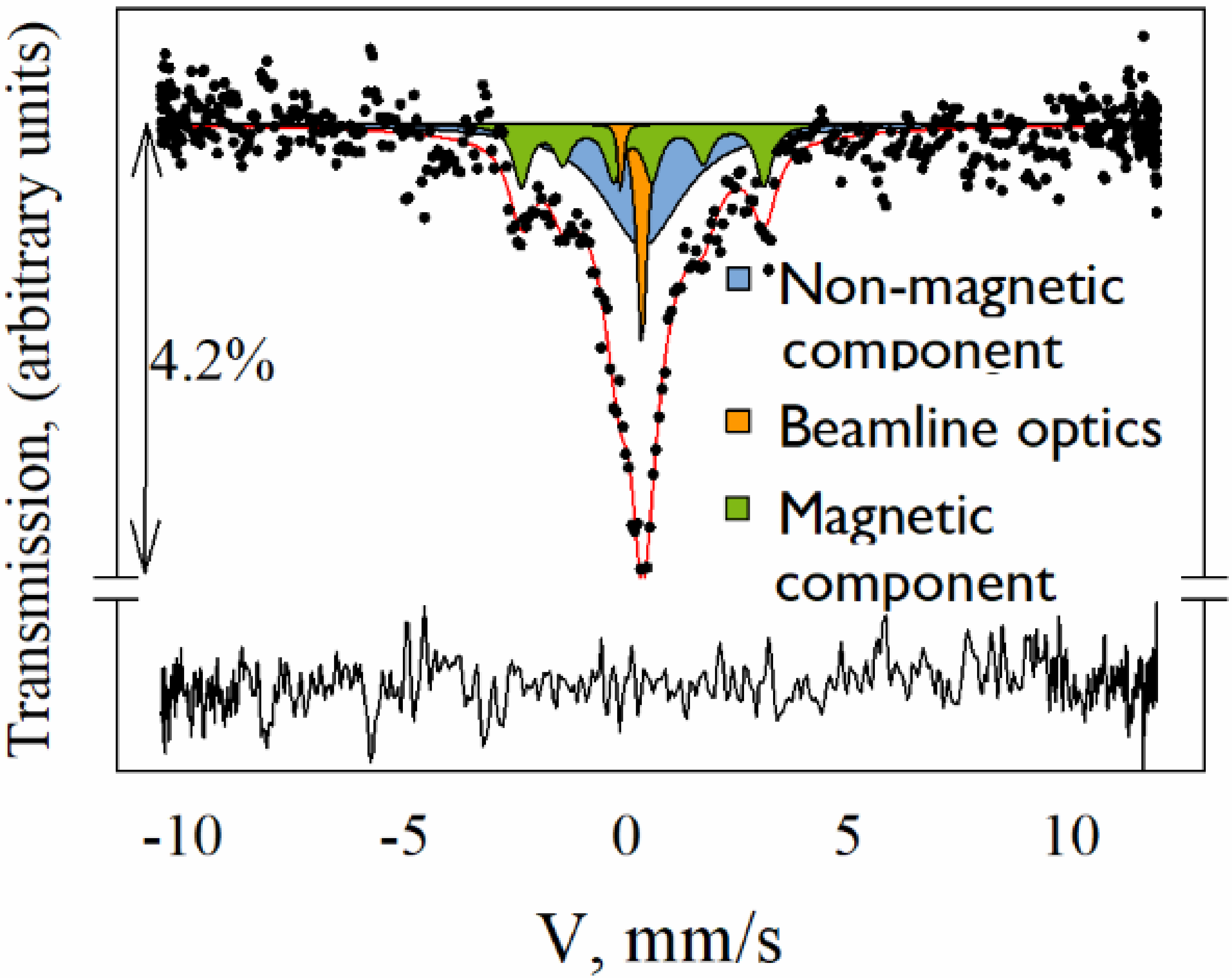
Transmission, (arbitrary units)
4.2%
Non-magnetic component
Beamline optics
Magnetic component
-10
-5
0
5
10
V, mm/s

High Pressure iron oxides in the presence of oxygen

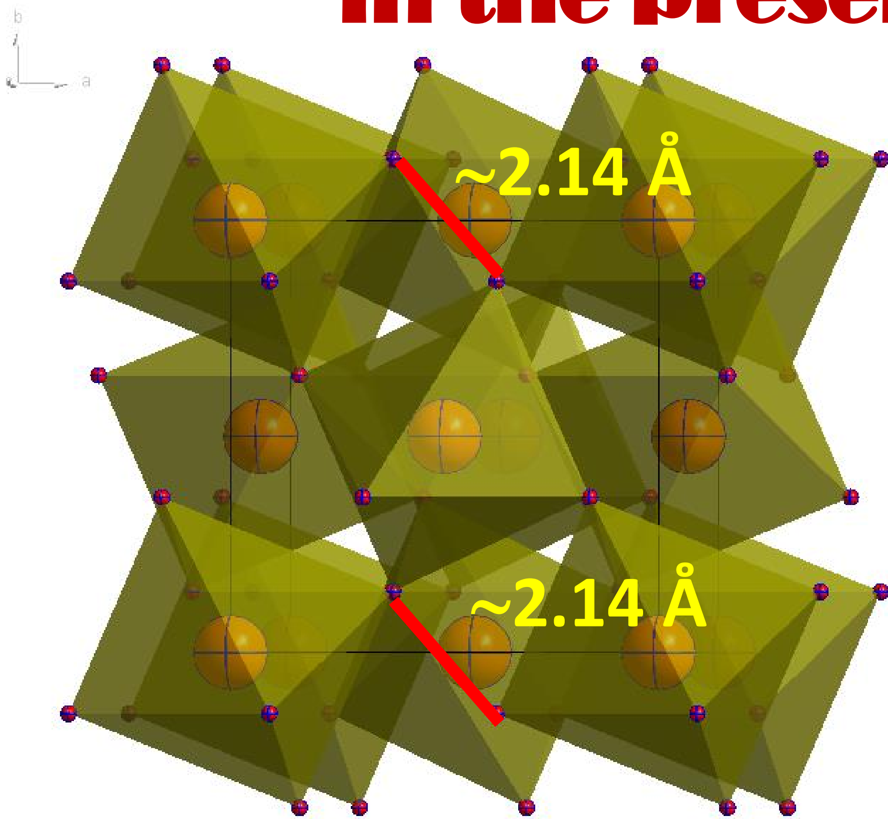

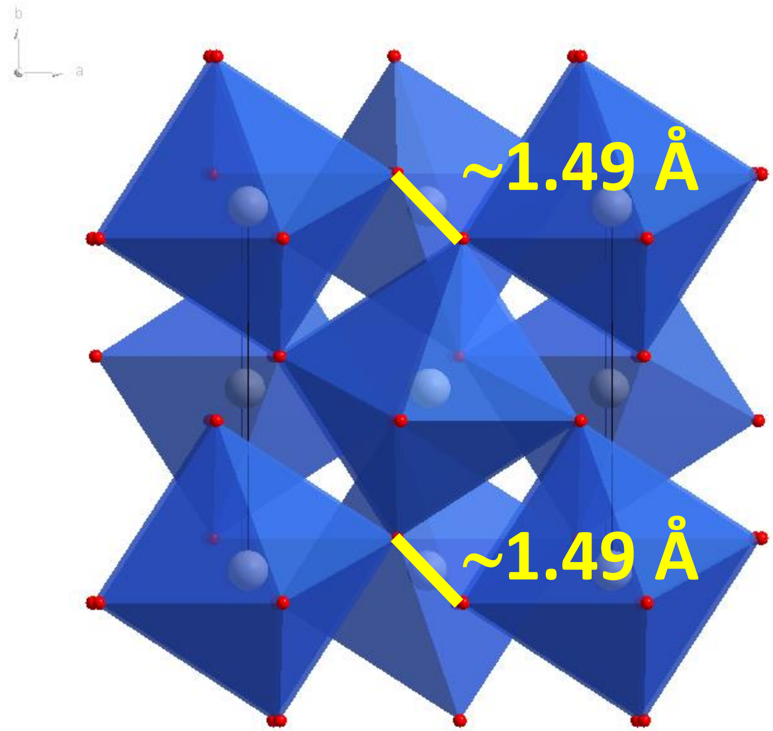

FeO_2, 68(1) GPa

HP-PdF_2-type structure

O^{2-}

MgO_2, 0 GPa

Pyrite-type structure

O_2^{2-}

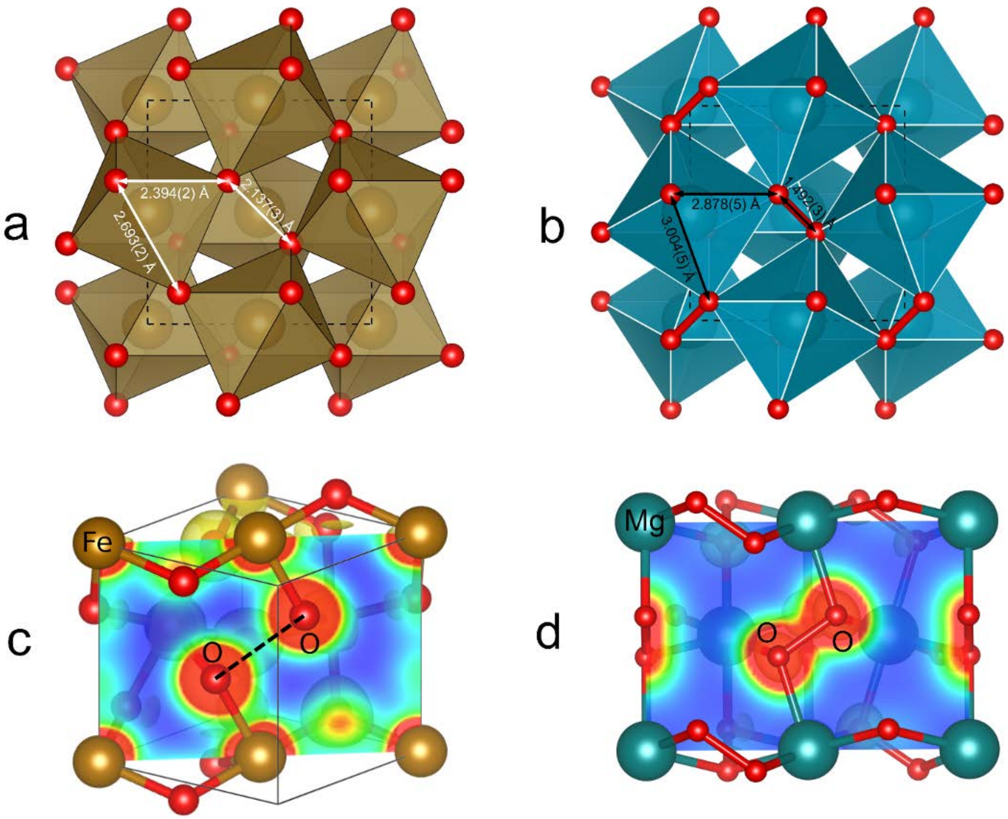

a
2.394(2) Å
2.137(3) Å
2.693(2) Å
b
2.878(5) Å
1.492(3) Å
3.004(5) Å
c
Fe
O
O
d
Mg
O
O

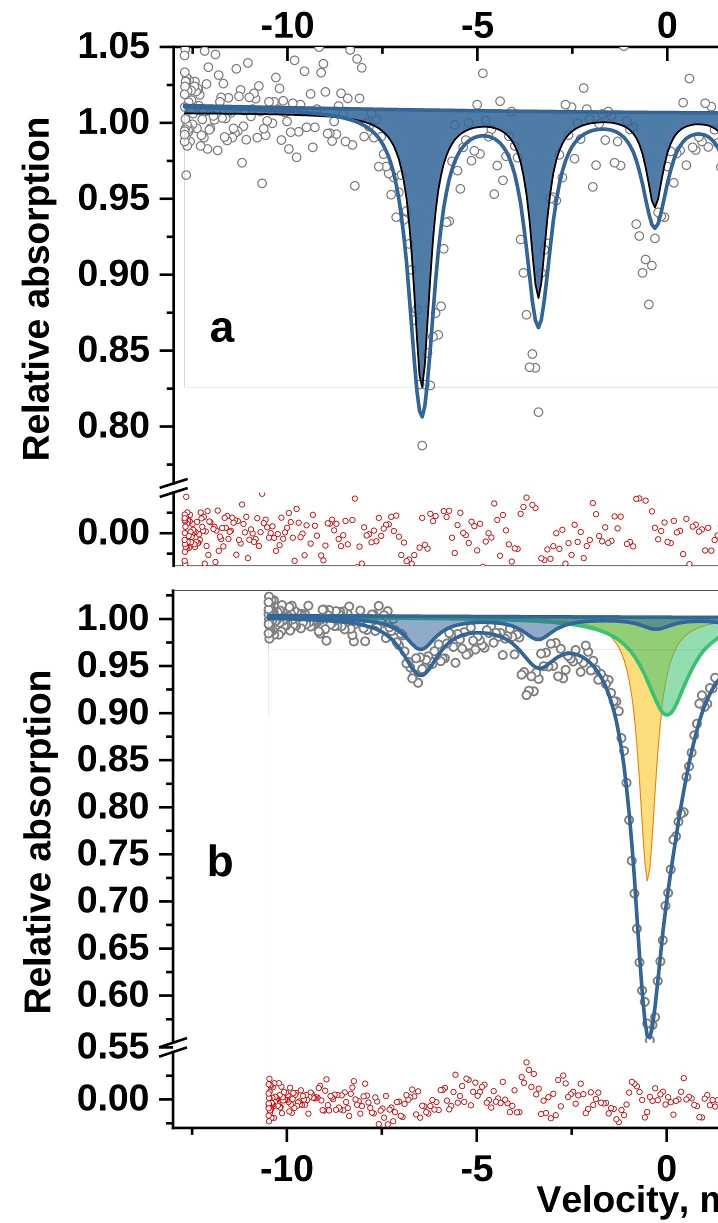

-10
-5
0
1.05
1.00
0.95
0.90
0.85
0.80
0.00
Relative absorption
a
1.00
0.95
0.90
0.85
0.80
0.75
0.70
0.65
0.60
0.55
0.00
Relative absorption
b
-10
-5
0

(Hirose and Lay, *Elements*, 2008)

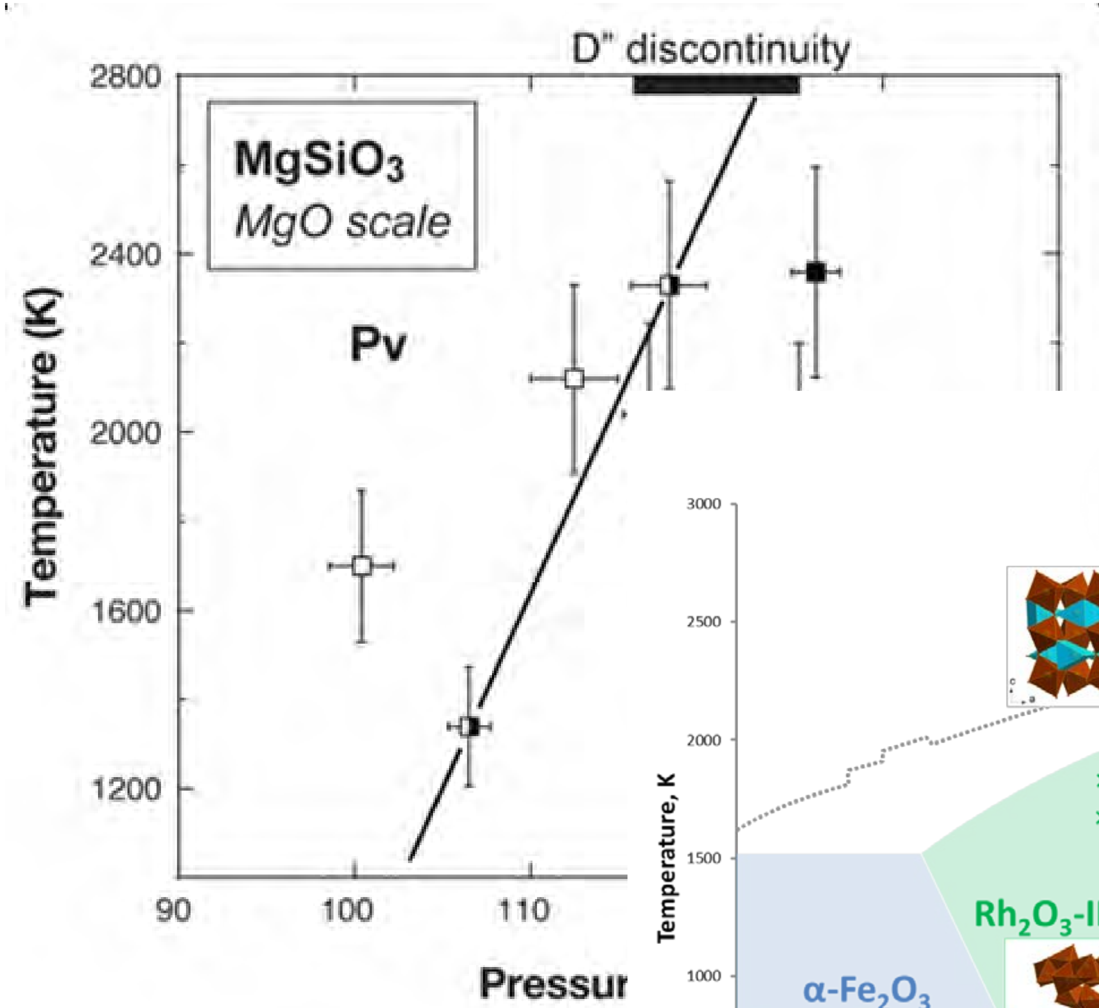

Fe_2O_3

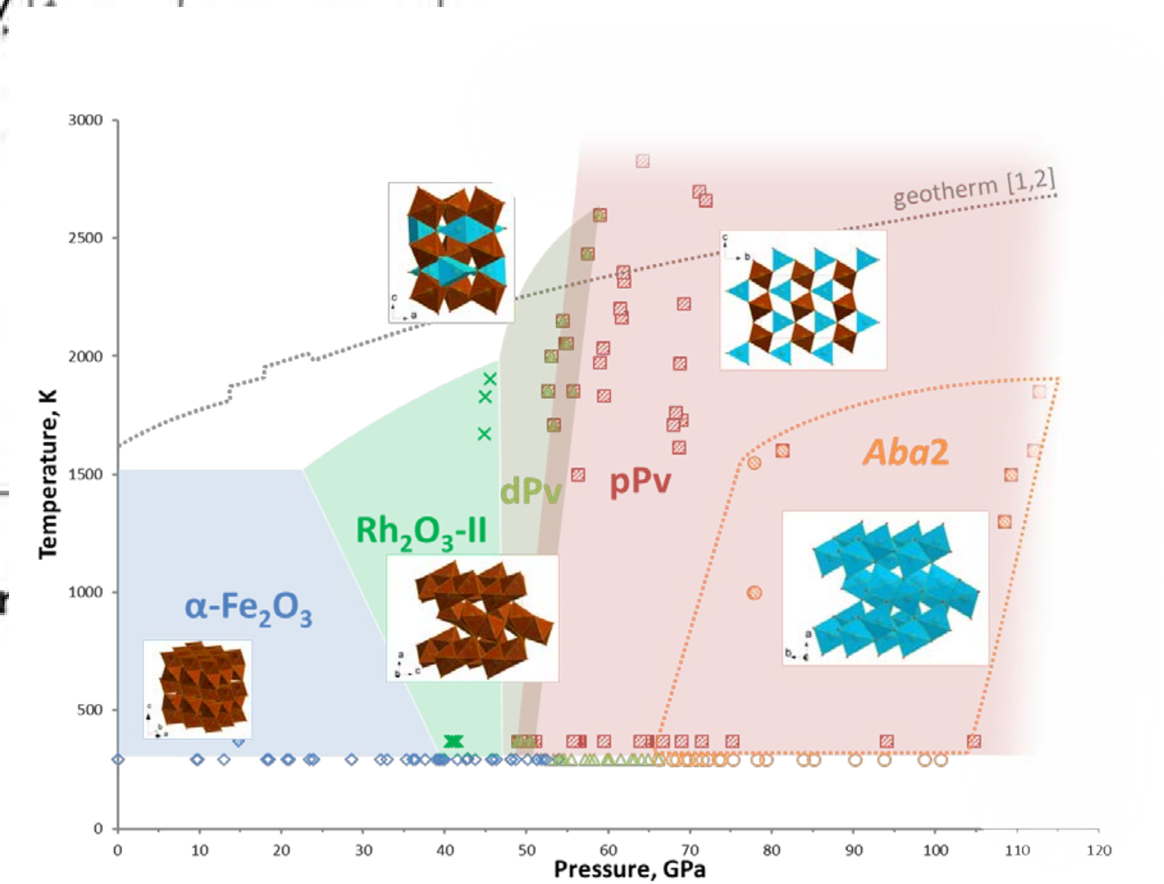

E. Bykova (2016), Nat. Commun.**7** (2016)
(DOI:/10.1038/ncomms10661).

Stability of PPv-Fe_2O_3 up to 200 GPa and 3000 K

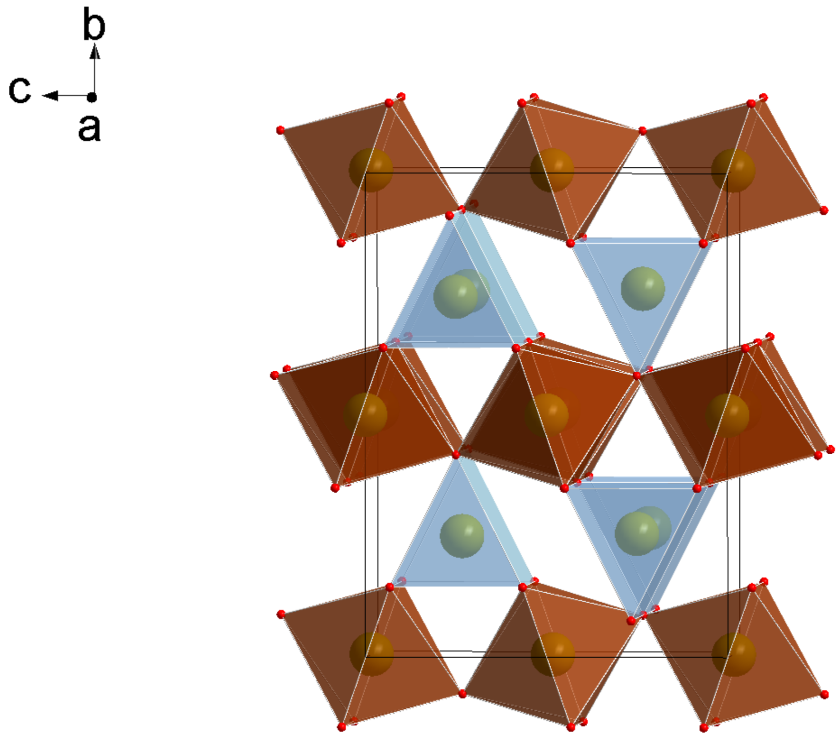

PPv-Fe_2O_3

Cmcm

a=2.5134(8) Å

b=8.1328(12) Å

c=6.073(3) Å

V=124.14(7) Å^3

Z=4

R1=7.1%

Decomposition of Fe_2O_3 at 187 GPa and 3000 K

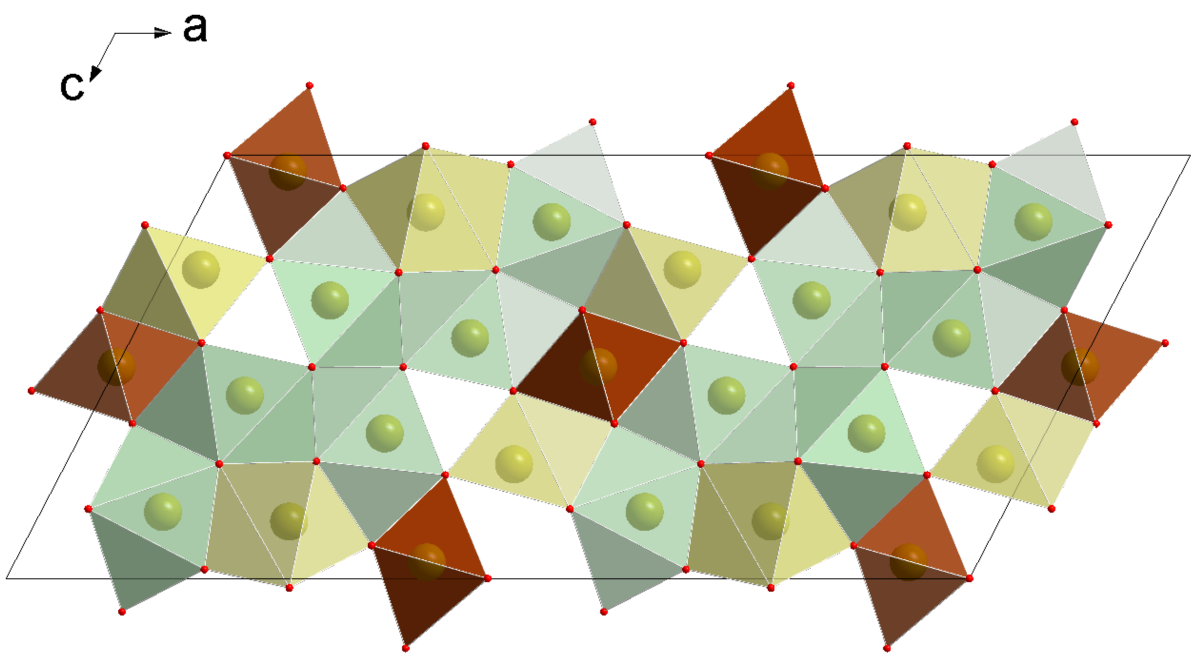

$Fe_{13}O_{19}$

C2/m

a=18.9445 (18) Å

b=2.5297 (13) Å

c=9.393 (11) Å

β=117.57˚ (3)

V=399.1 (5) $Å^3$

Z=2

R1=5.9%

M. Merlini (2015), Am. Min, Vol. **100**, 2001–2004

Decomposition of Fe_2O_3 at 187 GPa and 3000 K

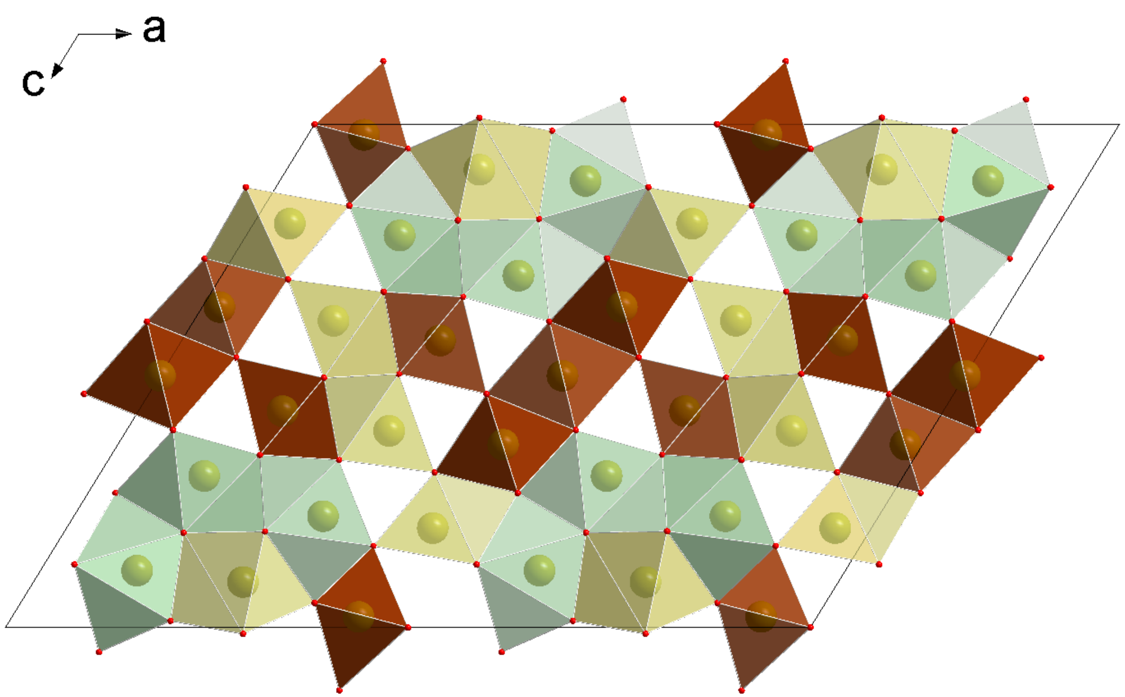

$Fe_{19}O_{27}$

C2/m

a=19.001 (3) Å

b=2.5464 (16) Å

c=13.932 (3) Å

β =121.57 ˚ (2)

V=574.3 (4) $Å^3$

R1=9.5%

Decomposition of Fe_2O_3 with formation of Fe_3O_4 at pressures 187-213 GPa

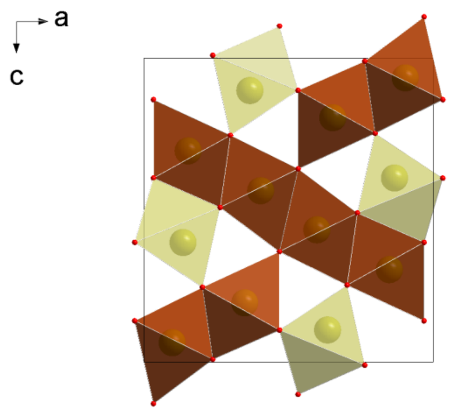

$CaTi_2O_4$-type

Fe_3O_4
Pnma
a=7.991 (3) Å
b=2.5965 (5) Å
c=8.384 (2) Å
V=173.95 (8) Å^3
Z=4

R1=5.3%

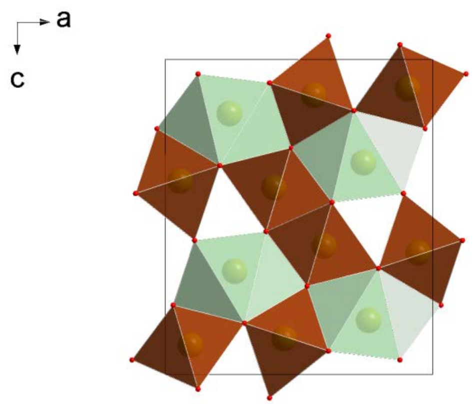

$CaFe_2O_4$-type

Fe_3O_4
Pnma
a=7.796 (5) Å
b=2.4369 (6) Å
c=9.1831 (19) Å
V=174.47 (13) Å^3
Z=4

R1=9.9%

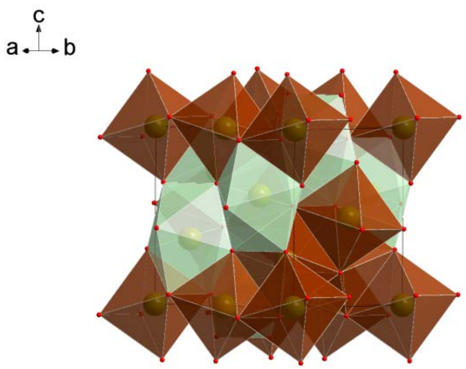

distorted Th_3P_4 -type

Fe_3O_4
$I4_1/amd$
a=5.576 (2),
b=5.622 (2)
V=174.81 (11)
Z=4

R1=4%

Chemical reactions of decomposition of Fe_2O_3 at pressures above 200 GPa

$13 \cdot Fe_2O_3 \rightarrow 2 \cdot Fe_{13}O_{19} + 0.5 \cdot O_2$

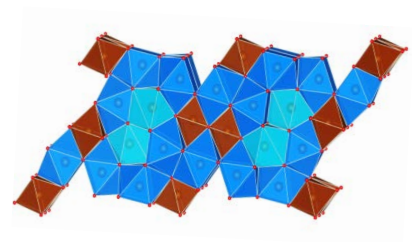

$Fe_{13}O_{19}$

$19 \cdot Fe_2O_3 \rightarrow 2 \cdot Fe_{19}O_{27} + 1.5 \cdot O_2$

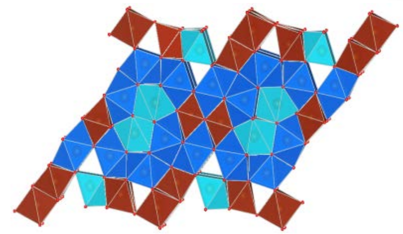

$Fe_{19}O_{27}$

$3 \cdot Fe_2O_3 \rightarrow 2 \cdot Fe_3O_4 + 0.5 \cdot O_2$

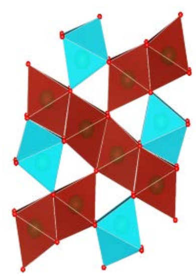

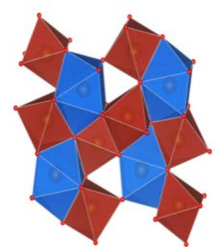

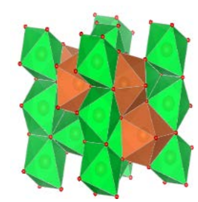

Fe_3O_4

JOURNAL OF APPLIED PHYSICS **118**, 035905 (2015)

Pressure, stress, and strain distribution in the double-stage diamond anvil cell

Sergey S. Lobanov,[1,2,a)] Vitali B. Prakapenka,[3] Clemens Prescher,[3] Zuzana Konôpková,[4] Hanns-Peter Liermann,[4] Katherine L. Crispin,[1] Chi Zhang,[5] and Alexander F. Goncharov[1,6,7]

P max 240 GPa

Microcrystalline CVD- diamond

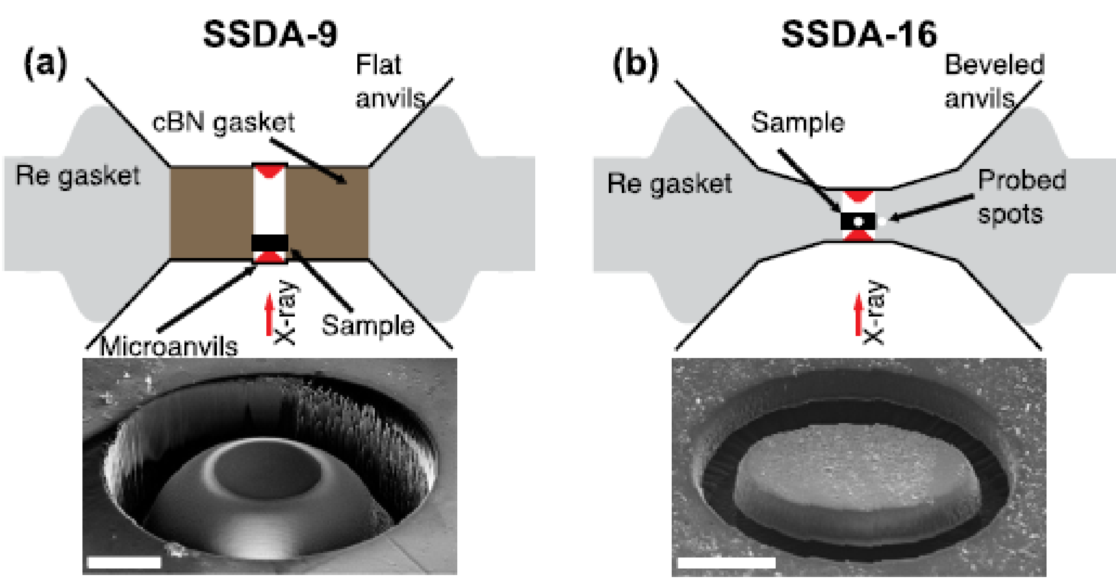

FIG. 1. Type-1 (a) and type-2 (b) DAC assemblage (top) and SEM micrographs of the SSDA (bottom) in the CVD substrate before placing on the first stage anvils. White bars in SEM images correspond to 10 μm.

"A **maximum pressure of 240 GPa** was reached independent of the first stage anvil culet size. We found that **the stress field generated by the second stage anvils is typical of conventional DAC experiments**. The maximum pressures reached are limited by strains developing in the secondary anvil and by cupping of the first stage diamond anvil in the presented experimental designs. Also, our experiments show that **pressures of several megabars may be reached without sacrificing the first stage diamond anvils.**"

REVIEW OF SCIENTIFIC INSTRUMENTS **86**, 033905 (2015)

High-pressure generation using double stage micro-paired diamond anvils shaped by focused ion beam

Takeshi Sakai,[1,a)] Takehiko Yagi,[2] Hiroaki Ohfuji,[1] Tetsuo Irifune,[1,3] Yasuo Ohishi,[4] Naohisa Hirao,[4] Yuya Suzuki,[5] Yasushi Kuroda,[5] Takayuki Asakawa,[5] and Takashi Kanemura[5]
[1]*Geodynamics Research Center, Ehime University, Matsuyama 790-8577, Japan*
[2]*Geochemical Research Center, Graduate School of Science, The University of Tokyo, Tokyo 113-0033, Japan*
[3]*Earth-Life Science Institute, Tokyo Institute of Technology, Tokyo 152-8550, Japan*
[4]*Japan Synchrotron Radiation Research Institute, Hyogo 679-5198, Japan*
[5]*HITACHI High-Technologies, Hitachinaka 312-0033, Japan*

(Received 20 January 2015; accepted 28 February 2015; published online 17 March 2015)

Micron-sized diamond anvils with a 3 μm culet were successfully processed using a focused ion beam (FIB) system and the generation of high pressures was confirmed using the double stage diamond anvil cell technique. The difficulty of aligning two second-stage micro-anvils was solved via the paired micro-anvil method. Micro-manufacturing using a FIB system enables us to control anvil shape, process any materials, including nano-polycrystalline diamond and single crystal diamond, and assemble the sample exactly in a very small space between the second-stage anvils. This method is highly reproducible. High pressures over 300 GPa were achieved, and the pressure distribution around the micro-anvil culet was evaluated by using a well-focused synchrotron micro-X-ray beam. © *2015 AIP Publishing LLC.* [http://dx.doi.org/10.1063/1.4914844]

P over 300 GPa

NPD – nano-polycrystalline diamond *(Irifune et al. Phys. Earth Planet. Inter. (2014))*
SD- single crystal diamond

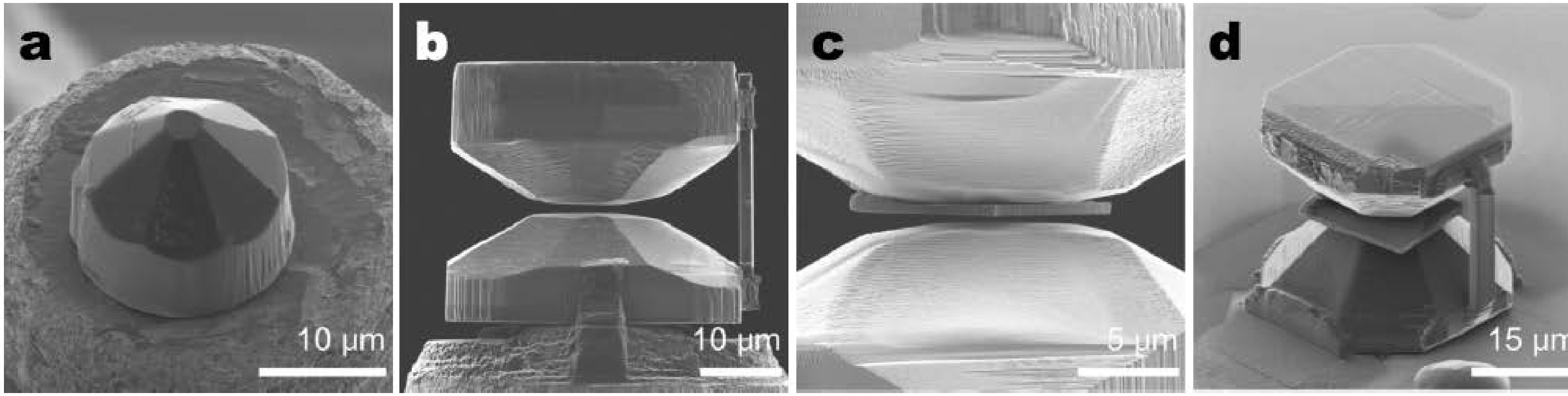

FIG. 1. (a) SIM image of the NPD micro-anvil (nonbeveled) (Run Micro01). (b) SIM image of the paired NPD micro-anvil (beveled) (Run Micro03). (c) Close-up view of platinum sample (Run Micro03). (d) SIM image of the paired SC micro-anvil (beveled) with platinum sample on the first-stage anvil (Run Micro04).

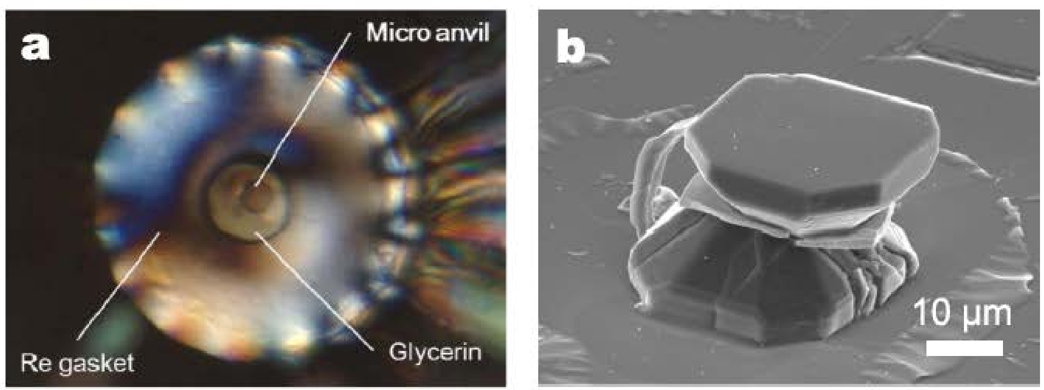

FIG. 8. (a) Microscopic image of the sample chamber before compression (Run Micro04). (b) Scanning electron microscopy image of the recovered sample (60° tilted).

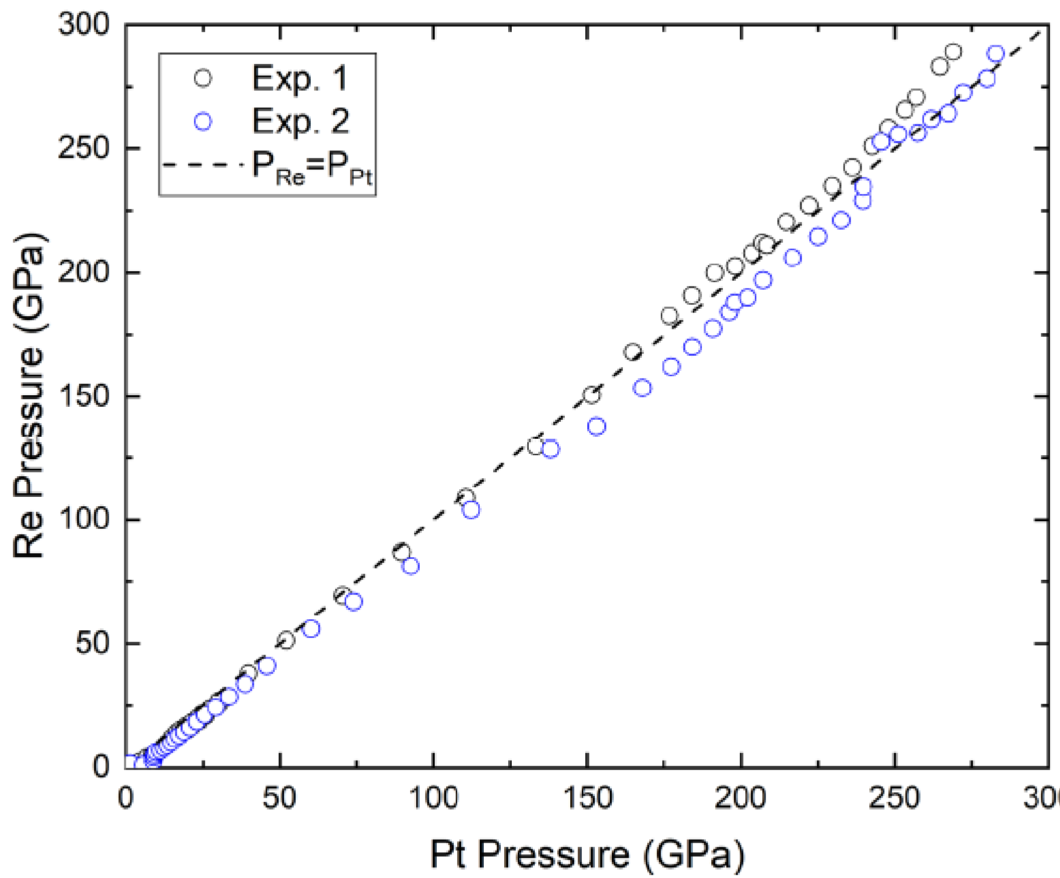

Figure S1. Pressure of the central culet area determined by the Re scale reported by Dubrovinsky et al.[4] as a function of the pressure determined by the Pt scale reported by Yokoo et al.[3]. The dashed line corresponds to $P_{Re}=P_{Pt}$. In one Pt experiment the maximum pressure determined by the Pt scale reported by Yokoo et al.[3] is less than 10 GPa higher than the pressure determined by the Re scale reported by Dubrovinsky et al.[4]. In the other Pt experiment the Re scale shows a pressure ~10 GPa higher than the Pt scale. Also note that we compared the Pt scales of Holmes et al.[5] and Yokoo et al.[3] and the difference at the maximum pressure of both the Pt experiments is < 4 GPa.

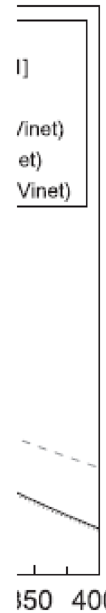

amonds are data obtained using a
and Yokoo et al.'s platinum scale
e ds-DAC based on Yokoo et al.'s
ırves are compression curves of
ɔrovinsky et al. [1], and Anzellini

Jenei et al., 2018

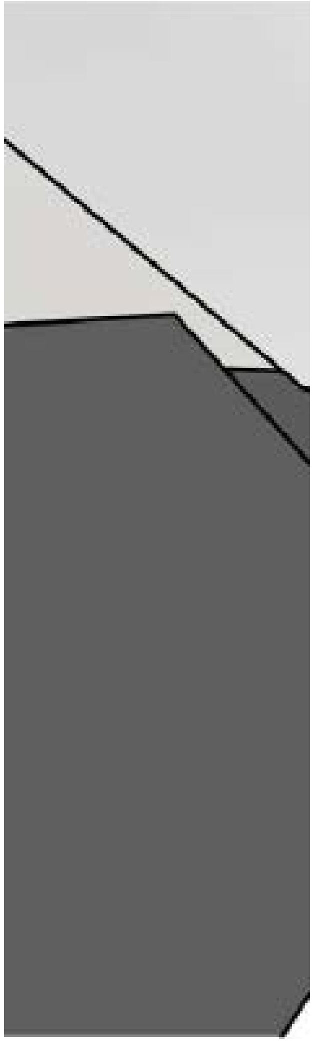

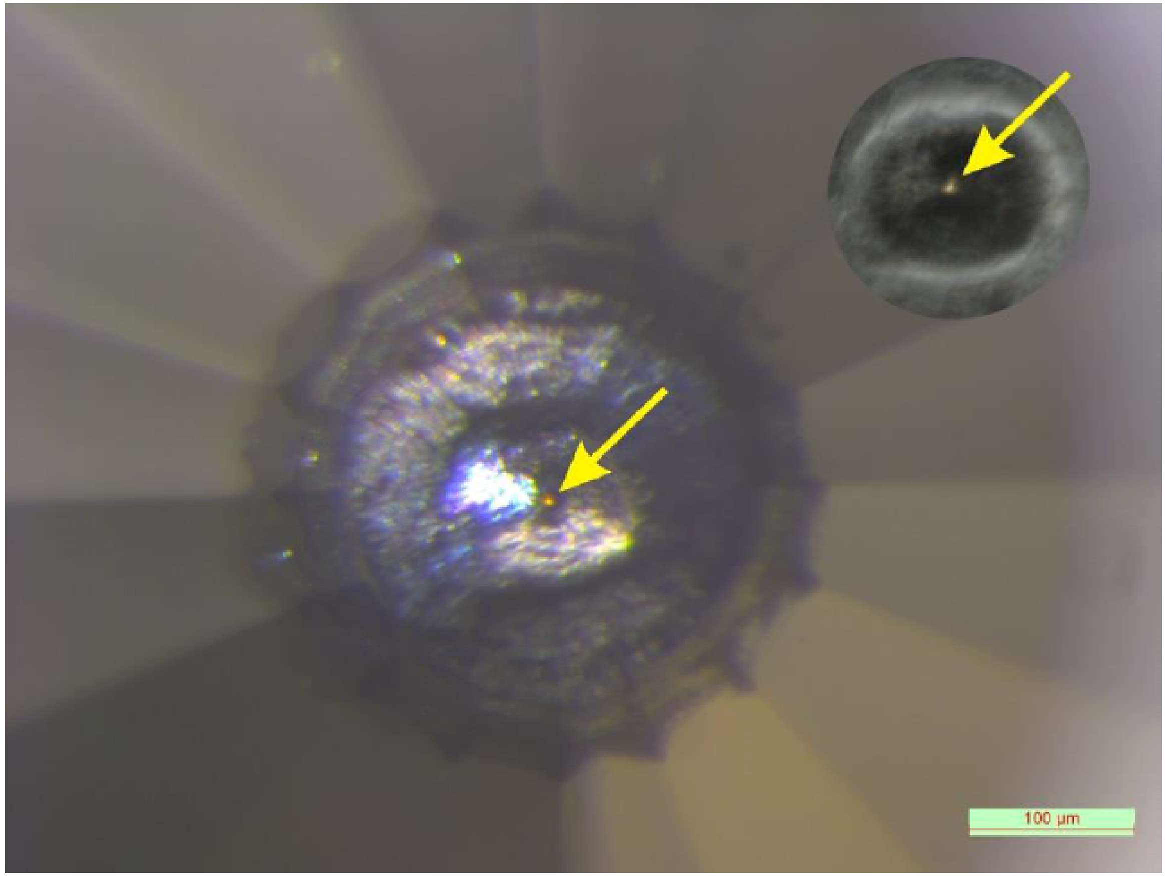

fig. S5. Optical photograph of the sample (Au and paraffin wax) compressed in a gasketed ds-DAC at 688(10) GPa, as seen through the diamonds and NCD secondary anvils. The size of the pressure chamber is of about 5 µm and gold occupies only a portion of it. As a result, one can clearly see the transmitted light (pointed out by the yellow arrow) passing through the material (paraffin wax) that confirms that NCD remains optically transparent even at such high pressures. Insert in the upper right corner shows the central part of the gasket and the pressure chamber under just slight illumination by the reflected light.

Dubrovinskaia et al., Sci Adv., 2016

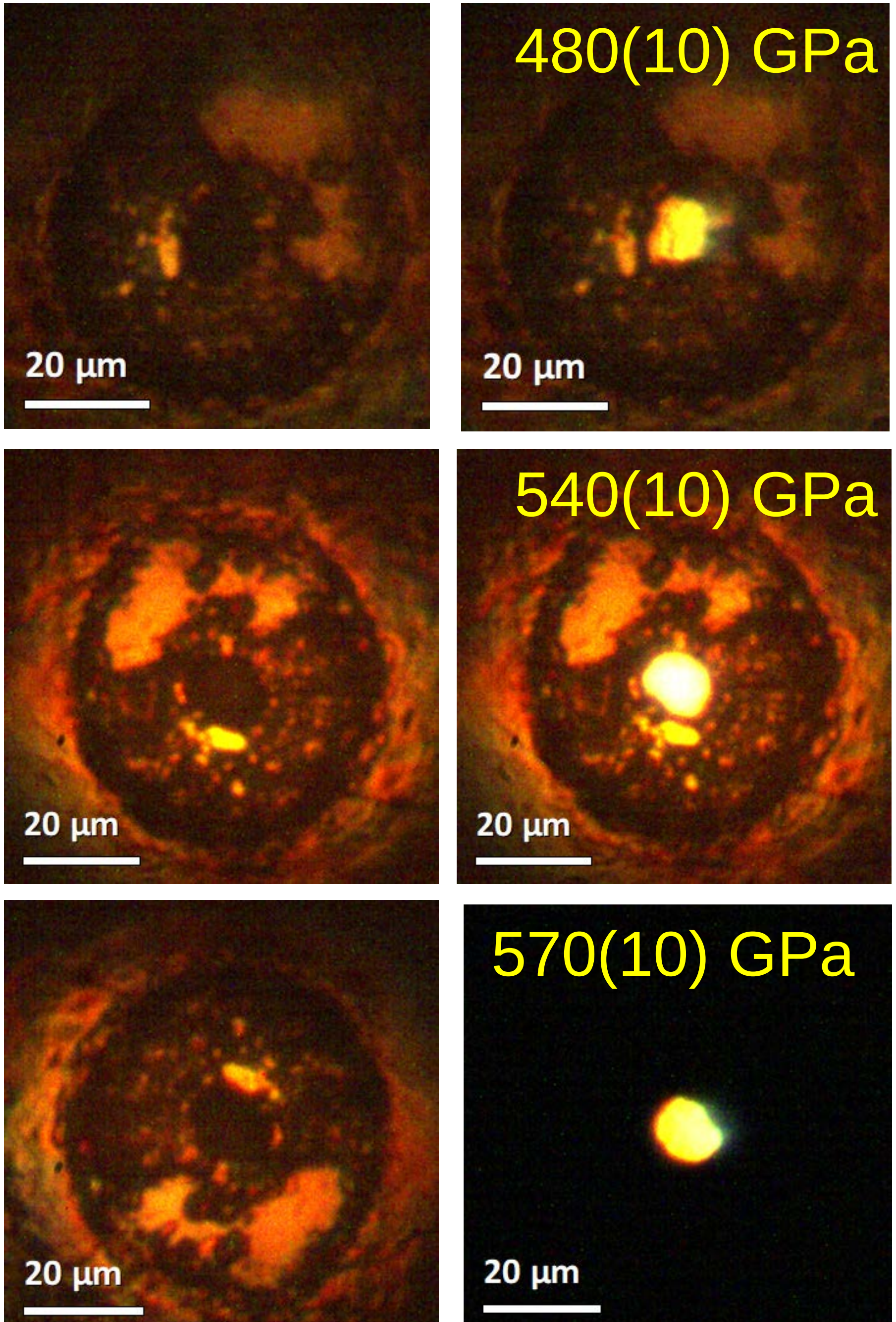
480(10) GPa
540(10) GPa
570(10) GPa
20 µm
20 µm
20 µm
20 µm
20 µm
20 µm

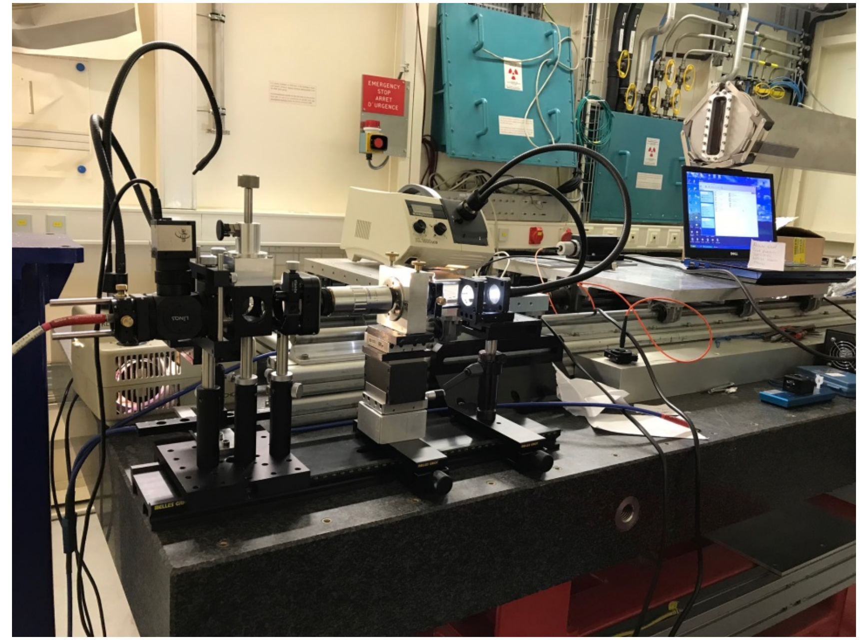

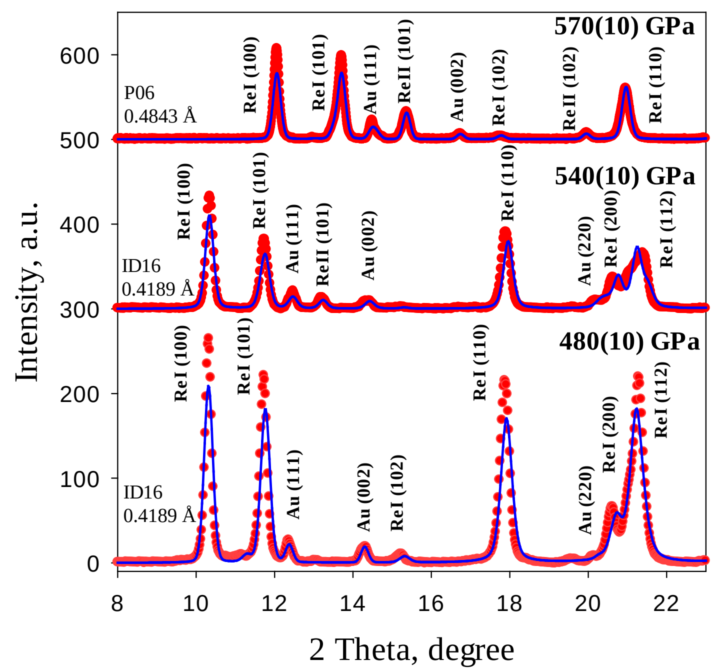
570(10) GPa
P06
0.4843 Å
ReI (100)
ReI (101)
Au (111)
ReII (101)
Au (002)
ReI (102)
ReII (102)
ReI (110)
540(10) GPa
ID16
0.4189 Å
ReI (100)
ReI (101)
Au (111)
ReII (101)
Au (002)
ReI (110)
Au (220)
ReI (200)
ReI (112)
480(10) GPa
ID16
0.4189 Å
ReI (100)
ReI (101)
Au (111)
Au (002)
ReI (102)
ReI (110)
Au (220)
ReI (200)
ReI (112)
Intensity, a.u.
0
100
200
300
400
500
600
8
10
12
14
16
18
20
22
2 Theta, degree

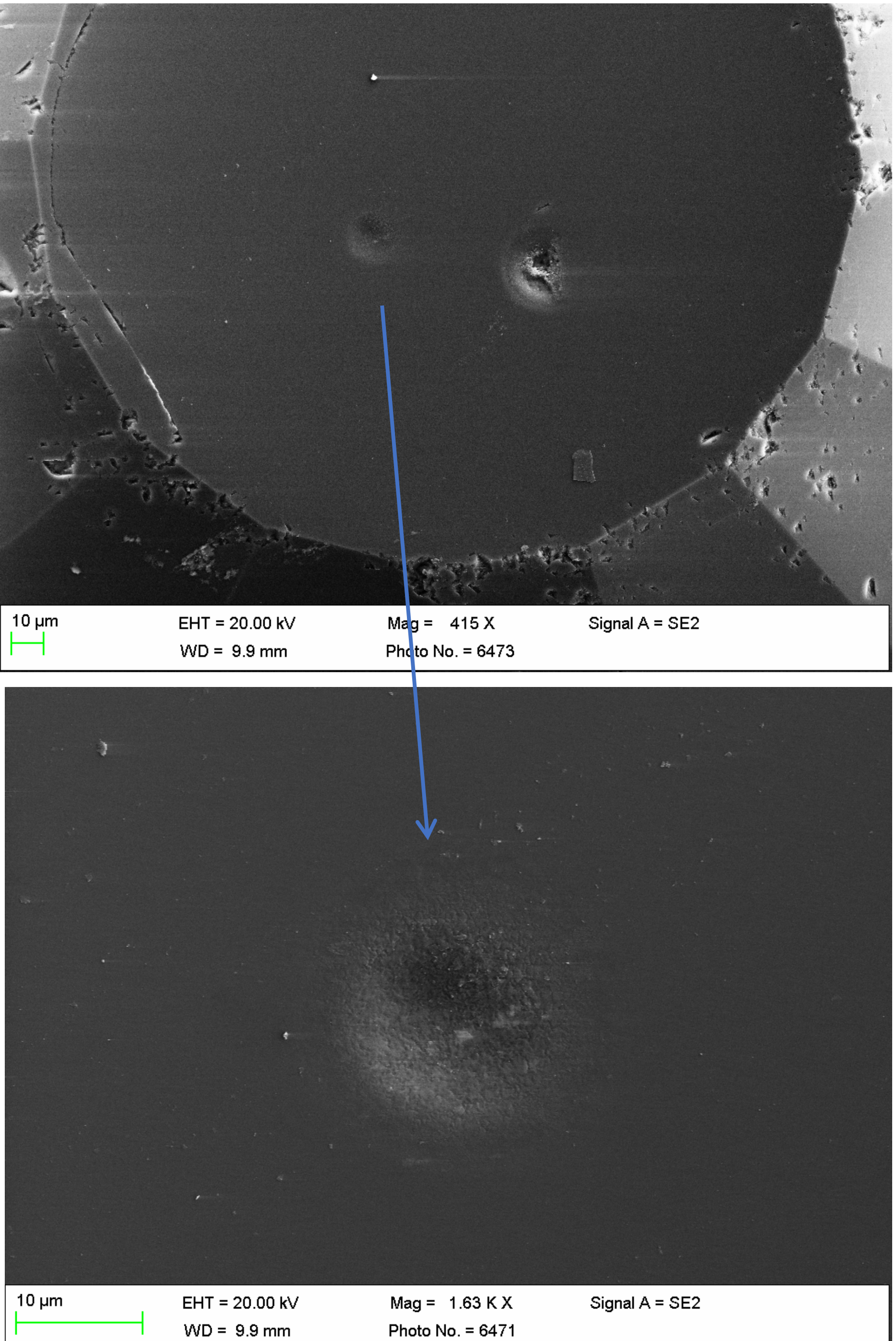

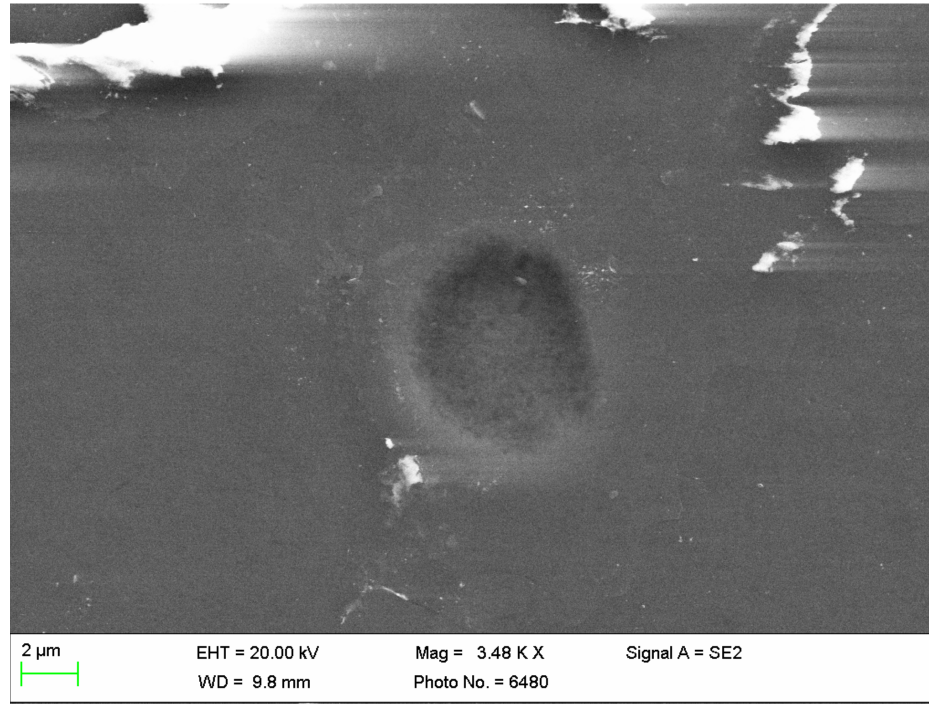

Spherical indentations on single crystal diamond (the (100) face, left) and NPD (above) by nanocrystalline diamond balls

Dubrovinskaia et al., Sci Adv., 2016

- **Could single crystal diamond be used for secondary anvils?**
- **How to prepare experiments above 500 GPa reproducibly ("algorithmically")?**
- **What factors do affect pressure characterization in dsDACs (and probably in a toroidal DAC) ?**

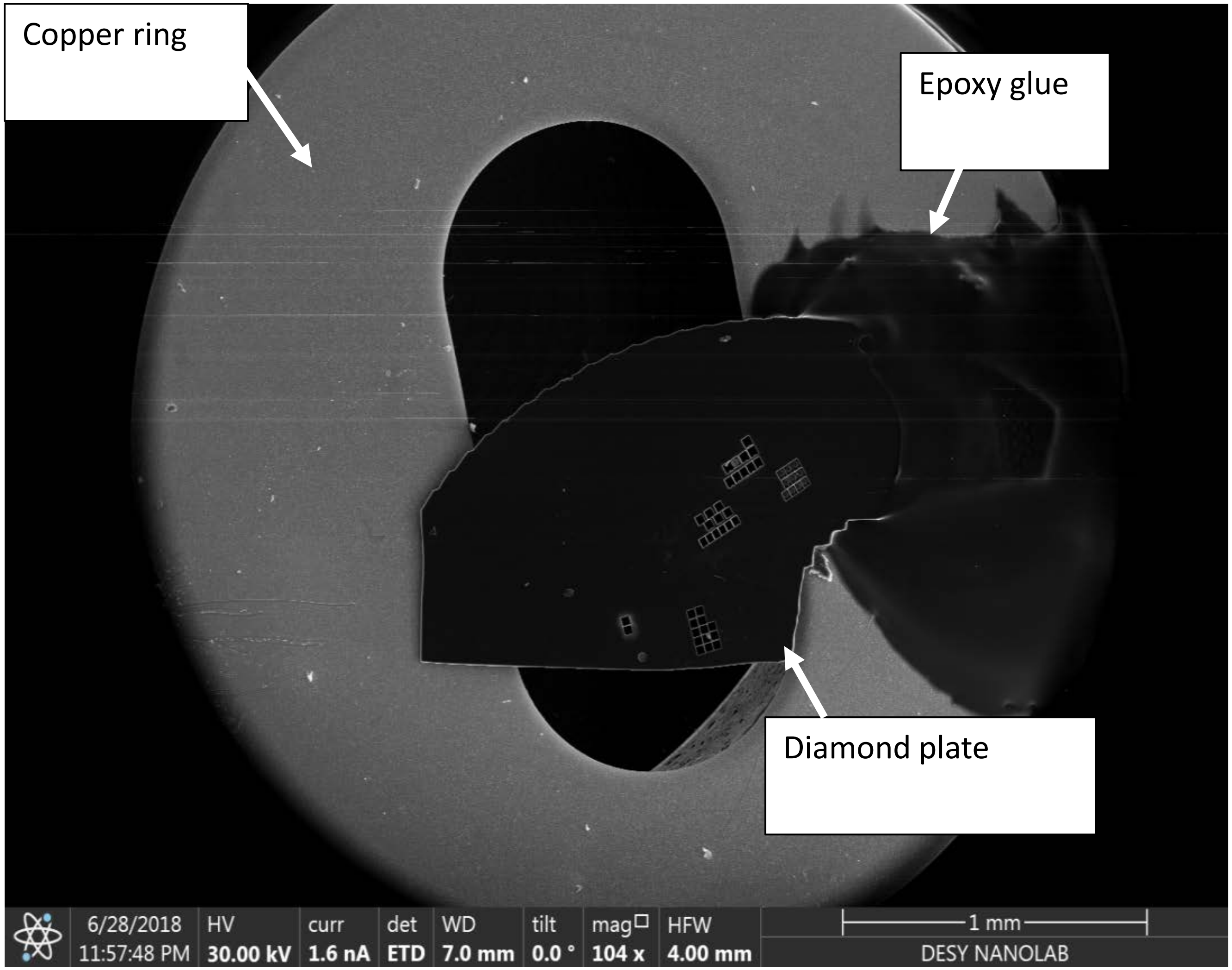

SEM-image of a single-crystal diamond plate (type Ia, diameter 3.00 mm, thickness 10 µm (100)-oriented, Almax easyLab).
The plate is glued on a copper ring (a holder for TEM-samples) with epoxy glue.

Disk illing

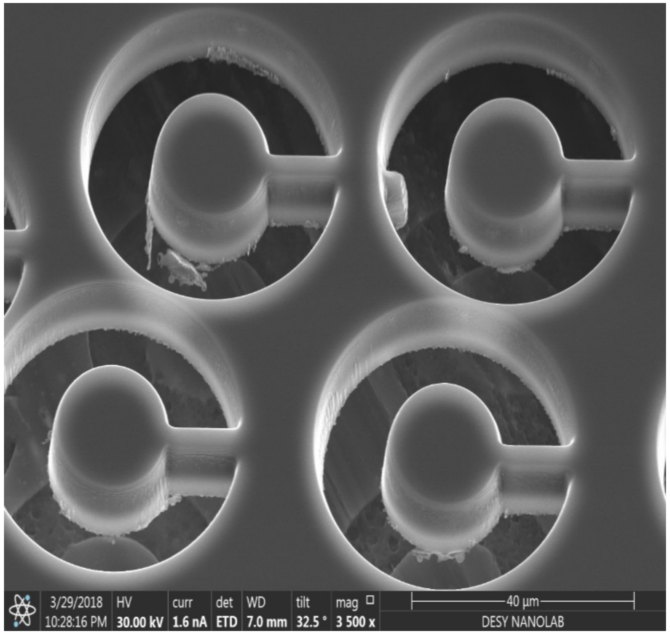
3/29/2018 10:28:16 PM
HV 30.00 kV
curr 1.6 nA
det ETD
WD 7.0 mm
tilt 32.5 °
mag 3 500 x
40 µm
DESY NANOLAB

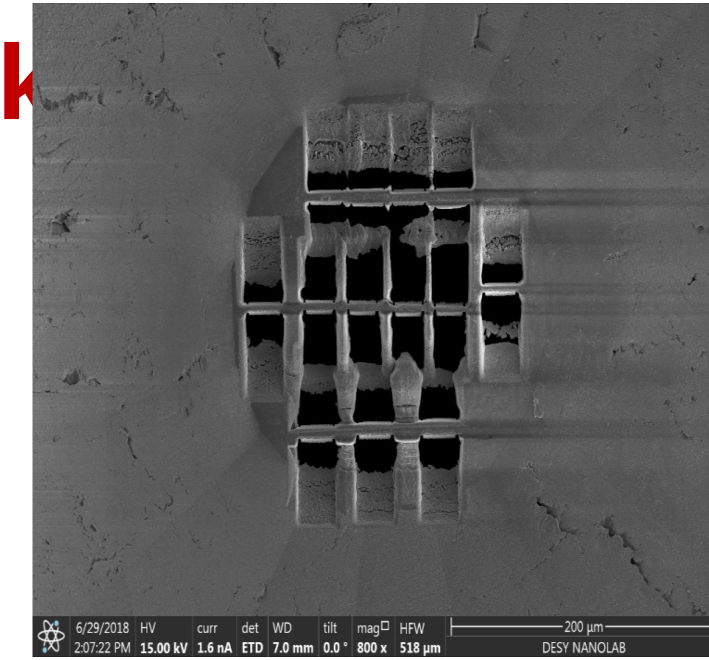
6/29/2018 2:07:22 PM
HV 15.00 kV
curr 1.6 nA
det ETD
WD 7.0 mm
tilt 0.0 °
mag 800 x
HFW 518 µm
200 µm
DESY NANOLAB

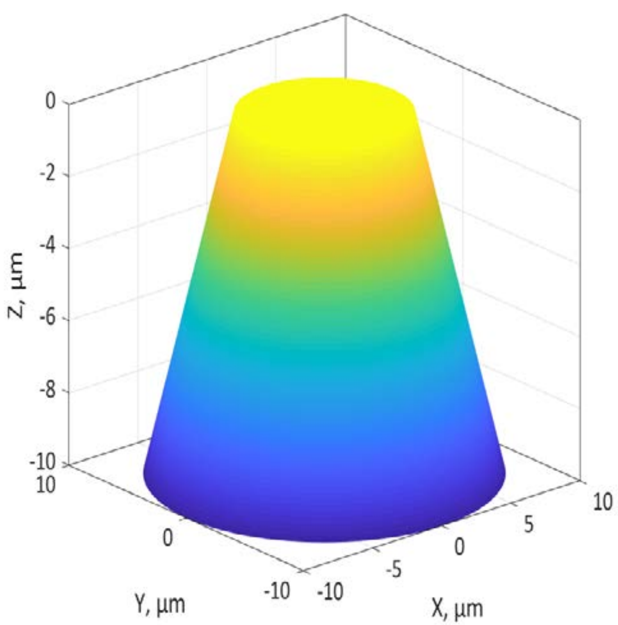
Z, µm
0
-2
-4
-6
-8
-10
Y, µm
10
0
-10
X, µm
-10
-5
0
5
10

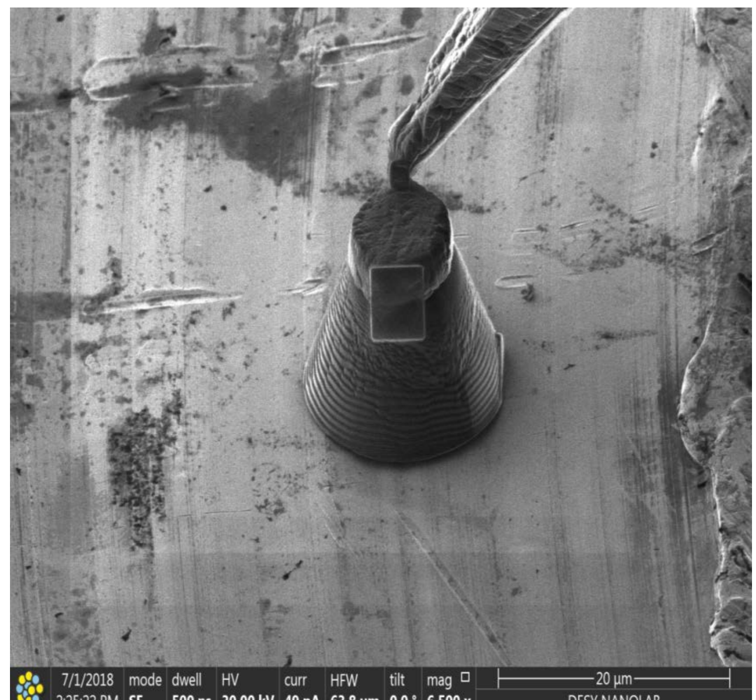
7/1/2018 2:25:22 PM
mode SE
dwell 500 ns
HV 30.00 kV
curr 49 pA
HFW 63.8 µm
tilt 0.0 °
mag 6 500 x
20 µm
DESY NANOLAB

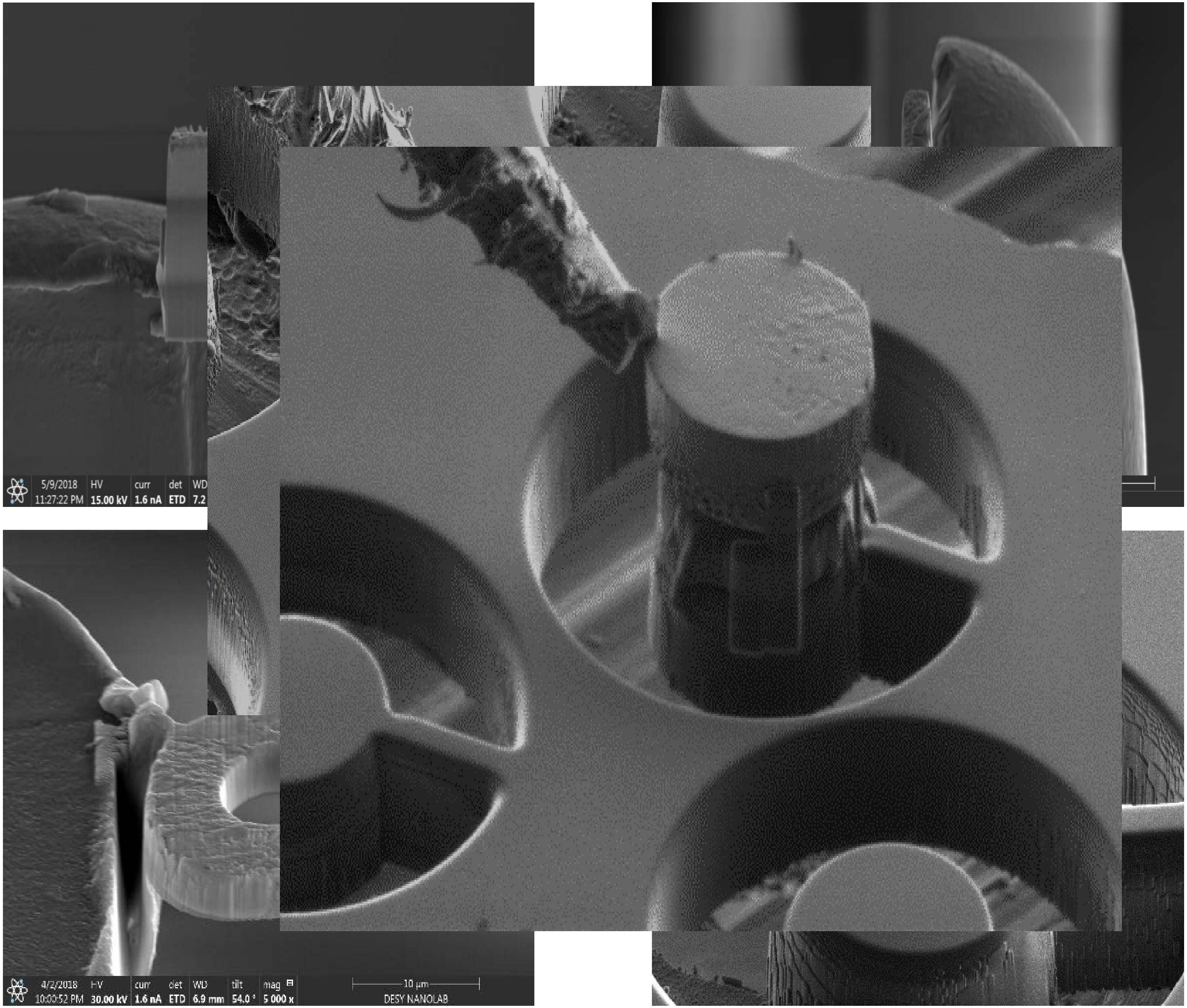
5/9/2018 HV curr det WD
11:27:22 PM 15.00 kV 1.6 nA ETD 7.2
4/2/2018 HV curr det WD tilt mag
10:00:52 PM 30.00 kV 1.6 nA ETD 6.9 mm 54.0 ° 5 000 x
10 µm
DESY NANOLAB

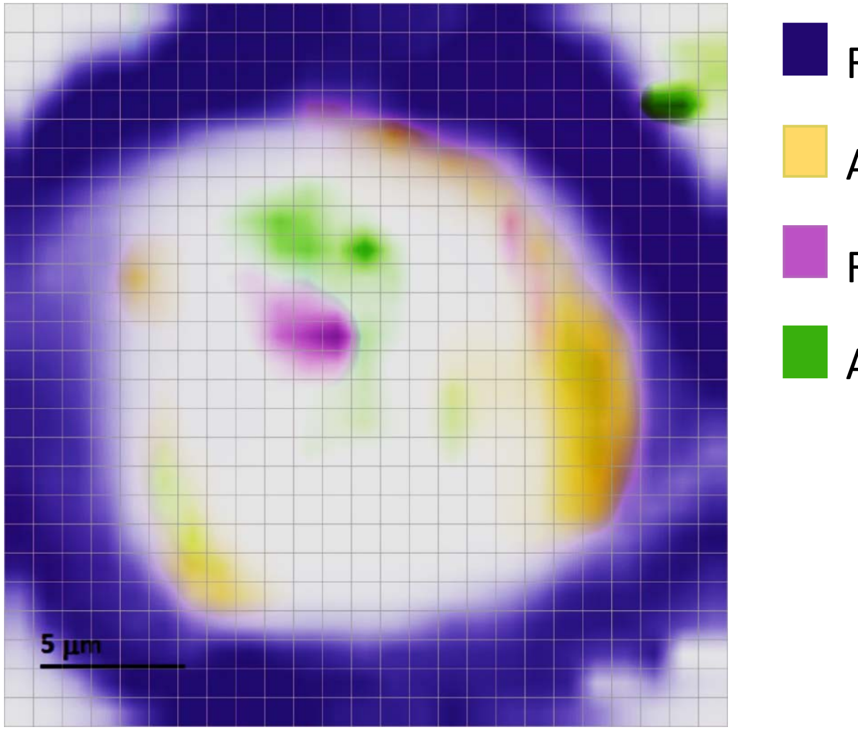

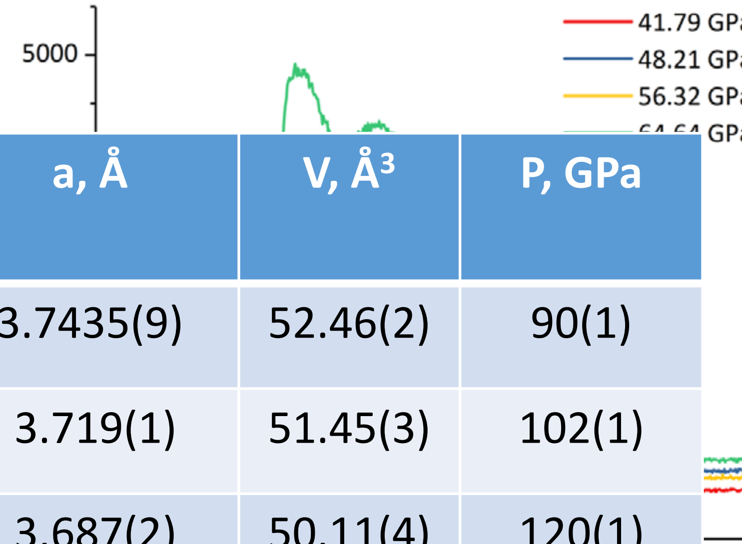

Au	a, Å	V, Å^3	P, GPa
P01	3.7435(9)	52.46(2)	90(1)
P02	3.719(1)	51.45(3)	102(1)
P03	3.687(2)	50.11(4)	120(1)
P04	3.664(3)	49.21(7)	135(1)

Pressure step	$P_{(Raman)}$	$P(Re)_{LP(diff)}$	$P(Re)_{HP(diff)}$
P01	41(3)	41(1)	94(2)
P02	48(3)	47(1)	124(1)
P03	56(3)	56(1)	153(2)
P04	64(3)	64(1)	168(2)

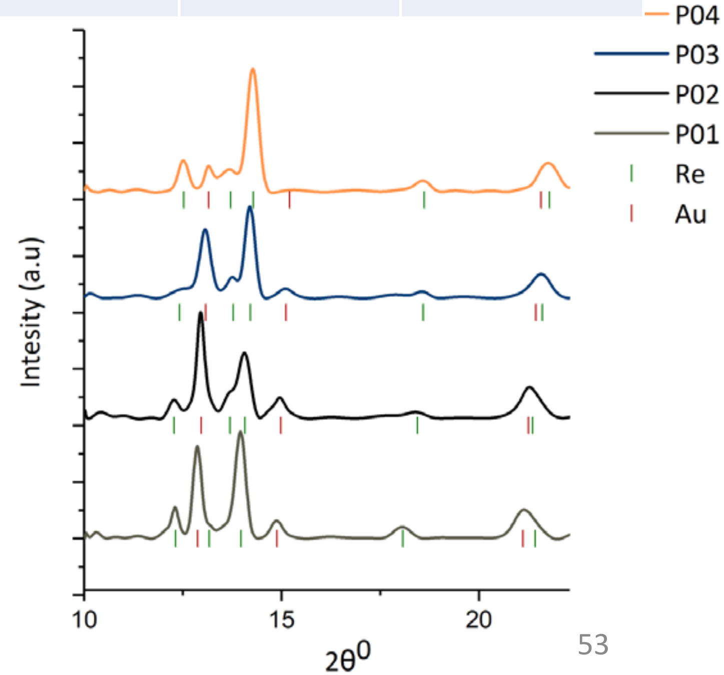

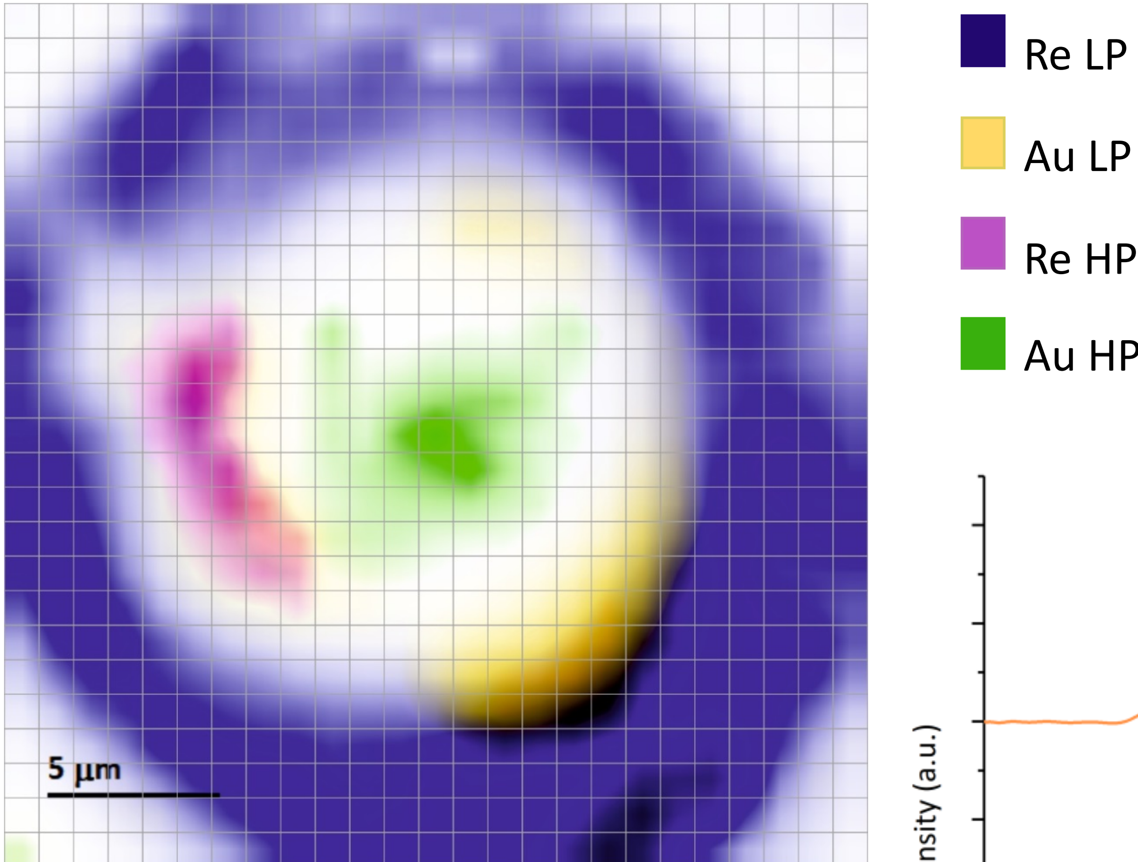

Pressure step	$P(Re)_{LP(diff)}$	$P(Re)_{HP(diff)}$
P01	21(1)	49(1)
P02	26(1)	89(1)
P03	37(1)	148(1)
P04	42(1)	185(1)

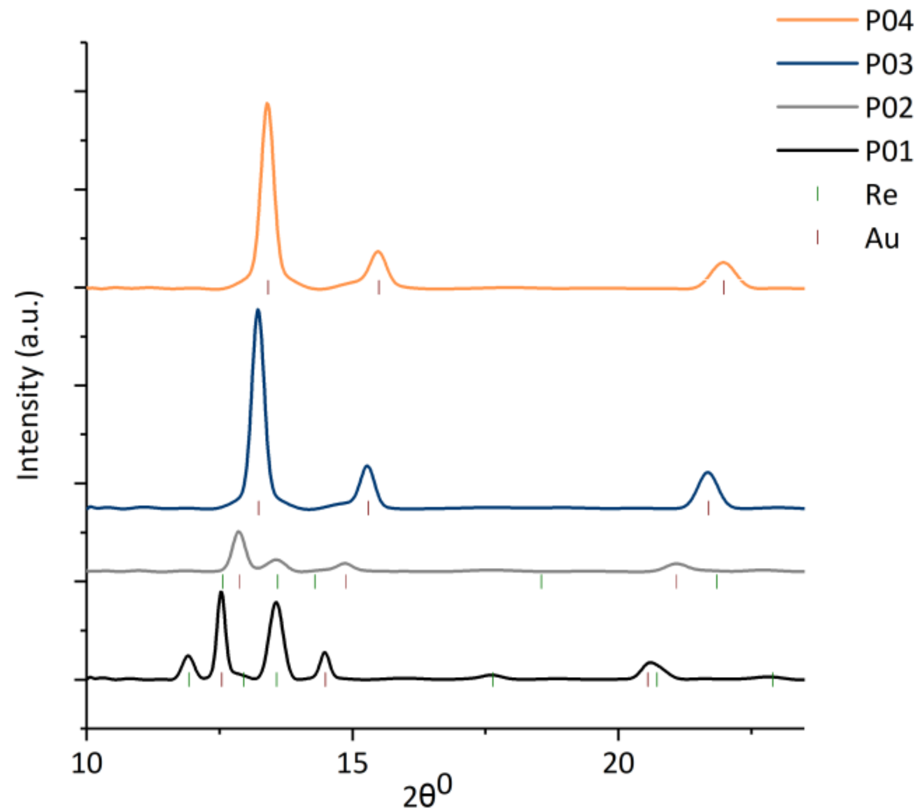

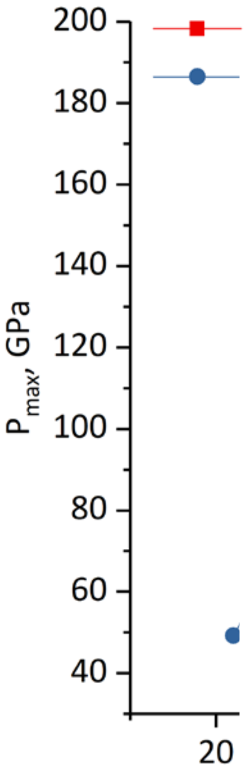

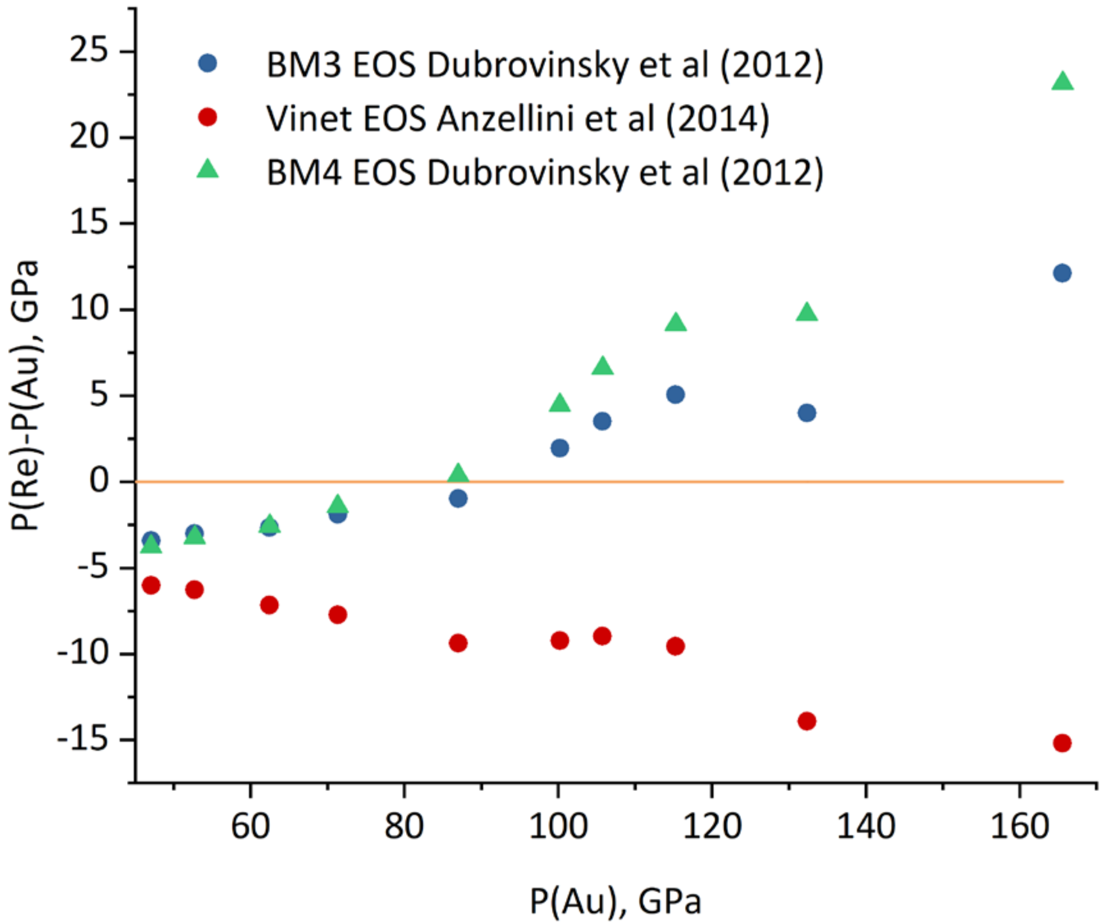

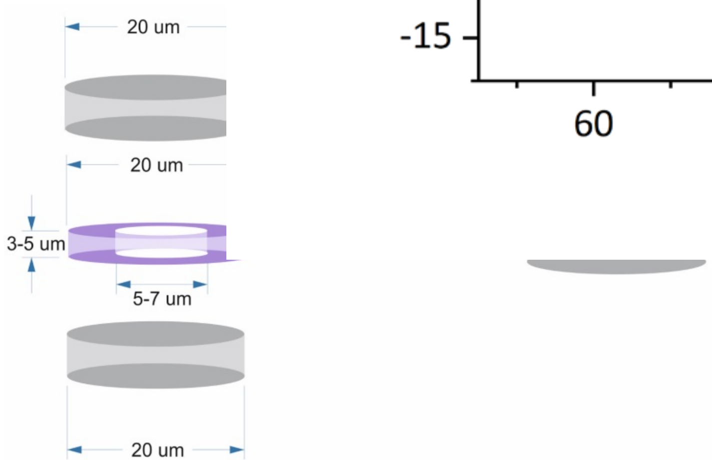

			, GPa
			(1)
47(1)	124(1)	26(1)	89(1)
56(1)	153(2)	37(1)	148(1)
64(1)	168(2)	42(1)	185(1)

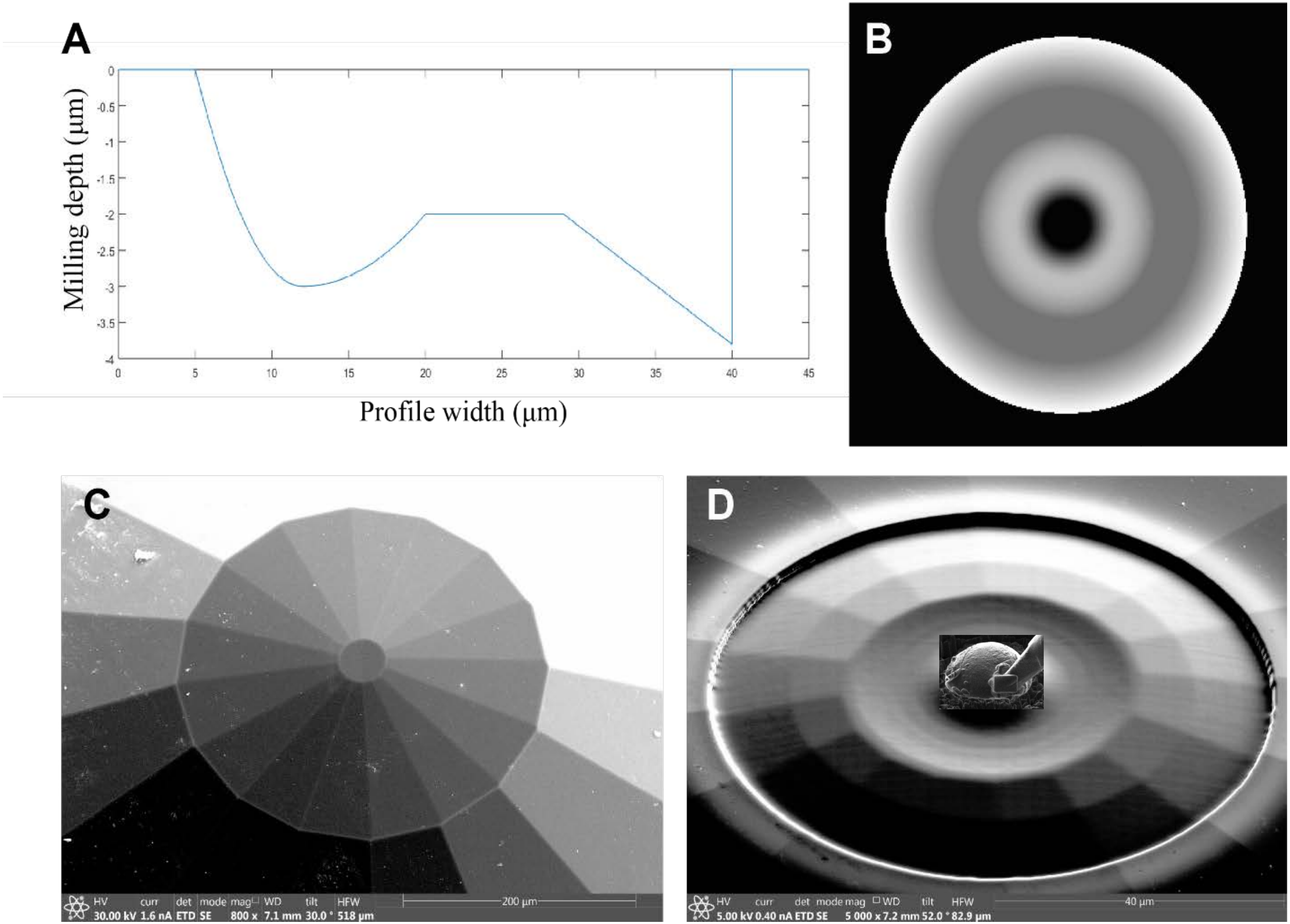

Pictures: S. Petitgirard

Pulsed laser heating in dsDAC

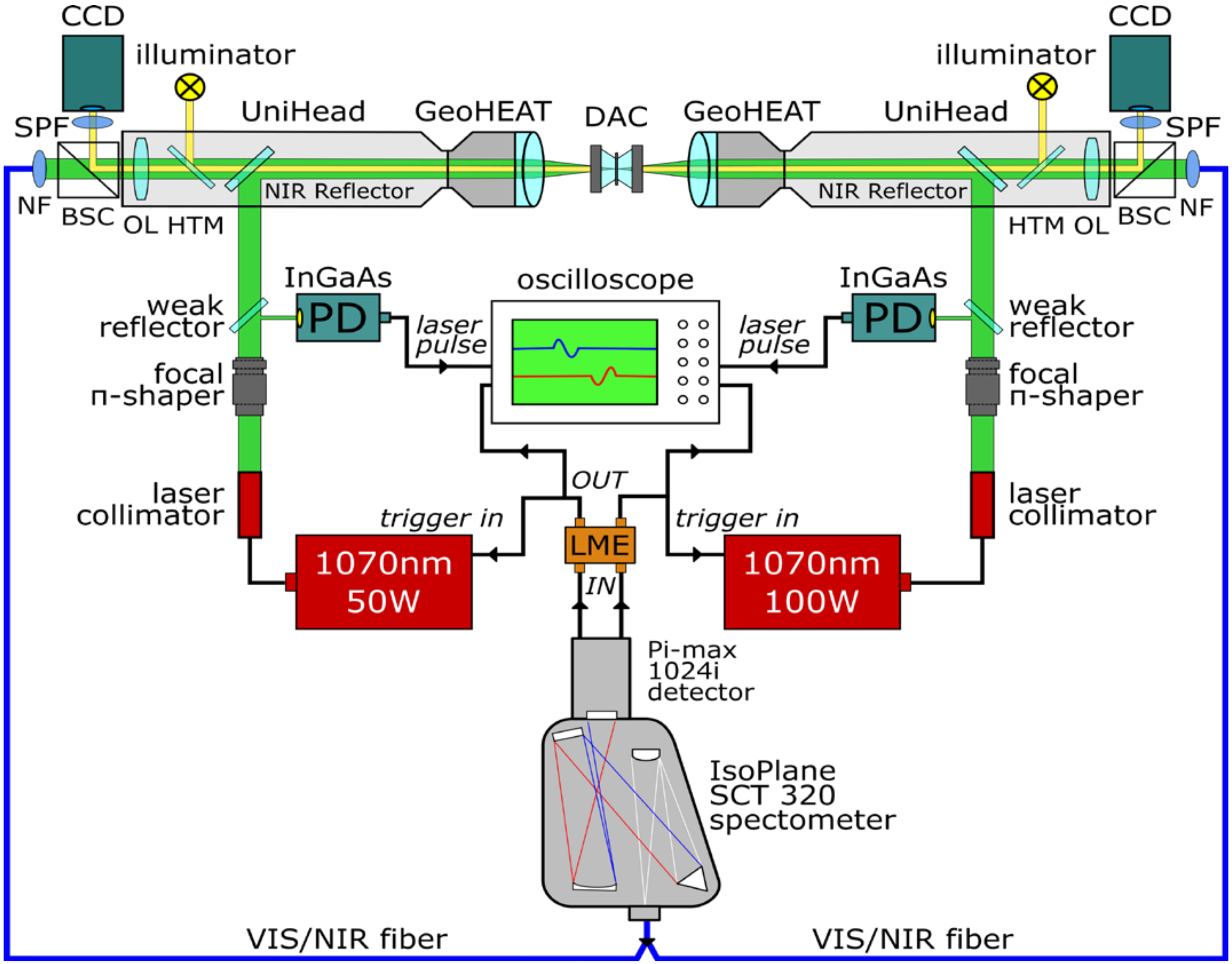

Aprilis et al., 2017

903(10) GPa (Anzellini et al., 2014)
1155(10) GPa (Dubrovinsky et al., 2012)

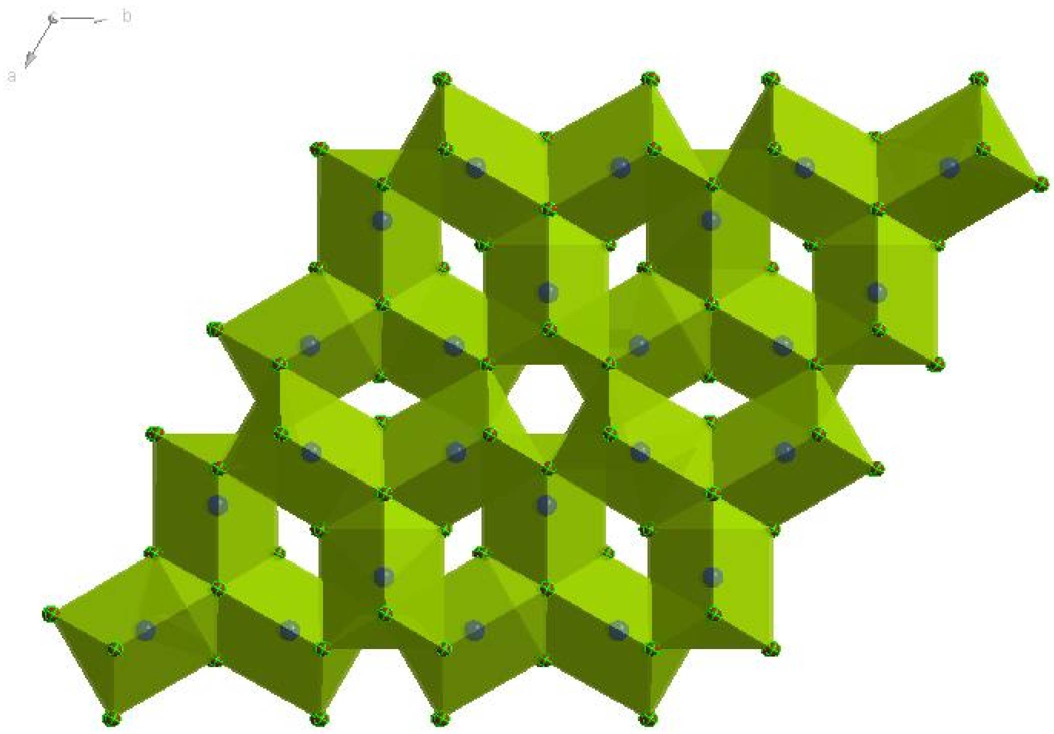

Re_7N_3

$P6_3mc$

a=6.278(2) Å

c=4.000(2) Å

V=136.57(9) Å^3

Z=2

394 reflections

Rint=2.8%

R1=7.1%

Acknowledgements

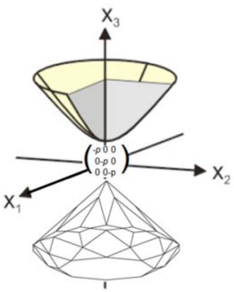

in incudibus veritas

G. Aprilis
E. Bykova
M. Bykov
S. Chariton
T. Fedotenko
E. Koemets
S. Petitgirard

UNIVERSITÄT BAYREUTH

BGI Bayerisches Geoinstitut

CarboPaT FOR2125

DESY

ID11, ID15, ID27, ID18, ID16, at ESRF
P02, P06 at PETRA III
IDD-13 at APS

ARGONNE NATIONAL LABORATORY

GEFÖRDERT VOM
Bundesministerium für Bildung und Forschung

DFG Deutsche Forschungsgemeinschaft

ESRF

Heisenberg-Programm
Deutsche Forschungsgemeinschaft

Chemistry at Extreme Conditions

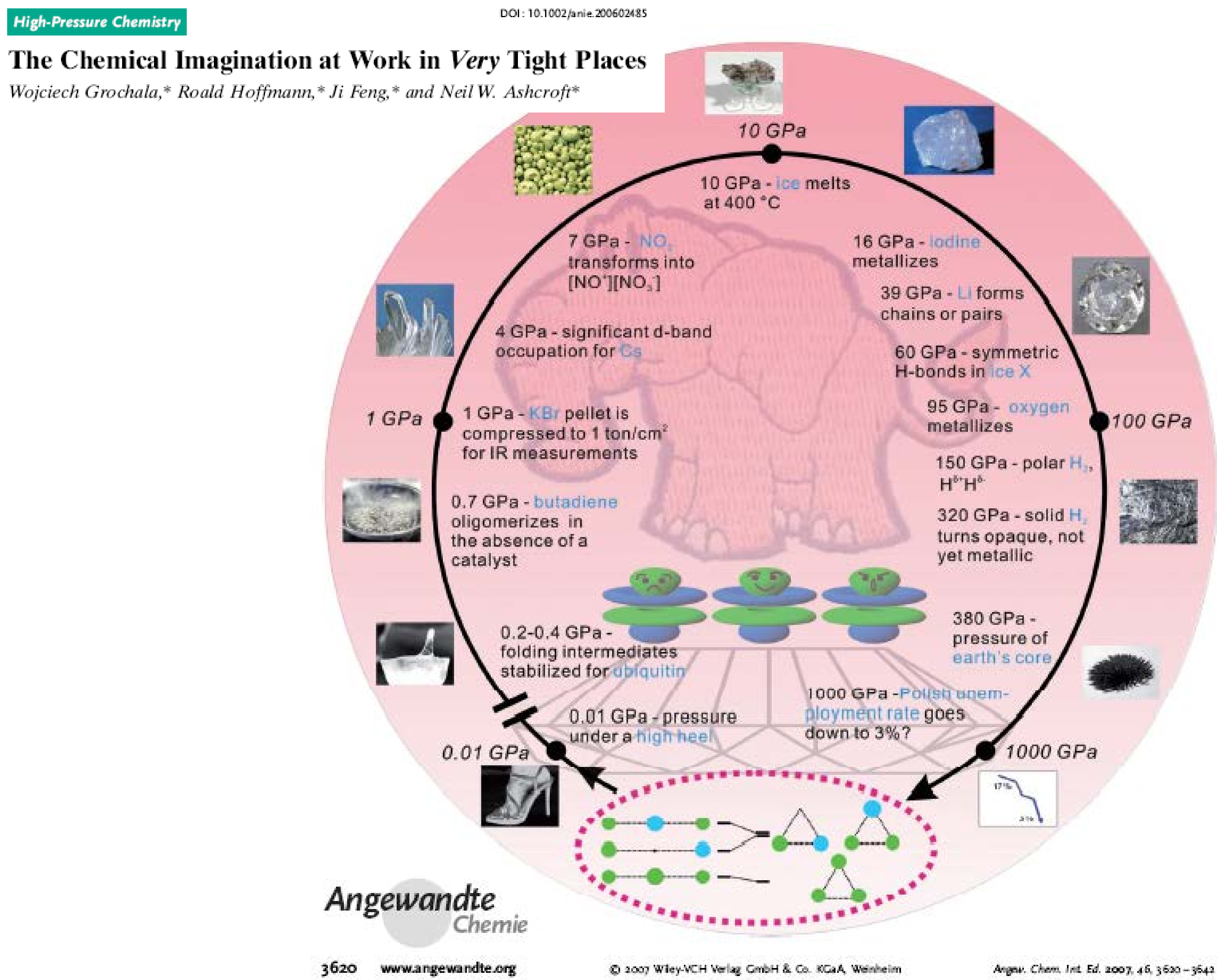

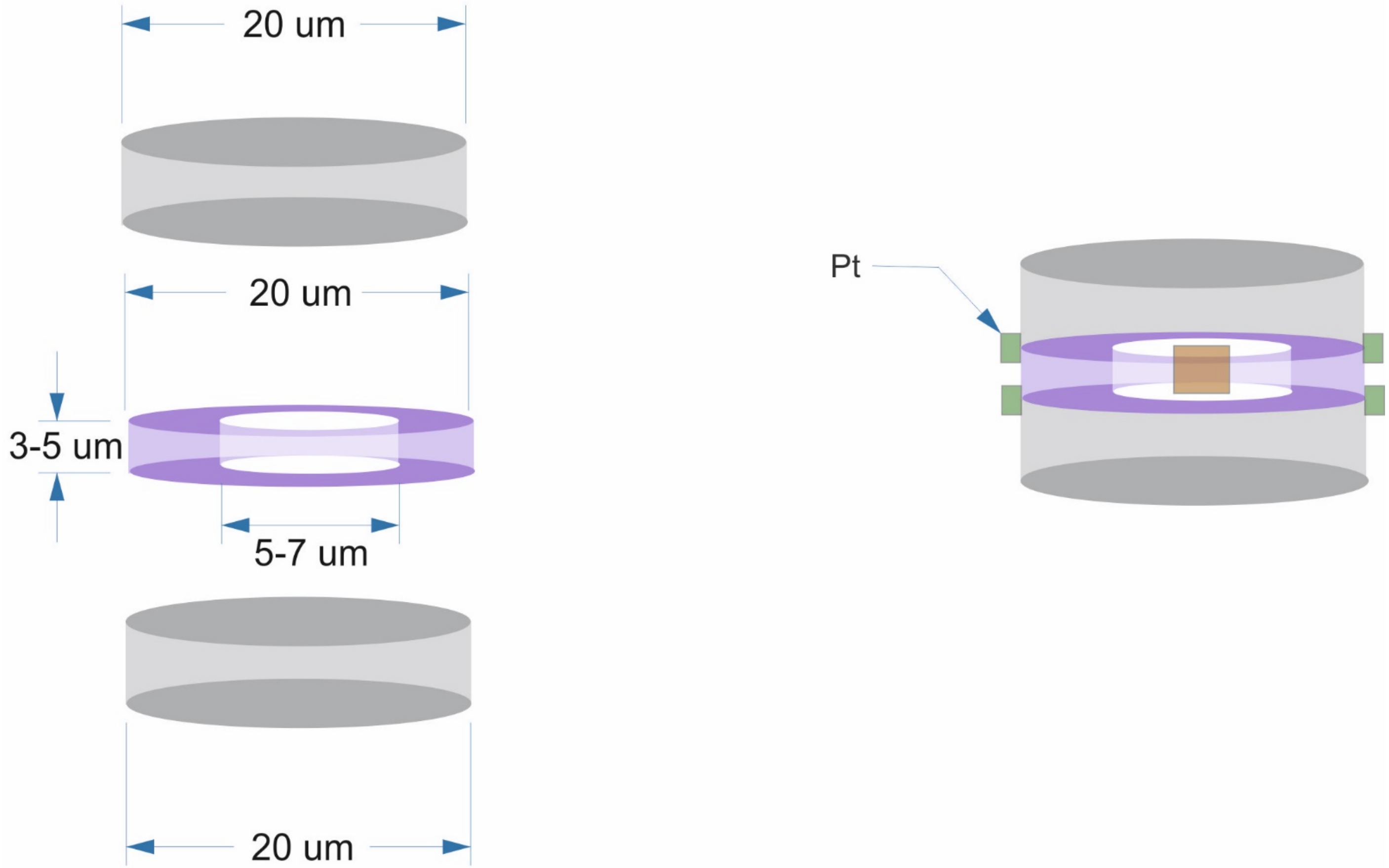

20 um
20 um
3-5 um
5-7 um
20 um
Pt

	a, Å	c, Å	V, Å^3	P, GPa
p01	2.609(1)	4.227(4)	24.92(3)	94(2)
p02	2.6165(7)	4.066(2)	24.11(2)	124(1)
p03	2.5873(9)	4.043(4)	23.44(3)	153(2)
p04	2.5660(9)	4.060(5)	23.15(3)	168(2)

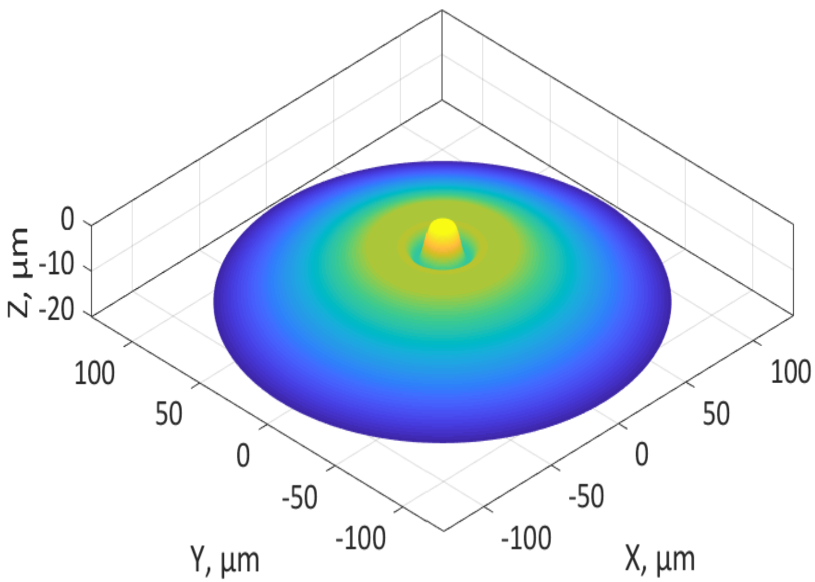
0
-10
-20
Z, µm
100
50
0
-50
-100
Y, µm
100
50
0
-50
-100
X, µm

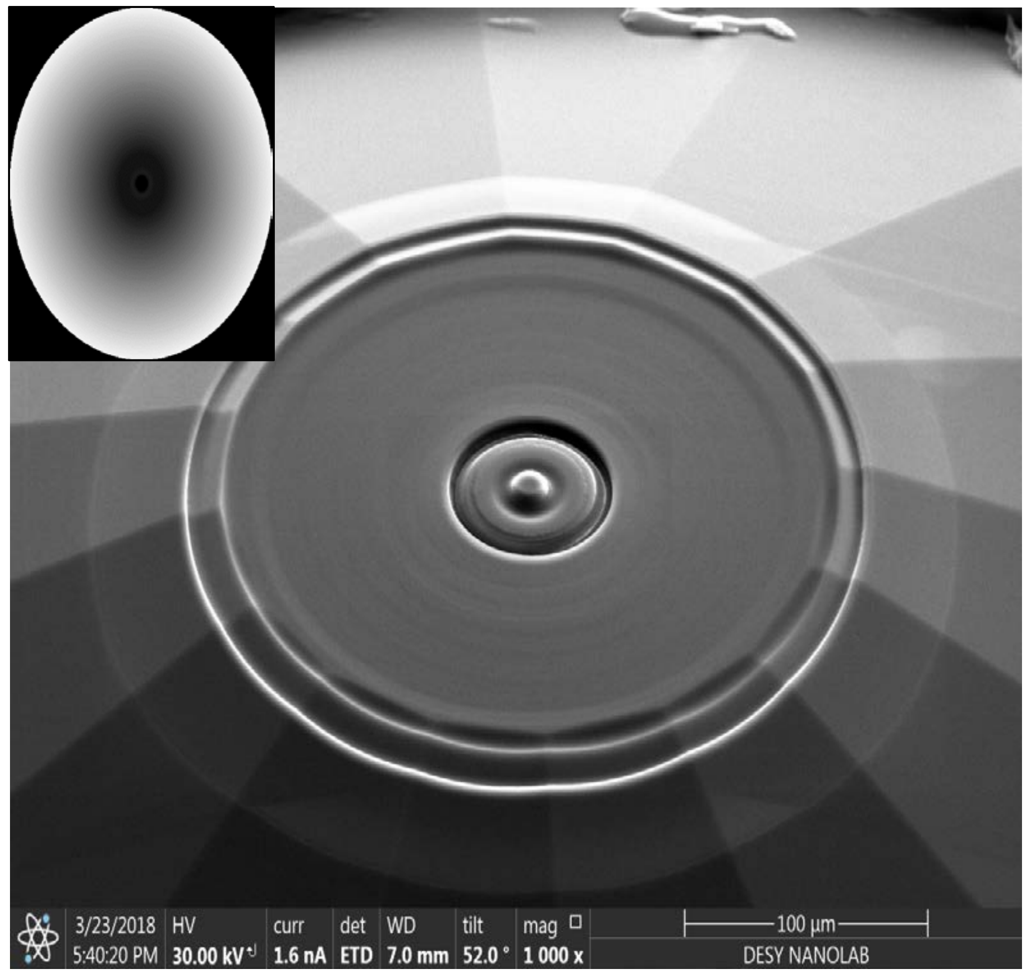
3/23/2018
5:40:20 PM
HV
30.00 kV
curr
1.6 nA
det
ETD
WD
7.0 mm
tilt
52.0 °
mag
1 000 x
100 µm
DESY NANOLAB

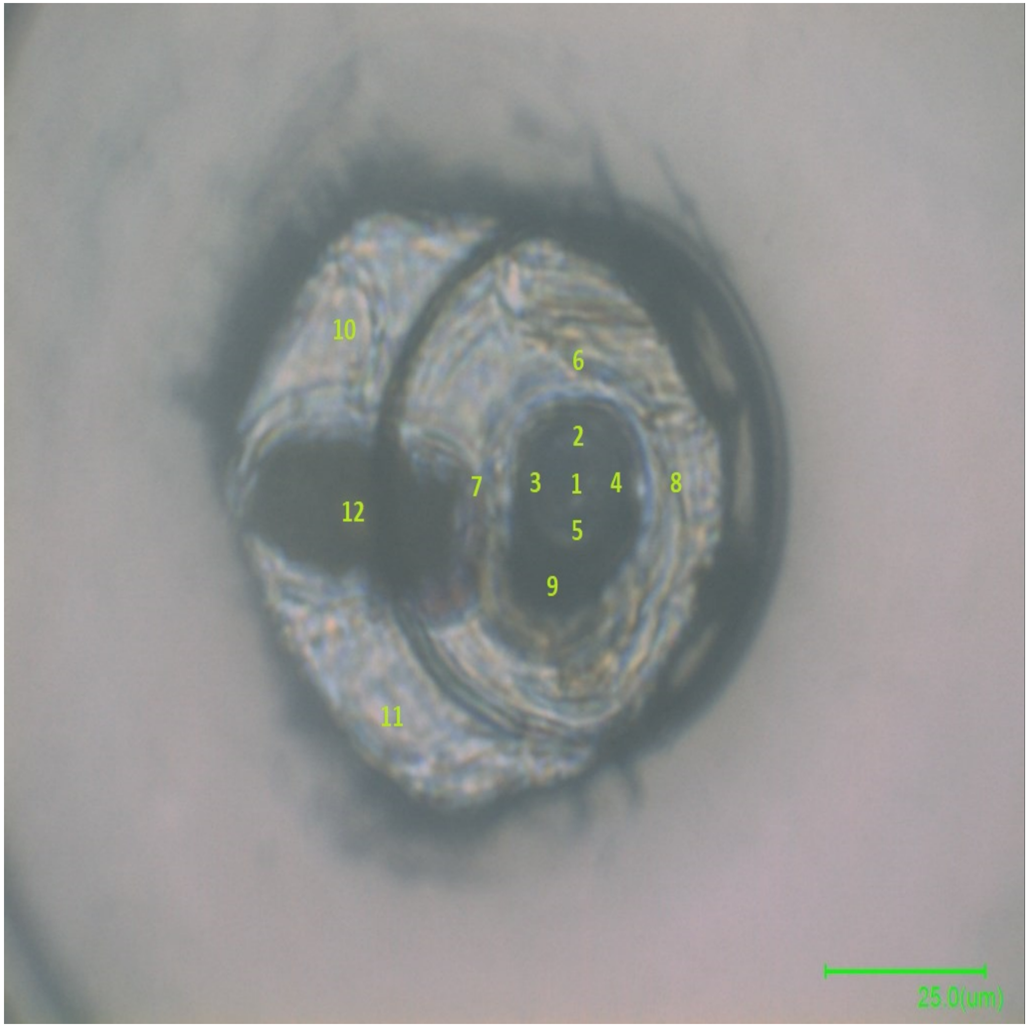
10
6
2
7
3
1
4
8
12
5
9
11
25.0(um)

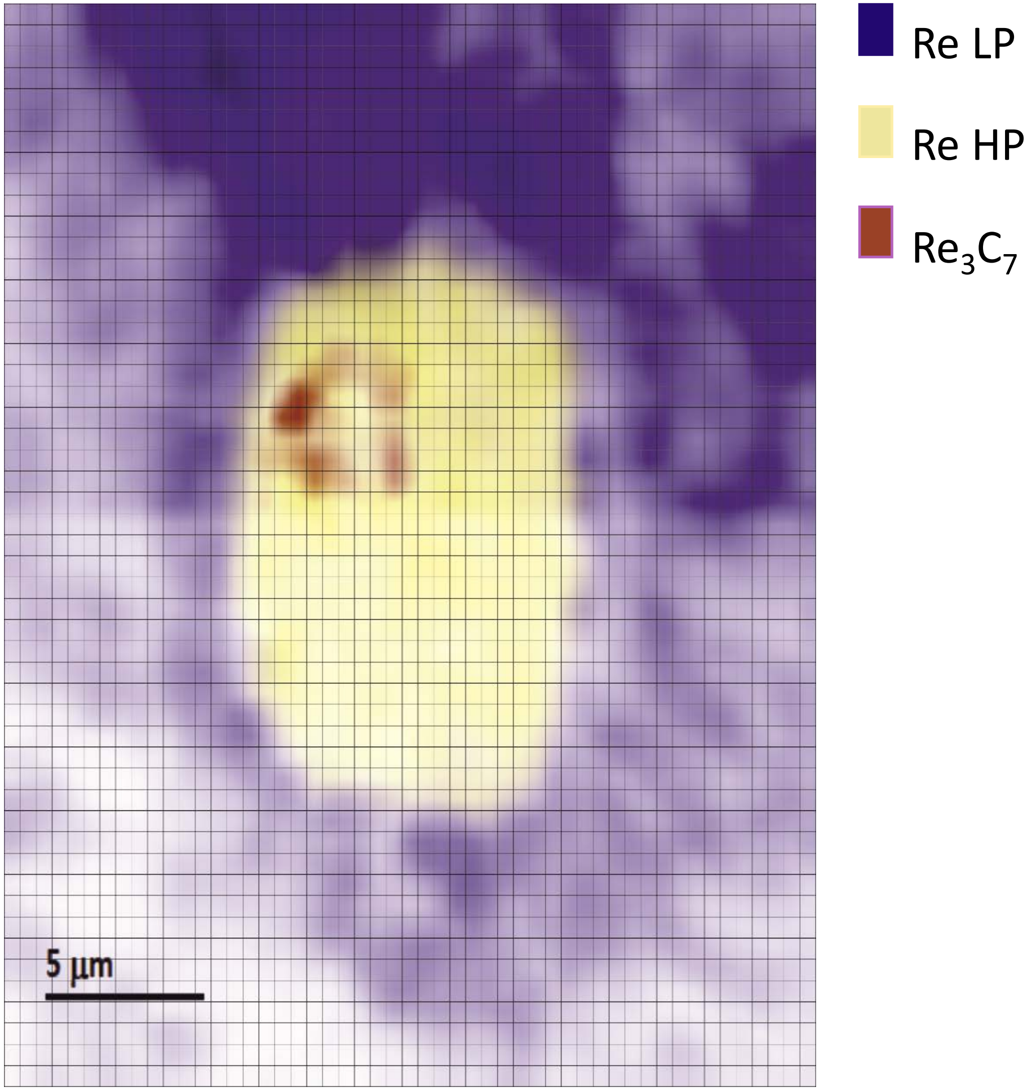
5 µm
Re LP
Re HP
Re_3C_7

Observed Fe_2O_3 phases

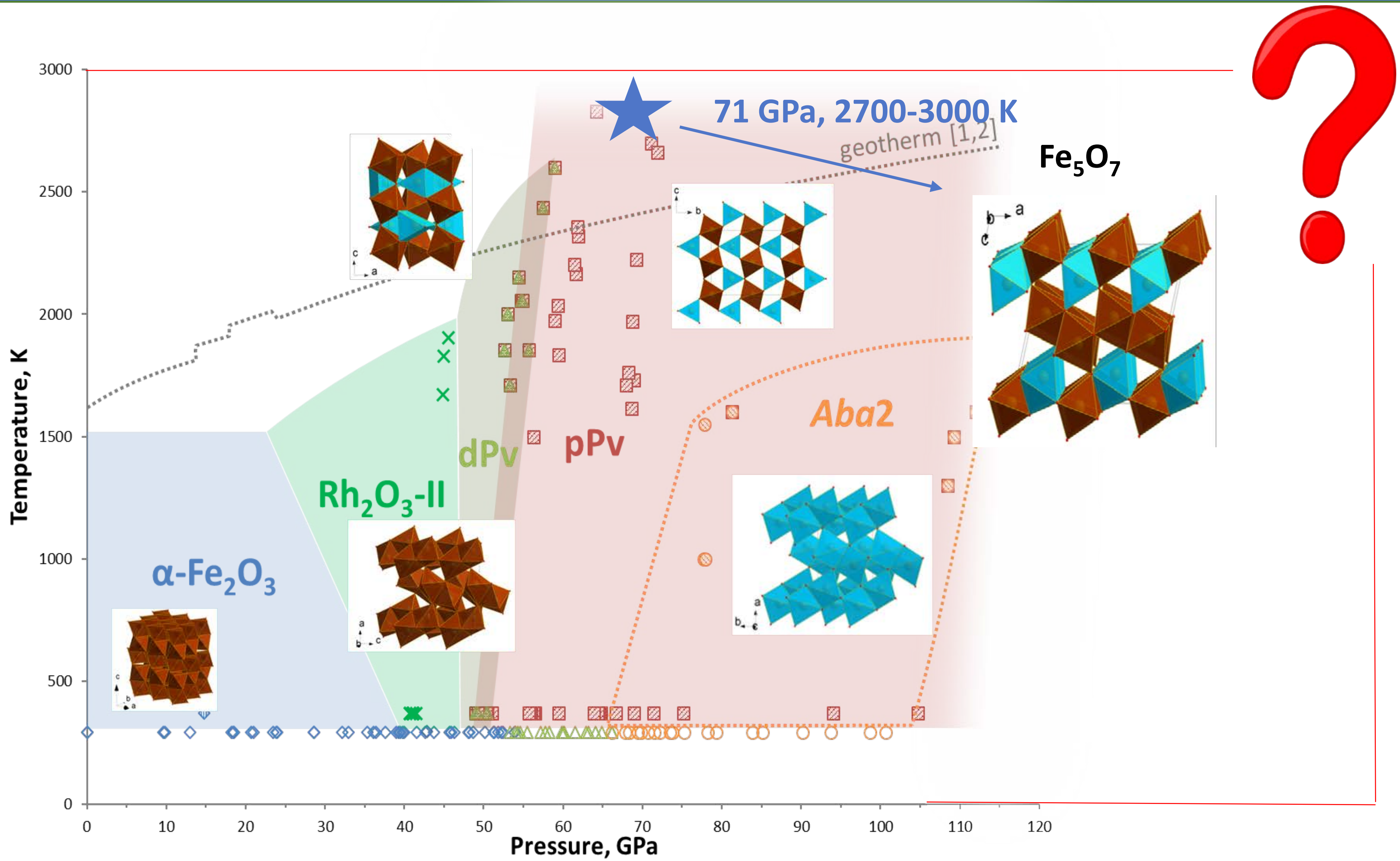

Phase diagram of Fe_2O_3:
Bykova et al, 2016

PPv-Fe_2O_3 exist at least up to 215 GPa

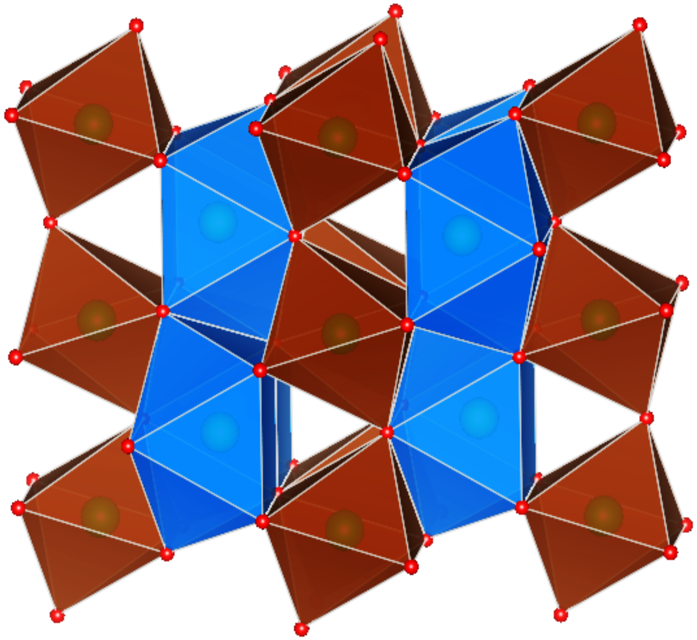

Building blocks:

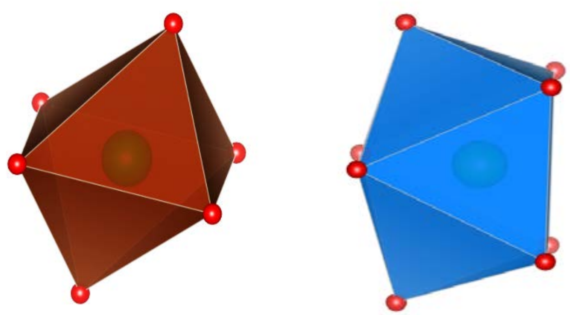

FeO6 FeO8

PPv-Fe_2O_3

Cmcm

a=2.5134(8) Å

b=8.1328(12) Å

c=6.073(3) Å

V=124.14(7) Å^3

Z=4

R1=7.1%

E. Bykova (2016), Nat. Commun.7 (2016) (DOI:/10.1038/ncomms10661).

Decomposition of Fe_2O_3 at 190 GPa and 3000 K

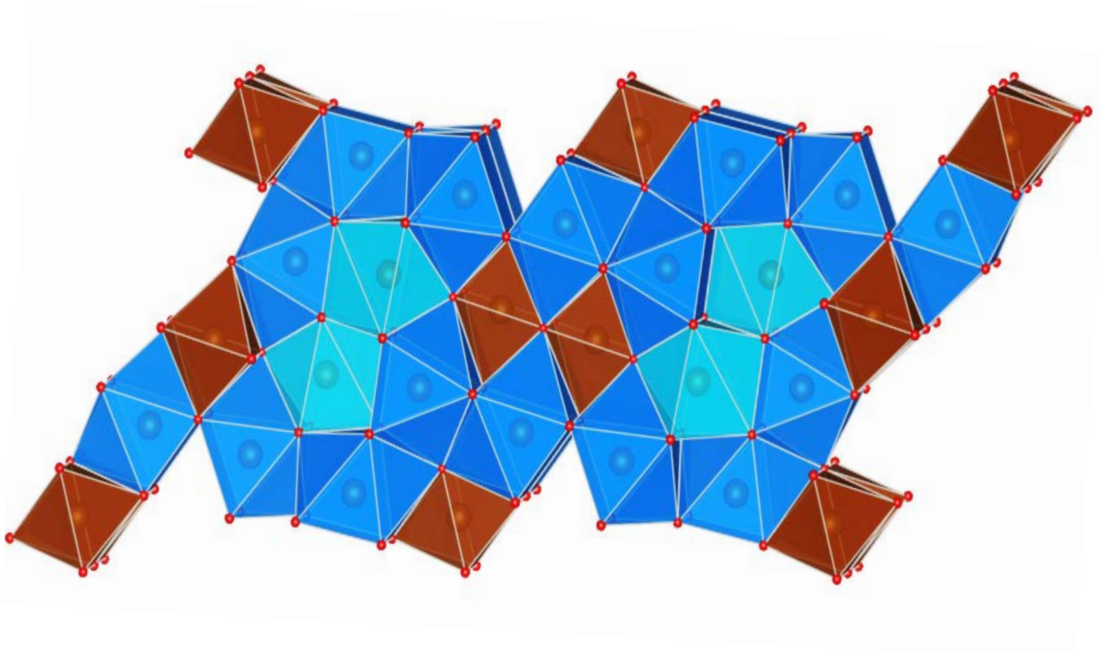

$Fe_{13}O_{19}$
C2/m

a=18.9445 (18) Å

b=2.5297 (13) Å

c=9.393 (11) Å

β=117.57˚ (3)

V=399.1 (5) Å^3

Z=2

R1=5.9%

Building blocks:

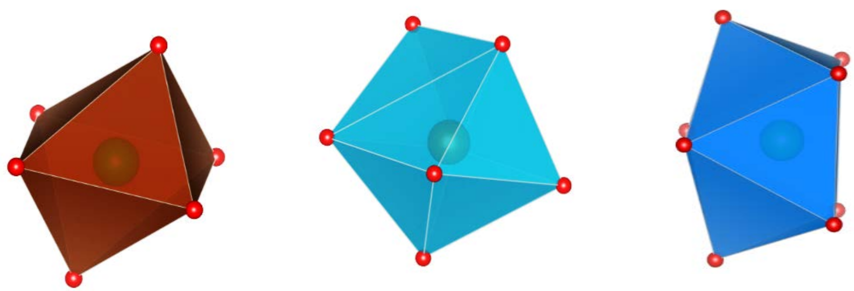

FeO6 **FeO7** **FeO8**

M. Merlini (2015), Am. Min, Vol. **100**, 2001–2004

Decomposition of Fe_2O_3 at 190 GPa and 3000 K

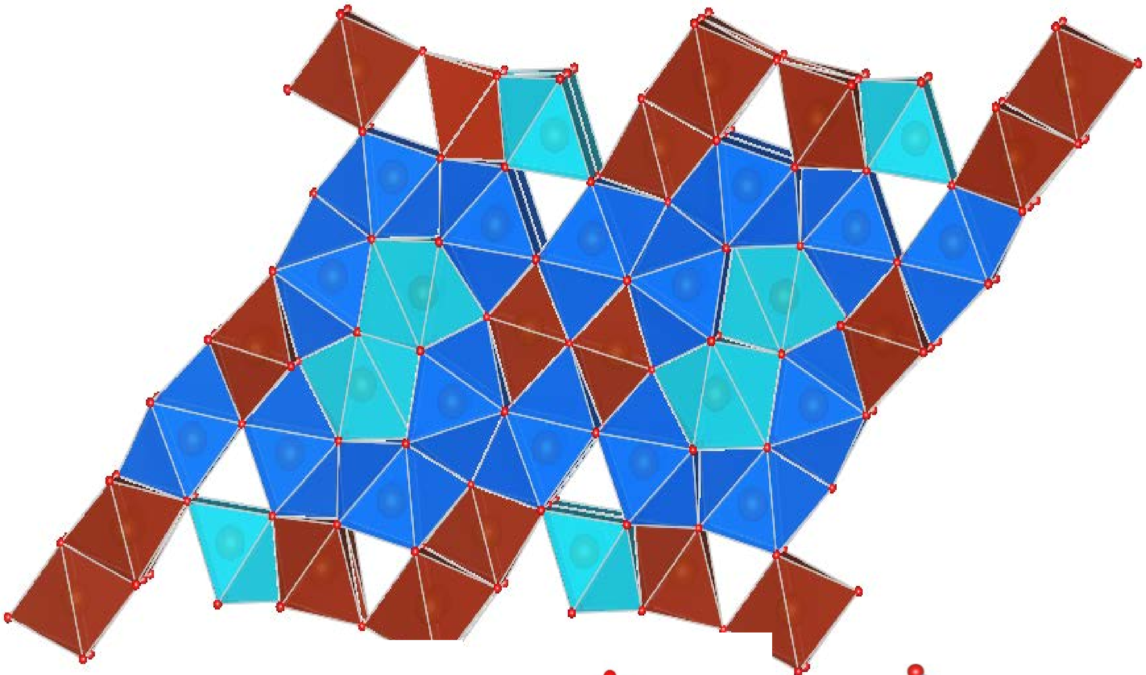

Building blocks:

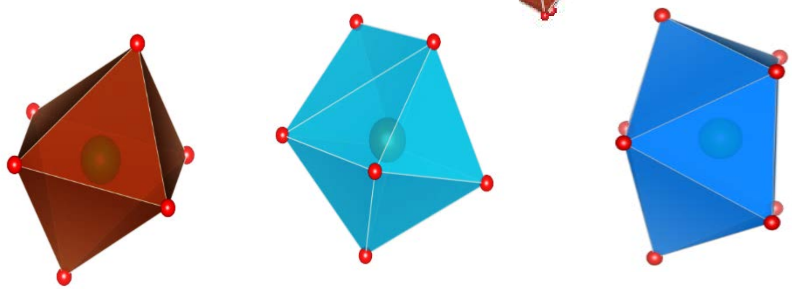

FeO6 **FeO7** **FeO8**

$Fe_{19}O_{27}$

C2/m

a=19.001 (3) Å

b=2.5464 (16) Å

c=13.932 (3) Å

β =121.57 ˚ (2)

V=574.3 (4) $Å^3$

R1=9.5%

Decomposition of Fe_2O_3 with formation of Fe_3O_4 at pressures 190 and 215 GPa

Fe_3O_4
Pnma

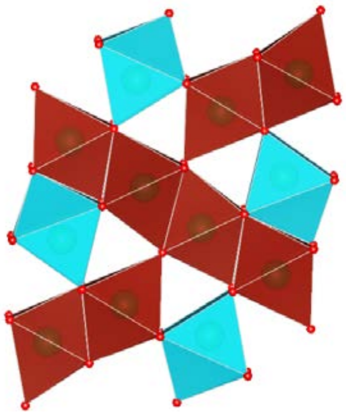

Distorted $CaTi_2O_4$-type

Fe_3O_4
Pnma

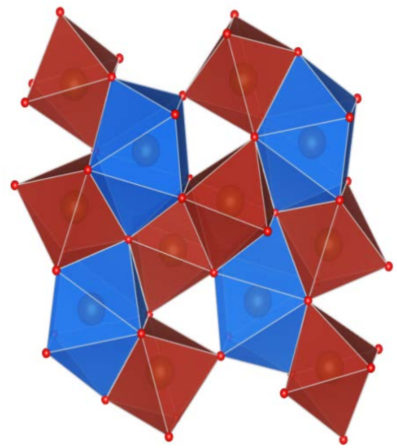

$CaFe_2O_4$-type

Fe_3O_4
$I4_1/amd$

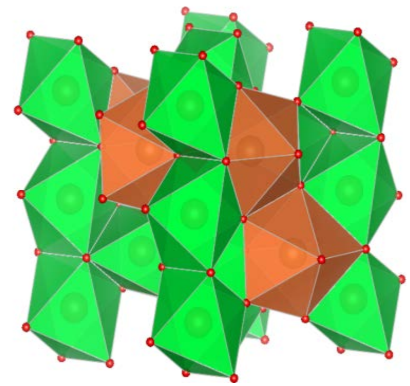

distorted Th_3P_4 structures

Building blocks:

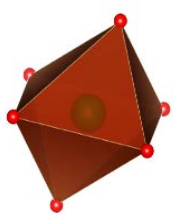

FeO6

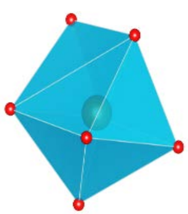

FeO7

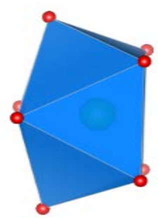

FeO8

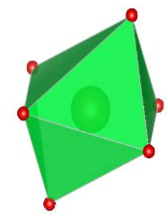

FeO6

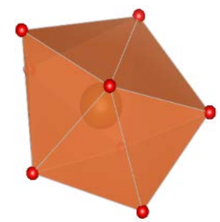

FeO8

Decomposition of Fe_2O_3 at pressures above 200 GPa

$13 \cdot Fe_2O_3 \rightarrow 2 \cdot Fe_{13}O_{19} + 0.5 \cdot O_2$

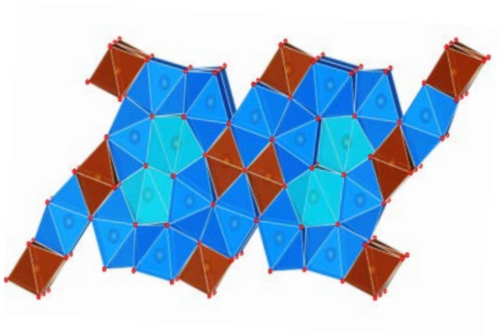

$19 \cdot Fe_2O_3 \rightarrow 2 \cdot Fe_{19}O_{27} + 1.5 \cdot O_2$

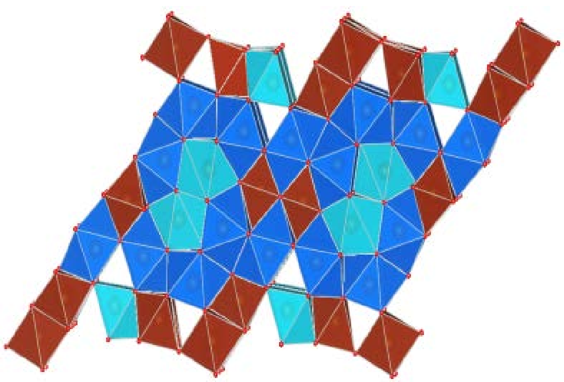

$3 \cdot Fe_2O_3 \rightarrow 2 \cdot Fe_3O_4 + 0.5 \cdot O_2$

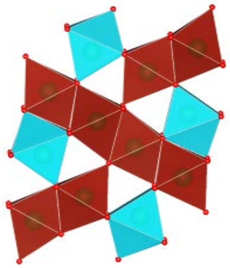

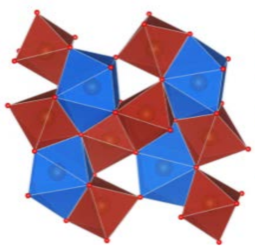

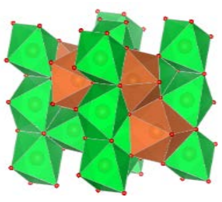

Fe_7O_{12} at 215 GPa and 3000 K

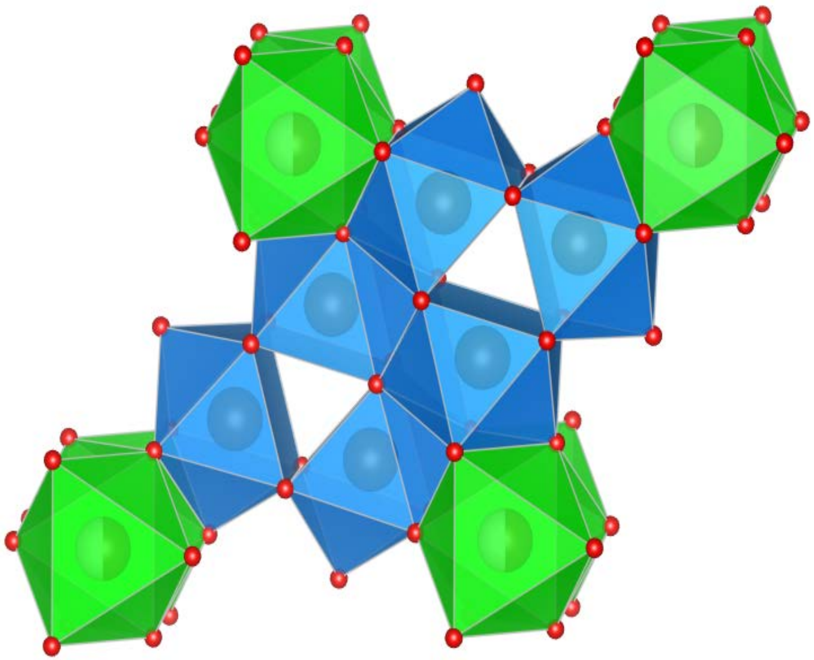

Fe_7O_{12}
$P6_3/m$
a=7.2464 (15) Å
c=2.7221 (6) Å
V=123.79 (5)$Å^3$
Z=1

R1=8.1%

Building blocks:

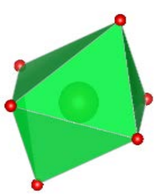

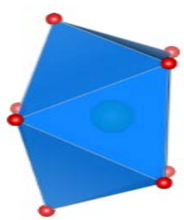

$$7Fe_2O_3+1.5\cdot \mathbf{O_2} \rightarrow 2\cdot Fe_7O_{12}$$

Distribution of several iron oxides in DAC at 215 GPa

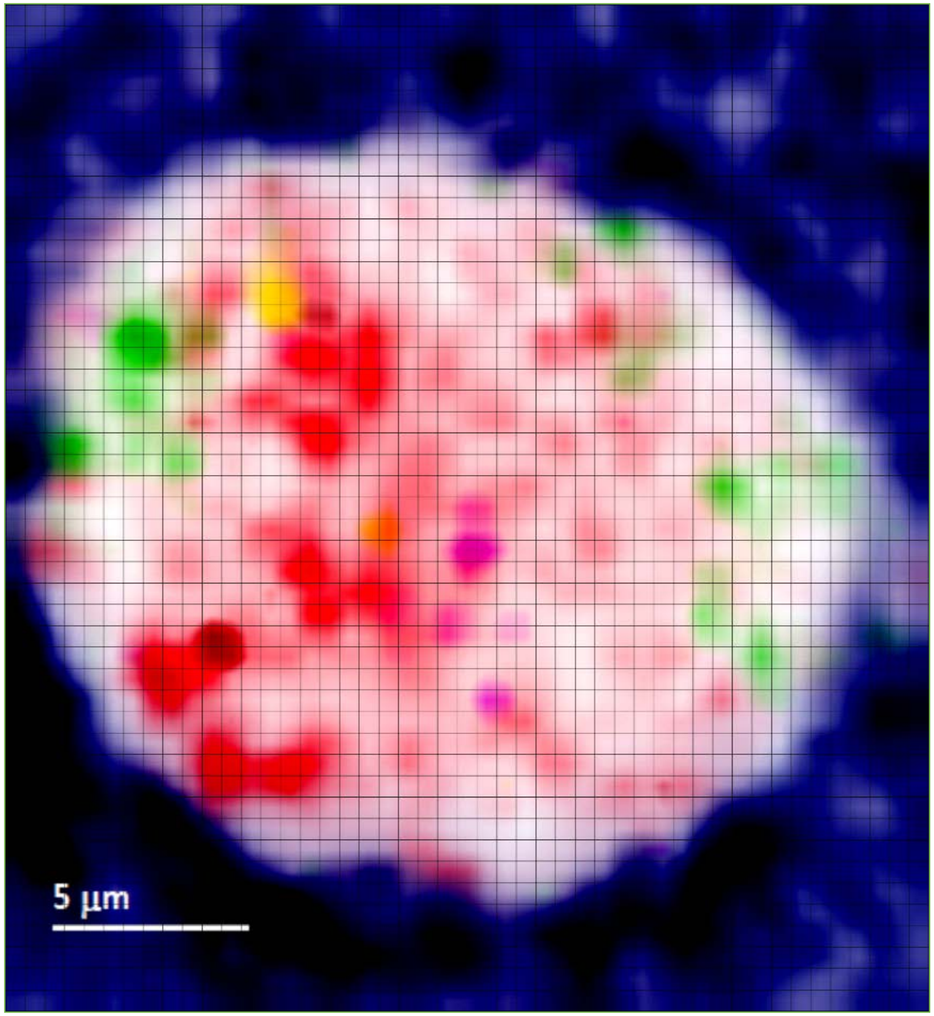

- Re
- PPv-Fe_2O_3
- Fe_3O_4 ($CaTi_2O_4$-type)
- Fe_3O_4 ($CaFe_2O_4$-type)
- $Fe_{13}O_{19}$
- Fe_7O_{12}